

**THE MECHANICS OF FIBER-BASED ABSORBENT
EVAPORATIVE COOLING (fbaEC) FOR TRANSPORT**

A Dissertation
presented to
the Faculty of the Graduate School
University of Missouri

In Partial Fulfillment
of the Requirements for the Degree
Doctor of Philosophy

by
XIAOYU GUO
Dr. Luis G. Occeña, Dissertation Supervisor

DECEMBER, 2016

The undersigned, appointed by the dean of the Graduate School, have examined the dissertation entitled

THE MECHANICS OF FIBER-BASED ABSORBENT
EVAPORATIVE COOLING (fbaEC) FOR TRANSPORT

presented by Xiaoyu Guo, a candidate for the degree of doctor of philosophy, and hereby certify that, in their opinion, it is worthy of acceptance.

Professor Luis Occeña

Professor Cerry Klein

Professor Yuwen Zhang

Professor Ronald McGarvey

DEDICATION

This dissertation is dedicated to my beloved wife, DENG Ximu, and my great parents LI Jinping and GUO Jiyuan, for their vision and wisdom, selfless and unconditional love, endless support and sacrifice with absolutely no regrets.

ACKNOWLEDGEMENTS

The completion of this dissertation could not have been possible without the participation and support of so many people whose names may not all be enumerated. Their contributions are sincerely appreciated and gratefully acknowledged. I would like to express my deep appreciation and indebtedness particularly to the following:

Dr. Luis Occeña, academic mentor and research advisor, for his endless support and valuable advising for past seven years;

Mr. Richard Oberto, for his endless technical support and assistance;

Dr. Cerry Klein, Dr. Yuwen Zhang, and Dr. Ronald McGarvey, for their great academic advice and support.

To all relatives, friends and others who in one way or another shared their support, thank you.

TABLE OF CONTENTS

ACKNOWLEDGEMENTS	ii
LIST OF FIGURES	vii
LIST OF TABLES	x
ABSTRACT.....	xii
CHAPTER 1 INTRODUCTION	1
1.1 Food Safety Crisis	1
1.2 Evaporative Cooling Principle	2
1.3 Evaporative Cooling in Food Storage	4
1.4 Mathematical Study of Evaporative Cooler	6
1.5 Evaporative Cooler for Transport.....	7
1.6 Research Objective.....	7
1.7 Dissertation Outline.....	8
CHAPTER 2 REVIEW OF LITERATURE AND RELATED TOPICS.....	10
2.1 Literature Review	10
2.2 Food Transportation Regulations and Related Standards	20
2.2.1 Refrigerated Truck.....	20
2.2.2 Food Transportation Regulations and Related Standards.....	21
2.2.3 Vehicles Used to Transport Meat, Poultry, and Egg Products	21
2.2.4 Monitor Operations for Employees	22
2.2.5 Air Quality for Fresh-Cut Fruits and Vegetables.....	23

2.2.6	Pre-Cooling and Cold Storage for Fresh-Cut Fruits and Vegetables.....	23
2.3	Absorbent Fibers	24
2.4	Review of Absorbent-Evaporative Cooler	26
2.4.1	The Advantages for The New Design.....	29
2.5	Review of The Data Collection Process.....	32
2.5.1	Cooling Efficiency Calculation	33
2.5.2	Experiment Environment.....	34
2.5.3	Experiment Equipment Information.....	34
2.5.4	Experiment Procedures.....	39
2.6	Prior Experiments Result	44
CHAPTER 3 METHODOLOGY DEVELOPMENT.....		45
3.1	Heat Transfer Mathematical Model On Single-Scaffold Structure.....	46
3.2	Mass Transfer Mathematical Model On Single-Scaffold Cooling Structure	49
3.3	Experiments On Testing the fbaEC in Real Transport Environment	50
3.3.1	Experiment Purpose and Cooling Efficiency Calculation.....	50
3.3.2	Experimental Environment and Assumptions	50
3.3.3	Experimental Equipment.....	50
3.3.4	Experiment Procedure	52
3.3.5	Experiment Results Analysis	54
3.4	Heat and Mass Transfer Mathematical Model On Multi-Scaffold Structure	54
3.5	Summary	55

CHAPTER 4 HEAT AND MASS TRANSFER MATHEMATICAL MODEL FOR A SINGLE-SCAFFOLD STRUCTURE OF FIBER-BASED ABSORBENT EVAPORATIVE COOLER	57
4.1 Heat Transfer	57
4.2 Mass Transfer	61
4.3 Results and Discussion.....	63
4.4 Summary	69
CHAPTER 5 EXPERIMENTS ON TESTING THE fbaEC COOLING PERFORMANCE IN REAL TRANSPORT ENVIRONMENT	72
5.1 Experiment Result.....	72
5.1.1 Speed 0 MPH.....	73
5.1.2 Speed 15 MPH.....	75
5.1.3 Speed 30 MPH.....	76
5.1.4 Speed 45 MPH.....	78
5.1.5 Extra Compare Cases.....	79
5.2 Water Consumption.....	81
5.3 Statistical Analysis	81
5.3.1 Temperature Comparison	81
5.3.2 Basic Assumptions and Analysis	82
5.3.3 Linear Regression Analysis	87
5.3.4 Analysis on Effect of Speed on Water Consumption	94
5.4 Discussion and Summary	96

CHAPTER 6 HEAT AND MASS TRANSFER MATHEMATICAL MODEL FOR A MULTI-SCAFFOLD STRUCTURE OF FIBER-BASED ABSORBENT EVAPORATIVE COOLER	100
CHAPTER 7 CONCLUSION AND FUTURE STUDY	104
7.1 Research Summary.....	104
7.1.1 Heat and Mass Transfer Mathematical Model Development for Single-scaffold Structure	105
7.1.2 Cooling Effect Validation in Transport Environment.....	105
7.1.3 Heat and Mass Transfer Mathematical Model Extension for Multi-Scaffold Structure.....	107
7.2 Future Study	108
7.2.1 Validation Experiment of Multi-Scaffold Structure’s Cooling Efficiency	108
7.2.2 fbaEC Structure Improvement.....	109
7.3 Contribution	109
REFERENCE.....	112
APPENDIX.....	119
VITA	128

LIST OF FIGURES

Figure	Page
Figure 1-1 Direct evaporative cooling (Western Environmental Services Corporation, n.d.)	3
Figure 1-2 Indirect evaporative cooling (Western Environmental Services Corporation, n.d.)	4
Figure 2-1 A sample of Zero-energy cool chamber	13
Figure 2-2 Zeer pot used in Nigeria	14
Figure 2-3 Reefer Truck	21
Figure 2-4 Woolen thread	25
Figure 2-5 Cotton thread	26
Figure 2-6 Linen piece	26
Figure 2-7 A typical wetted-pad evaporative cooler (“Evaporate Cooling Heating & Cooling Alabama Power”)	27
Figure 2-8 General structure sketch	27
Figure 2-9 Top view of refrigeration section	29
Figure 2-10 Evaporative cooler with a water pump to recirculate water from bottom to top (“Used Evaporative Coolers Coolers,” 2014).....	31
Figure 2-11 (a) Solidworks drawing and (b) product of single scaffold unit.....	35
Figure 2-12 (a) Solidworks drawing and (b) product of container (water tank).....	36
Figure 2-13 (a) Cotton threads, (b) woolen threads, and (c) linen piece (a type of weave made of cotton)	36
Figure 2-14 5V / 12V AC Cooling Fan.....	37
Figure 2-15 Thermocouples	37

Figure 2-16 Moisture sensor	38
Figure 2-17 Data acquisition program	38
Figure 2-18 I/O connector.....	39
Figure 2-19 600 ml water in a plastic bottle	39
Figure 2-20 (a) Wrapping cotton thread and (b) wool thread onto scaffold vertically	40
Figure 2-21 (a) Wrapping cotton thread, (b) wool thread onto scaffold horizontally, and (c) linen piece wrapping around scaffold.....	40
Figure 2-22 (a) Drawing of prescribed position; (b) sensors at diagnostic position; (c) front view of prescribed position model; (d) top view of prescribed position model..	41
Figure 2-23 Scaffold with cotton threads in container.....	42
Figure 2-24 Pour water into container while the scaffold stands inside the water container.....	42
Figure 2-25 Measuring water level change.....	43
Figure 3-1 Data Acquisition System Connected with Sensors and Laptop and Sensor T1 position.	52
Figure 3-2 Cooler Set Up on Vehicle	53
Figure 4-1 Airflow blow around the scaffold’s surface	60
Figure 4-2 The sectional view and top view of the positions of T2 and T3	62
Figure 4-3 Comparison between actual water consumption and calculation results ...	67
Figure 4-4 Error summary between actual water consumption and calculation results	68
Figure 5-1 Thermal couples’ positions.....	72
Figure 5-2 Temperature vs. time of three replications in case that driving test at speed of 0 mph.....	73
Figure 5-3 Temperature vs. time of three replications in case that driving test at speed	

of 15 mph	75
Figure 5-4 Temperature vs. time of three replications in case that driving test at speed of 30 mph	77
Figure 5-5 Temperature vs. time of three replications in case that driving test at speed of 45 mph	79
Figure 5-6 Temperature vs. time example of three replications in case that driving test at speed of 15 mph, 30 mph and 45 mph, while running without water inside	80
Figure 5-7 The average amount of consumed water among three replication at each driving speed while testing	81
Figure 5-8 Correlation analysis among variables for group #1 (v = 0mph)	82
Figure 5-9 Correlation analysis among variables for group #2 (v = 15mph)	83
Figure 5-10 Correlation analysis among variables for group #3 (v = 30mph)	83
Figure 5-11 Correlation analysis among variables for group #4 (v = 45mph)	83
Figure 5-12 Scatter plots among environment relative humidity and four cooling efficiency variables	85
Figure 5-13 Scatter plots among environment relative humidity and four cooling efficiency variables	86
Figure 5-14 Regression results from two methods comparison.....	90
Figure 5-15 Regression model statistics validation result	93
Figure 6-1 2 × 2 Multi-scaffold illustration.....	101

LIST OF TABLES

Table	Page
Table 2-1 Comparison between refrigerated cooler and fiber-based absorbent evaporative cooler.....	30
Table 2-2 Material and wrapping methods	32
Table 2-3 Case content.....	43
Table 3-1 Experiment case content	53
Table 4-1 Contents of Selected Cases for Validation.....	64
Table 4-2 Calculation Results of Water Consumption on Scaffold	65
Table 4-3 Measurement Results of Total Water Consumption of Whole Cooler.....	65
Table 4-4 Water Consumption from Surrounded Water Area	66
Table 4-5 Actual Water Consumption of Scaffold	66
Table 4-6 Error Summary between Actual Water Consumption of scaffold and Calculation Results	68
Table 4-7 Heat Transfer Coefficient Summary	69
Table 5-1 Summary of effects of environment relative humidity and speed on the cooling efficiency.....	91
Table 5-2 F-test result on the predictor variables to the amount of water consumption	94
Table 5-3 F-test result on the regression model among speed and water consumption	96
Table 5-4 Comparison between driving experiment result and dew-point.....	97
Table 5-5 Comparison between prior lab experiment result and dew-point.....	97
Table 5-6 Driving Test Experiment Result Summary	98

Table 7-1 Comparison Among Different Experiment Results 106

THE MECHANICS OF FIBER-BASED ABSORBENT EVAPORATIVE COOLING (fbaEC) FOR TRANSPORT

XIAOYU GUO

Dr. Luis G. Occeña, Dissertation Supervisor

ABSTRACT

For the purpose of food quality and safety during short-term transport and storage in developing or rural areas, low-energy consumption and environmental-friendly methods are needed for use in cooling systems and related applications. In prior research, a new evaporative cooling system model using absorbent fabric wrapping in curtain structure on a scaffold for short-term transport and storage was built in a laboratory scale, and a series of laboratory scale experiments to statistically verify the basic concept of the new model were performed. Three kinds of absorbent fabric materials in common use were evaluated based on their water absorbent characteristic to decrease temperature and then to increase humidity, which contribute to keeping food and other products that require low temperature and high humidity to stay fresh longer. To gain an understanding of the mechanics for the fiber-based absorbent evaporative cooling, an in-depth study that results in the mathematical modeling of the heat and mass transfer that takes place during cooling for both single-scaffold structure and multi-scaffold structure was built. From that model we can calculate the heat transfer coefficient based on the fiber material, airflow speed and scaffold characteristics, to develop a methodology to predict the water consumption during cooling. To validate the fbaEC's cooling effects in a transport scenario, a series of experiments in a real transport environment was designed and conducted. The driving testing transport experiments were conducted in a moving vehicle at 15 mph, 30 mph and 45 mph,

respectively. Cotton was the absorbent fiber material based on its cooling performance in prior laboratory experiments. Statistical analysis of the results showed a promising cooling performance for the fbaEC in a transport environment, with the lowest temperature generated at 17.6°C while the environment temperature was 31.9°C. The cooling efficiency was at 44.48% without resorting to electricity, but only wind power. The contribution of this study is summarized, and the future study direction is also discussed.

Keywords

Food safety, Absorbent, Fiber, Transport, Scaffold, Evaporative cooling

CHAPTER 1

INTRODUCTION

1.1 Food Safety Crisis

Proper temperature control during food transport and storage plays an important role in the field of food quality and safety. Improper or extreme temperatures could give rise to recalls and spoilage problems that have become recently more frequent and widespread in the food industry. According to statistics from agriculture organizations and research, loss of the post-harvest due to inappropriate management in transportation, storage, and even selling process takes a huge percentage of total fruit and vegetable production.

Especially in developing countries, the lack of advanced facilities and scientific management procedures are the main reasons that lead to a food safety crisis. For example, in India and Nigeria, a lot of fruit and vegetable products are wasted during post-harvest because of improper storage and transport equipment. Post-harvest losses in South East Asia can range from 10%-50% depending on a particular country. In Africa, post-harvest losses are not properly documented but experts have projected the losses to be up to 80%. 54% of wasted food, says the report, "Food Wastage Footprint: Impacts on Natural Resources" by the Food and Agriculture Organization of the United Nations (FAO), is lost during production, postharvest treatment and storage. Particularly badly affected are the poorer countries of Africa and Asia where shortcomings during harvesting and logistics destroy 6 to 11 kg of food per capita each year (Ndukwu & Manuwa, 2014).

The world loses or wastes one-quarter to one-third of all food produced for human consumption, according to the latest issue of the World Bank's quarterly Food Price Watch citing Food and Agriculture Organization of the United Nations and World

Resources Institute estimates. In regions with undernourishment, such as Africa and South Asia, this shocking loss translates to 400 to 500 calories per person, per day—and up to 1520 calories in the developed world (World Bank, 2014). Jim Yong Kim, President of the World Bank Group said, “Millions of people around the world go to bed hungry every night, and yet millions of tons of food end up in trashcans or spoiled on the way to market”.

The United Nations (UN) estimates that in the developing countries, one child in six is undernourished, which amounts to an absolute figure of 100 million, and undernourishment causes the deaths of 2.6 million children under five years old per year (Popular Plastics and Packaging, 2014).

All of above have forced government manufacturing and logistics operators to address the food safety crisis.

1.2 Evaporative Cooling Principle

Evaporative cooling has been reported to be effective for achieving a favorable environment in greenhouses (Jain, 2006), and the storage structure for fruit and vegetables (Helsen & Willmot, 1991). The degree of cooling depends on the original humidity of air and the efficiency of the evaporative surface. If the ambient air has low humidity, then a large reduction in temperature can be achieved (Thompson AK, 1996).

The evaporative cooling is a heat and mass transfer process that uses evaporation of water to vapor, and consequently the air temperature decreases (Amer, Boukhanouf, & Ibrahim, 2015). The basic principle relies on cooling by evaporation. When water evaporates it draws energy from its surroundings that produce a considerable cooling effect. Since air temperature and humidity are the two major parameters affecting thermal comfort significantly (Abbouda & Almuhanha, 2012), evaporative cooling occurs when air that is not too humid passes over a wet surface; the faster the rate of

evaporation, the greater the cooling. The efficiency of an evaporative cooler depends on the humidity of the surrounding air. Very dry air can absorb a lot of moisture so greater cooling occurs. In the extreme case of air that is totally saturated with water, no evaporation can take place and no cooling occurs.

As one of the most effective and low cost cooling technologies, which builds on phase-change theory that heat transfer happens during the property phase-change process, e.g. water to vapor, various types of evaporative cooling systems have been designed for industrial and personal use. From the aspect of energy dependency, we can classify the current cooling practice as electricity dependent cooling that relies on electricity to supply power, and electricity independent cooling that does not rely on electricity, instead using the power of nature, for example, wind power. According to heat exchange format, the main types of evaporative cooling include direct and indirect evaporative cooling.

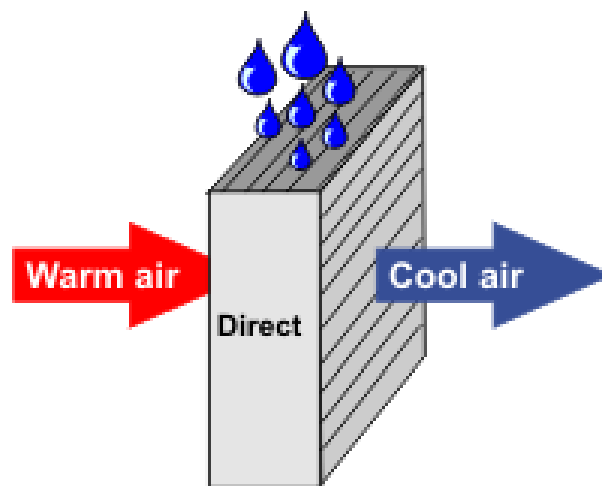


Figure 1-1 Direct evaporative cooling (**Western Environmental Services Corporation, n.d.**)

Direct evaporative cooling (DEC) is the oldest and the simplest type of evaporative cooling in which the process air contacts directly with water. The most commonly used direct evaporative coolers are essentially metal cubes or plastic boxes with large flat vertical air filters, called “pads”, in their walls (Xuan, et al, 2012).

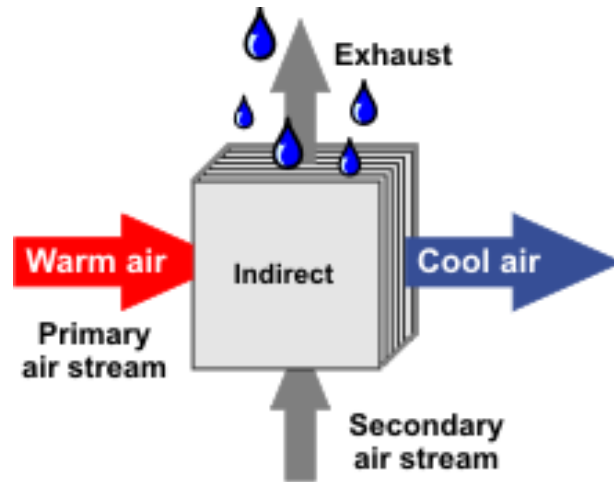


Figure 1-2 Indirect evaporative cooling (Western Environmental Services Corporation, n.d.)

In the case of indirect evaporative cooling, water evaporates in a secondary air stream that exchanges sensible heat with the primary air stream in a heat exchanger (Gómez, et al, 2010). In this way, the inlet air stream is cooled when keeping in contact with the surface through which the heat exchange is produced, without modifying its absolute humidity; whereas the other side of this surface the secondary air stream is being evaporative cooled (Patil, Hirde, & Badnera, 2013).

From the perspective of thermodynamics, in direct or indirect evaporative cooling process, it is a synchronized process in which flowing, heat exchange, and mass exchange happen at the same time. The main method for receiving energy from nature for evaporative cooling technology is directly using the difference between dry and wet bulb temperature; it barely consumes primary energy resources and is environmental friendly.

1.3 Evaporative Cooling in Food Storage

Refrigerated and cool storage are the best method of preserving fruits and vegetables, but they are expensive to buy and run. Consequently, for developing rural areas, there is an interest in simple low-cost alternatives, and evaporative cooling technology has been traditionally regarded as a good way to keep cool in the summer

is simple and does not require any external power supply.

In the past 25 years, research has developed evaporative cooling technology in various industries, for example, power plants, air conditioning, and also applied in the food storage field. Only few researchers so far focus and build evaporative cooling systems to service food storage. The “Zero Energy Cool Chamber” (ZECC) is an example that was initially designed for food storage based on evaporation theory (S. K. Roy & Pal, 1991). The details about ZECC will be presented in chapter 2.

However, “Zero Energy Cool Chamber” (ZECC) was built for local food storage, made of bricks, sand and sawdust; it can be considered a micro warehouse. Due to the lack of flexibility and complicated installation, the ZECC is not suited for transport, which seeks to reduce the risks of food lost during transport, especially the long distance transport without the access to a refrigerated truck. As for a traditional evaporative cooler, the electricity-dependent structure has to rely on outsourced electricity that constraints the usage of a cooler. Since there was no appropriate electricity-independent evaporative cooler design for transport, a new fiber-based absorbent evaporative cooler with vertical curtain structure was developed for food storage that initially can be used in a moving transport environment (Guo, 2012).

Compared with ZECC structure and construction materials, the new fiber-based absorbent evaporative cooler uses absorbent fabric fiber as a water storage medium enables the coolers to be more flexible and clean. Compared with existing traditional evaporative coolers, which also use fiber as the water-storage media (e.g. the raw fiber material like coconut coir), the new fiber-based absorbent evaporative cooler changes the traditional structure of horizontal stacked pads to the structure of a vertical independent standing scaffold. The former structure has to rely on a water spray system, a cloud of very fine water droplets is produced using atomization nozzles (Montazeri,

Blocken, & Hensen, 2015), which cannot be independently operated without an electricity driven pump; the latter structure has a unique advantage to still work for cooling without electricity owing to the fabric fiber that can soak water up naturally and air flow to effect the evaporation. The detailed structure description will be presented later in chapter 3. Within a laboratory scale, the prior experiments have initially verified the concept of “fiber-based evaporative cooler” on single-scaffold structure, the cooling performance showed a significant temperature drop with certain type of fiber materials. In those experiments, different wrapping methods and different airflow speed have different cooling effects on evaporation efficiency. The relative humidity and the material type were also factors that affected the cooling performance. For all cases of experiments, they were given enough equal amounts of water during the cooling process.

1.4 Mathematical Study of Evaporative Cooler

With the development of the evaporative cooler design, the study of heat and mass transfer started with industry-based evaporative coolers, and researchers have conducted various heat and mass transfer studies for industrial-use evaporative cooling tower, air-conditioner, etc.

However, there are few recent studies for the evaporative cooler for food storage. Although a fiber-based evaporative cooler has been experimentally demonstrated as performed good performing cooling facility, mathematical studies on heat and mass transfer can help better understand the cooling process, and also contribute to structure improvement including changing dimension, etc. Most importantly, once we have completed the heat and mass transfer mathematical model, we can calculate the necessary amount of water for a specific cooling requirement, specifically with respect to time. This is critical to avoid water waste, particularly for hot and dry areas where

there is relatively limited access to water resources.

Derived from the single-scaffold fiber-based absorbent evaporative cooler (fbaEC) structure, the heat and mass transfer study of a multi-scaffold cooling structure is also necessary for verifying a practical configuration for an eventual implementation of fiber-based absorbent evaporative cooler.

1.5 Evaporative Cooler for Transport

As previously presented, implementing the function of transportable coolers is one of the advances when comparing with other existing cooling models for food storage. The prior experiments on a single-scaffold structure has simulated the moving status by using a fan to bring the airflow into the storage space. However, there are still many other factors that were considered while operating the laboratory scale experiments. To validate the cooling performance of fbaEC for transport, it is necessary to conduct a further study to test cooling performance in a realistic transport environment.

1.6 Research Objective

To implement fiber-based absorbent evaporative cooling and apply it to the low cost food storage and food transportation to derive a new way to help reduce the food safety crisis. Therefore, this dissertation aims to (1) review the fbaEC system, (2) build a series of mathematical models to study the heat and mass transfer process on both single scaffold and multi-scaffold structures during cooling, (2) use the model to predict the minimum water amount for the single scaffold structure, which will be consumed during cooling based on specific target, (3) analyze the collected data from prior experiments, find out the specific heat transfer coefficient for different materials, (4) complete the heat and mass transfer model, then validate heat and transfer model through the amount of water that consumed during experiment, (5) design a series of

experiments to validate the fbaEC's cooling effects in a realistic transport environment, (6) summarize the advantages, aspects to be improved, and the further study.

1.7 Dissertation Outline

In chapter 2, the literature is reviewed to introduce a brief history of the research related to evaporative cooling, and the application in food safety. Some related topics about food transport and common cooling technology applications are discussed. Related studies on heat and mass transfer in evaporative cooling are also compared. The initial concept, on which the fbaEC system is based, is reviewed and the process of data collection for prior experiments is described.

In chapter 3, the research methodology will be described. It starts from building heat and mass transfer equations with validation for single-scaffold structure. The experiments for testing the cooling performance of single-scaffold structure cooler in realistic transport environment is designed. And then the heat and mass transfer mathematical model is extended for a multi-scaffold structure fbaEC.

In chapter 4, the result of the mathematical heat and mass transfer model is presented to predict the minimum amount of water that is being consumed during cooling. Prior experiment results are reviewed. The data collected from the prior experiments are processed for the specific heat transfer coefficient, and the minimum amount of water consumption is validated through resulting experimental data.

In chapter 5, the experiments result of testing the fiber-based absorbent evaporative cooler's performance in the real transport environment is discussed. The experiment result is illustrated to show the temperature change during cooling process, the correlation among variables is statistically analyzed, the regression model to predict the water consumption is developed at the end.

In chapter 6, based on the heat and mass transfer mathematical model for single-

scaffold structure, the extended mathematical heat and mass transfer model is built for the multi-scaffold structure, to predict the minimum water consumption during cooling process.

In chapter 7, conclusion will be summarized, the contribution of this dissertation is discussed, and the direction for future study about this study is given to further improve the fiber-based absorbent evaporative cooling system.

CHAPTER 2

REVIEW OF LITERATURE AND RELATED TOPICS

2.1 Literature Review

Much of the post-harvest loss of fruits and vegetables in developing countries is due to the lack of proper storage facilities (Noble, 2003). Due to the short shelf life of these crops, it is estimated that about 30 to 35% of India's total fruits and vegetables production is lost during harvest, storage, grading, transport, packaging and distribution in a year, which reduces the growers' share. Only 2% of these crops are processed into value added products (Basediya, Samuel, & Beera, 2011). In Nigeria, large quantities of these products are lost annually due to poor processing and storage facilities. This situation is even worse in the remote rural areas where the fresh food materials are produced (Anyanwu, 2003). The fruits and vegetables, being perishable, need immediate post-harvest attention to reduce the microbial load and increase their shelf life, which can be achieved by storing them at low temperature and high relative humidity conditions. These conditions are usually achieved in cold storages (Basediya et al., 2011).

When talking about cooling technology development history, we can trace back to three hundred years ago, when many of the current mechanical refrigeration technologies were initially invented. However, as matter of fact, thousands of years previously, the people living in Greece had started to drink chilled wine (Love, 2009). In fact, in most ancient civilizations at least the wealthy appeared to have had access to ice or snow to cool their drinks. Sometimes people harvested ice from cold regions, which was transported to temperate climates and stored in insulated pits. In other cases, it seemed that ice was generated via radiation of heat from shallow pools into the night sky, while in other cases evaporative cooling was used to chill bottles filled with wine

(Love, 2009).

And in Asian countries, like China, people used to store ice from the winter season in warehouses under the ground, which has a much lower temperature. But for most of architectures in China, the unique structure and construction material can help people cool the interior space during summer and keep warm during winter. In rural areas, especially in northwestern China, people built cave dwellings along the edge of a loess plateau. Inside the cave house was naturally cooled in summer and warmed in winter.

The cooling technology is mainly based on phase-change methods and physics theory. The typical and also original phase-change cooling method is by using a chemical agent to release and absorb heat during phase changes, e.g. chlorofluorocarbon. A typical application of physical cooling technology is magnetic refrigeration, which can be defined as an adiabatic temperature change due to magnetization, or alternatively, isothermal magnetic entropy change (Boucekara, Kedous-Lebouc, Dupuis, & Allab, 2008).

The food cold chain, also called cold chain, based on low-temperature food technology, is a temperature-controlled supply chain. It uses refrigeration equipment and technology, in order to keep frozen food or low temperature-needed food in a certain range of temperature in whole material and logistics process that will promote best quality and marketing performance. While refrigerated cool stores are the best method of preserving fruits and vegetables, their high-cost which requires heavy initial capital investment and intensive consumption of energy involved in constructing cold storage cooler or cold warehouse is still a bottleneck for most developing countries or rural areas. Consequently, for a small scale company there is an interest in simple low-cost alternatives. Evaporative cooling has been traditionally regarded as a good way to keep food cool in the summer that is simple and does not require any external power

supply.

With the onset of energy crisis and environmental problems caused by conventional air-conditioners, the importance of evaporative cooling has grown (Kachhwaha & Prabhakar, 2009). In hot, dry climates, such as those encountered in some parts of Nigeria, evaporation from a water reservoir can reach significantly high proportions, and it has been reported that more than $1.2 \times 10^9 \text{ m}^3$ evaporates annually from the reservoirs of the Colorado and Missouri rivers (Anyanwu, 2003).

Owing to its characteristics of zero pollution, energy efficiency, simplicity and good in-door air quality (J.M. Wu, X. Huang, & H. Zhang, 2008), a number of researchers have focused on building evaporative coolers in past years. In industry, water-cooling towers, evaporative condensers, evaporated fluid coolers, air washers, and dehumidifying coils, are widely used. Generally, an evaporative cooling structure is made of porous material that is fed with water (Mehere, Mudafale, & Prayagi, 2014). In 2006, Jha SN, Chopra S (SN & S, 2006) proved the evaporative cooled storage structure is useful for short term, on-farm storage of fruits and vegetables in hot and dry regions. The Zero Energy Cool Chamber (ZECC) developed at IARI, New Delhi by Roy and Khurdiya (1986) was based on the principle of evaporative cooling (S. K. Roy & Khurdiya, 1986).

The process of evaporative cooling is an adiabatic exchange of heat, in which heat does not enter or leave the system concerned, that the heat airflow losses equals to the heat the water gains; when ambient air passes through a saturated surface to obtain low temperature and high humidity, which is desirable to extend the storage life of fruits and vegetables (Das SK & Chandra P, 2001). Storage of horticultural products inside the cool chamber has shown reduction in the physiological loss in weight, optimum color, and better firmness and extended shelf life by 1–2 weeks in other parts of the

country (Basediya et al., 2011). Researchers including Sandooja, Sharma, Pandit, & Batra, (1987), Wasker, Nikam, & Garande (1999) also published lower weight loss of fruits and vegetables under ZECC .

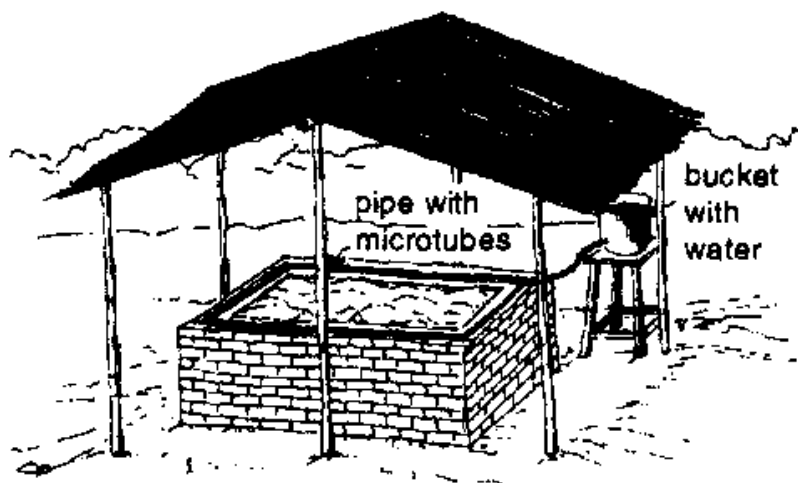


Figure 2-1 A sample of Zero-energy cool chamber

In figure 2-1, a sample of Zero-energy cool chamber shows a pipe connecting with a bucket with storage water, injecting water into a gap between two walls, soaking filler materials, for example, sand. Water evaporates from the gap between the walls and thereby cools the inside chamber.

Zero energy cool chambers along with packaging materials, ventilation and anti-fungal treatments can help in minimizing the losses of ascorbic acid in the stored lemon fruits to some extent compared to the storage under ambient conditions of storage (Prabha A, Sharma HR, Goel AK, & Ranjana V, 2006).

Khader (1999) designed a simple evaporative cooler that is basically a pot structure that is mainly made up of a wet porous bed through which air exchanges heat with water and be cooled. Mohammed Abbah, a teacher in Nigeria, developed a small scale storage pot-in-pot system (shown in figure 2-2) that uses two pots of slightly different size (Longmone AP, 2003). The smaller pot is placed inside the large pot and the space between is filled with sand (Amrat lal Basediya, D. V. K. Samuel, and Vimala

Beera 2011).



Figure 2-2 Zeer pot used in Nigeria

A zero-energy cool chamber was developed using locally available materials in New Delhi, India, by Roy and Pal in 1994. The chamber is designed for on-farm use, operates by evaporative cooling, and is constructed from double brick with sand-filled cavity walls. The shelf life of tropical fruits held in the chamber was increased by 2 to 14 days (15–27% increase) as compared to storage at room temperature, and the physiological loss in weight was lower (Amrat lal Basediya, D. V. K. Samuel, and Vimala Beera 2011). Roy & Khurdiya (1982) used porous bricks, riverbed sand, ordinary wooden box and ordinary fruit basket, respectively, and constructed 4 types of evaporative cooler chambers used to store vegetables. They also used sand to fill gaps.

Roy (1984) reported that a 6 ton cool chamber was constructed, where the side wall was constructed with two layers of bricks leaving approximately 7.5 cm gap in between them. This gap was filled with riverbed sand. The floor was made of wooden planks. Below the floor, a 33 cm deep tank was constructed with 4 air ducts made of bricks opening at the center and submerged under wet sand. The sand in the wall and surrounding the ducts were saturated with a drip system. The top of the chamber was insulated and incorporated with an exhaust fan. The air while passing through saturated duct and walls cooled sufficiently and took away heat from the produce (Amrat lal

Basediya, D. V. K. Samuel, and Vimala Beera 2011).

A solar-cum-wind aspirator ventilated evaporative cooling structure of 20-ton capacity for potatoes and other semi perishables was constructed at the Central Potato Research Station (CPRS), Jalandhar. The structure maintained a temperature of 21–25 °C with 80–90% RH at ventilation rate of 24m³/min when the outside temperature and RH were 40–42 °C and 30–35%, respectively (Chouksey RG, 1985).

Roy and Pal developed a low cost zero energy cool chamber—an on-farm rural oriented storage structure at IARI, New Delhi, using locally available raw materials such as bricks, sand, bamboo, dry grass, jute cloth etc., which operates on the principle of evaporative cooling (Amrat lal Basediya, D. V. K. Samuel, and Vimala Beera 2011). At the same time, Mogaji and Fapetu designed an evaporative cooling system that could be utilized to preserve tomatoes and carrots at their minimal storage temperature(Mogaji & Fapetu, 2011).

Umbarkar et al. (1998) constructed an evaporative cooler (EC) structure of 2 ton capacity based on the results of their previous studies (Umbarkar SP, Bonde RS, & Kolase MN, 1991). The walls of the structure were constructed with 10 cm thick brickbat pad sandwiched between two 10 cm thickness brick perforated walls.

As for energy-independent cooler system, a new zero energy cool chamber (ZECC) consisting of two cooling systems, a solar-driven adsorption (chemical agency) refrigerator and an evaporative cooling system (Md. Parvez Islam & Morimoto, 2014), was developed and then evaluated as a low-cost and eco-friendly cooling storage for storing fruit with moderate respiration rates. Since the inside too dry cool chamber will not provide the desired cooling effect and too moist chamber causes unnecessary wastage of water and may sometimes lead to fungus growth (Ganesan, Balasubramanian, & Bhavani, 2004), Rayaguru et al built a series of experiments in the

coastal area and found the optimum water level to achieve a steady and conducive storage environment for storage of fruits and vegetables in summer and winter months, respectively.

After several research of building an evaporative cooler structure, many studies started to focus on evaluation and measurement of evaporative cooling performance.

A numerical model is developed for the evaporating liquid meniscus in wick microstructures under saturated vapor conditions, in which four different wick geometries representing common wicks in heat pipes, wire mesh, rectangular grooves, sintered wicks and vertical micro wires, were modeled and compared for evaporative performance (Ranjan, Murthy, & Garimella, 2011).

A simulation model was developed to predict temperature, moisture content and water activity of evaporative-cooled tortillas by T.A. Talor et al. in 1998. The overall model was based on three parts: (1) the predicted equilibrium moisture isotherm for the product, (2) a correlation model for predicting the saturated water vapor pressure for a given temperature, and (3) the energy and mass balances for simultaneous convective heat and moisture transfer between product and cooling air. The simulation model was verified with experimental data and was found to accurately describe the behavior of the tortilla cooling system. The model predicted the simultaneous decrease in temperature, moisture content, and water activity of the product exposed to varying simulated processing conditions. It was found that cooling air velocity and temperature had the primary effect on product cooling and moisture loss rates (T.A. Talor et al.1998).

E.E. Anyanwu designed and measured performance of a porous evaporative cooler for preservation of fruits and vegetables in 2003 which illustrated the evaporative cooler has prospects for use in short term preservation of vegetables and fruits soon after harvest (Anyanwu, 2003). The experimental cooler, with a total storage space of

0.014 m³, consisted of a cuboid-shaped porous clay container located inside another clay container. The gap between them is filled with coconut fiber. A water reservoir linked to the cooler at the top through a flexible pipe supplied water to fill the gap (Anyanwu, 2003). The testing results published that the decreasing of ambient air varied 0.1-12°C during the period of test and proved that an evaporative cooler has superior performance over open-air preservation of post-harvest vegetables during daytime.

Thiagu et al. (2007) compared the tomatoes ripened in evaporative cooling (EC) storage conditions (20 °C–25 °C, 92–95% RH) with control fruits stored under room conditions (28 °C–33 °C, 45–65% RH) during summer in Mysore. EC-ripened tomatoes on the 15th day reached a 100% ripening index (RI) with a value of 2.48 for the ratio of redness to yellowishness (a/b) and hue angle (θ) of 22.1°, whereas the control tomatoes on the same day reached at a maximum 83.3% RI with a/b ratio of 1.59 and a hue angle of 32.9°. EC stored fruits showed lower values for rupture and shear stresses. The rate of moisture loss for control fruits was 6.5 times as great as for EC stored tomatoes (Amrat lal Basediya, D. V. K. Samuel, and Vimala Beera 2011).

The basic function of the evaporative cooler is heat treatment of air flow, and letting air flow meet request in respect to temperature, humidity, wind speed and cleanliness; and the key issue is the heat and mass exchange between air and water. Research on heat and mass transfer were reported in recent years.

J.M. Wu et al (2008) finished numerical investigation of the heat and mass transfer for a direct evaporative cooler. A simplified mathematical model was developed to describe the heat and moisture transfer between water and air in a direct evaporative cooler. The mass of evaporated water is treated as a mass source of air flow, and the related latent heat of water evaporation is taken as a heat source in the energy equation.

The momentum caused by water evaporation is taken into account in the momentum equations. The effective air viscosity and diffusion coefficient were decided experimentally. The models and methods were validated by comparing the numerical results with those of experiment for the same evaporative cooler. The influences of the inlet frontal air velocity, pad thickness, inlet air dry-bulb and wet-bulb temperatures on the cooling efficiency of the evaporative cooler were calculated and analyzed (J.M. Wu et al., 2008). Experimental results showed the inlet frontal air velocity is one of factors having significant effect on cooling efficiency.

William Adebisi Olosunde et al. (2009) evaluated the performance of absorbent materials in evaporative cooling system for the storage of fruits and vegetables. In this study, the absorbent materials were jute, hessian and cotton waste. The performance criteria included cooling efficiency, material performance and total amount of heat load removed from the evaporative cooler. The results showed that under the no-load condition, the average cooling efficiency was highest for jute at 86.2%, compared to 76.3% for cotton waste and 61.7% for hessian fiber. Material performance tests results showed that the highest resistance to mold formation was exhibited by hessian followed by cotton waste, while the jute fiber had very poor performance. The heat load determination also showed that products stored in the cooler with jute as water absorbent produced the least heat of respiration, followed by cotton waste and hessian in that order. The total results indicated that jute had the overall advantage over the other materials. However, if the cotton surface could be modified to offer larger surface required for evaporation, it would be the best alternative because the jute surface is prone to mold formation (William Adebisi Olosunde, J.C. Igbeka, & Taiwo Olufemi Olurin, 2009).

Kalpana Rayaguru et al. (2009) optimized water use in zero energy cool chambers

for short-term storage of fruits and vegetables in the coastal area. The quantity of water applied in ZECC was standardized. Since winter weather is drier than summer time, the optimum water level of 75 l/day and 90 l/day was required to achieve a steady and conducive storage environment for storage of fruits and vegetables in summer and winter months, respectively. The chamber kept the average temperature of its environment less by 5–8°C than the outside temperature, and maintained more than 90% RH. The ZECC was very effective in extending the storage life of potato, tomato, eggplant, mango, banana and spinach by 3 to 15 days as compared to ambient conditions (Kalpana Rayaguru, Md K. Khan, and Sahoo N. R. 2009).

According to S.K. Sharma, M.C. Nautiyal and K. Issar, there was a reduction of 7.1°C in mean minimum temperature and 12.2°C in mean maximum temperature in the ZECC as compared to the ambient conditions. Additionally, a humidity of 90% was maintained in the ZECC continuously during the fruit storage studies. So, apple fruits can be successfully stored under ZECC (temperature 3.10 to 19.80°C, RH~ 90%) for a period of about 100 days after treatment with 10 %wax and treatment with 2.5% CaCl₂ or Bavistin (200 ppm) after packing in micro perforated polythene bags, with minimum postharvest disease incidence, and quality changes (S.K Sharma, M.C. Nautiyal, and K. Issar n.d.).

Islam M.P. and Morimoto T. have reported an experiment to test cooling performance of ZECC and according to experimental results, the maximum and minimum temperatures inside the ZECC under shading condition were 24.2°C and 17.1°C while the outside maximum and minimum temperatures were 42.5°C and 25.0°C; the maximum and minimum temperatures inside the ZECC under no shading condition were 31.1°C and 24.6°C while the outside maximum and minimum temperatures were 45.6°C and 25.5°C. A shading curtain kept the ZECC temperature

lower.

Researchers have focused on heat and mass transfer study of above evaporative coolers and developed several optimization models (e.g. based on field synergy principle and the entransy dissipation extremum principle) improving heat transfer performance. In addition, Computational Fluid Dynamics (CFD) can be a valuable tool for assessing the potential and performance of evaporative cooling system. Several researchers have also developed mathematical models for experimental validation of the thermal behavior in the greenhouse after evaporative cooling; five factors mainly affect the temperature distribution inside the greenhouse: ventilation rate; crop transpiration and soil evaporation, the latter being neglected in what follows; percentage of shading; water evaporation from the pads; and heat loss coefficient of the cover. Results indicated the thermal gradient develops along the direction of the airflow inside of container.

2.2 Food Transportation Regulations and Related Standards

2.2.1 Refrigerated Truck

73% of all goods are shipped by truck, and 90% of the US food supply is transported by truck (Wojtala, n.d.). Delivery trucks can now be turned into mobile refrigeration units so that food can be kept colder while it is being delivered from place to place. These trucks are refrigerated at near or below freezing levels to keep any of the frozen food, e.g. seafood and ice cream, inside from spoiling. Many trucks pack their seafood with dry ice, which is a colder form of ice than regular ice and takes much longer to melt. These trucks use a lot of gas and electricity and are often expensive to operate. If a business is trying to transport perishable food using this method, it would probably be a good idea to look into delivering a lot of food at once to pay for the transport (Westlake, n.d.).



Figure 2-3 Reefer Truck

A Reefer truck shown in figure 2-3, has a refrigerated unit built either directly on the frame or is transported by trailer. It is refrigerated by diesel-powered generators and liquid carbon dioxide, or CO_2 . Reefer trucks range from simple ice cream trucks to large containers carrying perishable goods across the country (Wagner, n.d.).

2.2.2 Food Transportation Regulations and Related Standards

The U.S. Food and Drug Administration (FDA) has been asking commercial food transporters to follow the guidance the agency (FDA, 2010) issued in 2010 to reduce the chances of physical, chemical, biological and other risks during transportation of foods while the agency reviews current food safety transportation regulations.

According to FDA new regulation and guidance, different foods and different transportation methods have different standards:

2.2.3 Vehicles Used to Transport Meat, Poultry, and Egg Products

- Design and construct vehicles to protect product.

Vehicles should be designed and built to make locking and sealing easy, protect the cargo against extremes of heat and cold, and prevent infestation by pests.

Vehicle design should permit effective inspection, cleaning, disinfection, and temperature control.

Interior surfaces should be made of materials that are suitable for direct food

contact. For example, the surfaces may be made with stainless steel or be coated with food-grade epoxy resins.

- Sanitize and properly maintain vehicles.

Meat, poultry, and egg product transportation vehicles, accessories, and connections should be kept clean and free from dirt, debris, and any other substance or odor that may contaminate the product. They should be disinfected as needed. Cleaning and sanitation procedures should be specified in writing.

Different cleaning procedures may be necessary for the different types of meat, poultry, or egg products that are to be transported. The type of product transported and the cleaning procedure used should be recorded. Generally, wash water should be at least 180 °F (82 °C) and an approved sanitizer may be used to reduce the number of microorganisms and dissolve any fat particles adhering to interior surfaces.

Cargo pallets, load securing devices, and loading equipment should be kept clean and free of potential food contaminants and be regularly washed and sanitized.

Equipment used in transferring meat, poultry, and egg products, such as hand trucks, conveyors, and forklifts, should be well maintained and kept in a sanitary condition.

Secure transport vehicles to prevent tampering when not in use.

2.2.4 Monitor Operations for Employees

- Maintain a daily shift roster to easily identify persons who are/should be on the premises and indicate that they are in their appropriate location.
- Provide appropriate level of supervision to all staff, including food handlers, cleaning and maintenance staff, and computer support staff.
- Monitor employees for unusual behavior (e.g., staying unusually late, arriving unusually early, taking pictures of the establishment, or removing company documents

from the facility).

2.2.5 Air Quality for Fresh-Cut Fruits and Vegetables

Air inside a processing plant can be a vehicle for contamination of food by mold, yeast, dust, or pathogens if not properly controlled. Where fresh and fresh-cut fruits and vegetables are exposed to open air, it is recommended that air quality be monitored to ensure that it is of suitable quality.

It also recommends that fresh-cut processors consider the following to maintain appropriate air quality:

- Using air pressure differentials to direct potential airborne contaminants away from microbial sensitive areas. For example, negative air pressures in raw product areas, microbiology laboratories, and rest rooms may help to keep air from those areas from flowing into the processing areas. Similarly, positive air pressure can be maintained in areas such as the processing and packaging area.
- If air filtering equipment is used in a fresh-cut processing facility, filters should be performing at manufacturer specified levels of performance
- Filtering compressed air (such as oxygen (O₂), nitrogen (N₂), and carbon dioxide (CO₂) used in modified atmospheric packaging) when such air contacts fresh produce using a 0.3-micron filter (with an efficiency of approximately 75%)

2.2.6 Pre-Cooling and Cold Storage for Fresh-Cut Fruits and Vegetables

Sanitary cold storage of raw agricultural commodities (RACs) and fresh-cut produce is important to reduce the risk of microbial contamination and potential for subsequent growth. However, most current temperature recommendations for both whole and fresh produce are based on temperatures that maintain quality attributes. Although we recognize that more research needs to be done to identify the types of whole and fresh-cut produce that will support the growth of human pathogens and the

temperatures at which this pathogen growth will occur, certain practices can reduce the potential for pathogen growth and contamination during pre-cooling and cold storage.

It is recommended the following practices to reduce this risk:

- Holding RACs and fresh-cut produce at appropriate cold storage temperatures to reduce the potential for microbial growth
- Preventing condensate and defrost water from evaporator-type cooling systems (e.g., vacuum cooling, cold storage) from dripping onto fresh and fresh-cut produce
- Designing and maintaining forced air cooling to avoid contaminating fresh produce
- In most instances, vacuum cooling or use of fans poses the lowest risk of microbial contamination
- Holding cut melons and any other fresh-cut product determined to need temperature control for safety at $\leq 41^{\circ}\text{F}$ ($\leq 5^{\circ}\text{C}$)
- Locating temperature monitoring devices in the warm area of the refrigerator unit (e.g., near the door) and calibrating them on a regular basis
- Inspecting all refrigeration units on a regular basis and keeping them in good operating condition
- Storing similar commodities together (unprocessed product next to unprocessed product and finished product next to finished product) to avoid cross-contamination
- Using an appropriate inventory system to ensure first in first out (FIFO) use and FIFO shipment of raw materials and finished products

2.3 Absorbent Fibers

Absorbent fibers are those, which can allow penetrating water molecules well inside their sites (Mohit Saluja, 2011). Fabrics can absorb water because of their molecular structure; abundance of places made by molecules inside fabrics, tolerate a lot of water to be attracted inside. Different kinds of materials have different

arrangement of molecules, the more spaces among molecules, the more capacity of absorbency the fabrics have. Other fabrics, especially synthetic ones, have fewer places for water molecules to bond to; therefore, even though other fabrics will attract and hold some water, they do not have the capacity to absorb like cotton fibers that have strong absorbent capacity.

Other research studies have tested the cooling performance of a few naturally occurring fibers, for example, coconut fiber, cotton waste and some processed fibers, for example, jute clothing in evaporative cooling. These materials were used as filler material, but for a curtain structure that we wrap some materials onto the scaffold, we need other types of material such as the fabric thread and clothing piece shown in the following figures. Fabric materials are easy to buy, especially the most normal processed fabric in our life or manufacturing, cotton thread, wool thread and linen, which are low cost and convenient to find for people living in rural areas.



Figure 2-4 Woolen thread



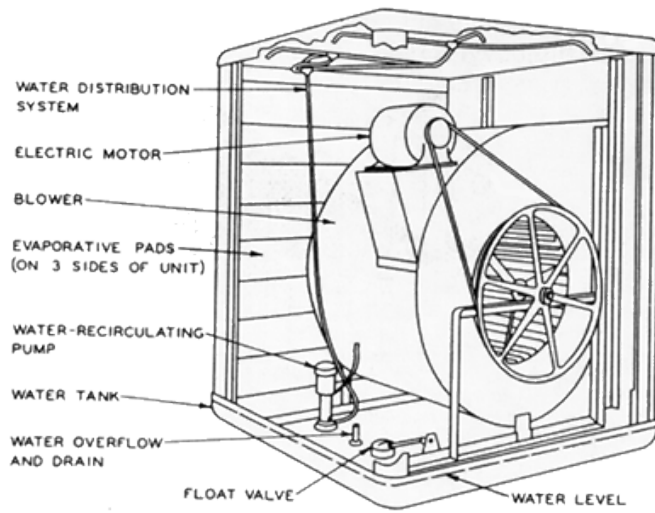
Figure 2-5 Cotton thread



Figure 2-6 Linen piece

2.4 Review of Absorbent-Evaporative Cooler

The typical evaporative cooler (shown in following figure 2-7) consists of eight major parts: container (metal or fiberglass), a blower, circulating water pump, water reservoir, float valve, pads, water distribution lines, and electric motor. In the absorbent-evaporative cooler, we changed the pad structure to fabric curtain; and we integrated a cooling part together with a storage cabinet as shown in figure 2-8:



Typical Wetted-Pad Evaporative Cooler

Figure 2-7 A typical wetted-pad evaporative cooler (“Evaporate Cooling | Heating & Cooling | Alabama Power”)

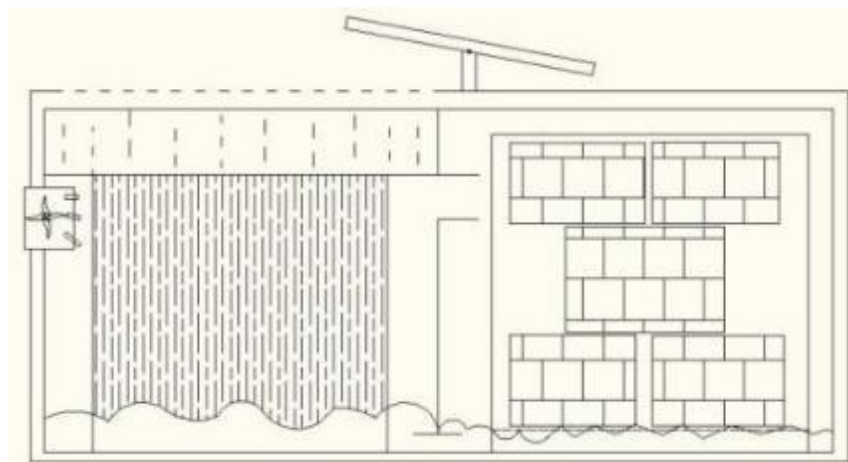


Figure 2-8 General structure sketch

Figure 2-8 shows a cooler construction including two parts: a freezing section on the right and a refrigeration section on the left. The top solar panel supplies electric power when needed. The freezing section is used for frozen food like seafood, meat, and ice cream. The refrigeration section is used for vegetables or other kinds of food that do not need a freezing temperature. We used water evaporation to provide cold air to decrease the temperature inside the two different containers. Air flows through the blower into the refrigeration section; and it will continue to enter into the freezing

section after the refrigeration section cools air.

In the refrigeration section, storage space is separated by scaffolds, which are wrapped by an absorbent fabric material in the style of a vertical curtain. The absorbent material will soak up the water, and the scaffold will be thoroughly wet. The water flow will rise by absorption.

The airflow accelerates evaporation, then increases cooling efficiency. Theoretically, when this cooler is used for transportation, the moving vehicle will bring the airflow into the container. The vehicle will take the place of the blower, which only needs an extra power supply when the cooler is placed in a warehouse.

When airflow goes through the absorbent fabric curtain, it exchanges heat with water, which rises from the bottom of the container. Then vapors evacuate through the sunroof also taking heat out; and the cooled airflow is left around the absorbent material. The cooled airflow will flow into the freezing section through the top valve (shown in figure 2-7), which will lower the temperature around the ice container. This has the effect of extending coolant melt time. The water used for evaporation comes from the melted coolant (e.g. ice), and it flows into the cooling section through the bottom valve.

The inside of freezing section has an ice container. The ice container is used for storing frozen foods, which are packaged in small boxes.

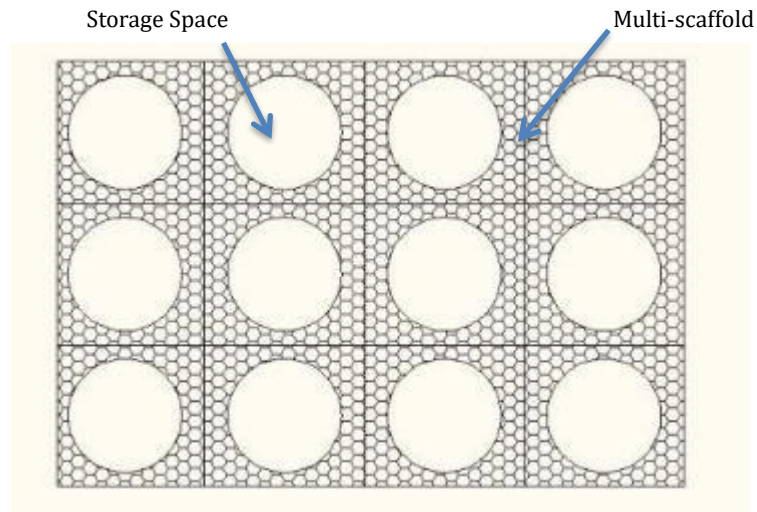


Figure 2-9 Top view of refrigeration section

As you can see from the top of the refrigeration section, as shown in figure 2-9, the shadowed part is the absorbent fabric curtain wrapped on scaffolds. In other words, cotton thread holding absorbed water. The circular part is the storage space used for storing food that does not require freezing temperatures.

2.4.1 The Advantages for The New Design

In developing rural areas, the existing refrigeration technology alternative (e.g. refrigerated truck) has the following major disadvantages:

a) Energy consumption:

Refrigerated trucks are mostly equipped with one of a variety of mechanical refrigeration systems powered by small displacement diesel engines, or utilize carbon dioxide (either as dry ice or in liquid form) as a cooling agent. These kinds of equipment consume a high-volume of fossil fuels and/or electricity. It is reported that about 20% of total energy all over the world is consumed by HVACs (Heat, Ventilation and Air Conditioning systems) (Yuan & Chen, 2012), According to the “Transport Refrigerators Technology Assessment” (Air Resources Board, 2014), the average engine utilization for a truck refrigerator can be as high as 16% of fuels.

b) Environment pollution:

Conventional cooling technologies employing harmful refrigerants usually need more energy, and lead to peak loads, which result in negative effect on the environment (Buker & Riffat, 2015). Since most refrigerated trucks rely on fossil fuels to supply the mechanical cooling equipment, a permanent fixture of the truck, emission of fluorinated gases and carbon dioxide pollute the air.

c) High facility and maintenance cost:

A mechanical cooling system has a much more complicated structure. This structure is too expensive to build and maintain for most people living in developing areas. Another problem with this structure is that the consumer may have to find a skilled technician to fix possibly even a small problem if the refrigeration stops running.

Contrasted with the refrigerated cooler, this new design of the evaporative cooler requires less power and is environment-friendly; it is also easy to construct and maintain.

Table 2-1 Comparison between refrigerated cooler and fiber-based absorbent evaporative cooler

Refrigerated truck	Absorbent-evaporative cooler
Consumes fossil fuel energy	Only solar consumption when stationary
Complicated structure, high facility and maintenance cost	Simple structure, low technical skill and cost, easy to set up
Environment pollution	Environment-friendly

Previous evaporative cooling products used for food storage, such as zero energy cool chambers, were fixed facilities and the main materials used were brick and sand. These kinds of evaporative coolers are fit for fixed storage, but not well suited for moving and transport, and lack flexibility.

The proposed absorbent-evaporative cooler is intended to be a movable container that can be used for both transport and temporary storage in a warehouse. The main

material to be used for the wall of the container will be metal and the scaffold can be made from plastic or other materials. The primary power comes in the form of solar energy used by the blower when the cooler is not moving, otherwise, there is no electricity needed for the cooler when the cooler is moving. There is no chemical emission during the cooling process.

Melted ice usage is very efficient. When the ice melts in the freezing section, in order to avoid heat exchange between water and ice, the proposed absorbent-evaporative cooler takes water from the freezing section into the refrigeration section. This very same water is the source for evaporation. Contrasted with previous evaporated coolers, the absorbent-evaporative cooler does not require adding water manually if the water for evaporation is exhausted.

Absorbent fabric material moves water from the bottom to top by absorption instead of using a pump to raise and lower water (conventional design shown in figure 2-10). Therefore, the fiber-based absorbent evaporative cooling (fbaEC) is different from other traditional evaporative cooling systems.

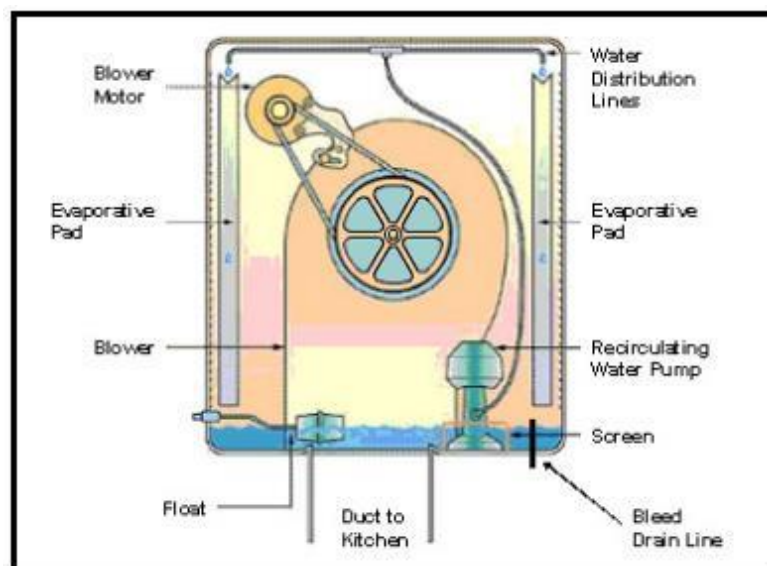


Figure 2-10 Evaporative cooler with a water pump to recirculate water from bottom to top (“Used Evaporative Coolers | Coolers,” 2014)

2.5 Review of The Data Collection Process

The core element in the absorbent-evaporative cooler with fabric curtain is the refrigeration section. The fabric curtain's performance plays a vital role in cooling efficiency. Prior experiments initially focused on testing the fabric curtain's performance in absorbent-evaporative cooling, which did not include the freezing section. Firstly, it tested the feasibility of the cooler with a vertical curtain structure. Then, it tested the performance of three types of fabric materials: (A) wool, (B) cotton, and (C) linen. These materials are relatively inexpensive, easy to find, and reliable. Experiments showed cotton and linen had better cooling performance than wool.

Factors affecting evaporation rate were temperature, wind, exposed surface area and ambient relative humidity. For cooling purpose, we need to eliminate outside heat; so that wind, exposed surface and relative humidity are the only factors we need to consider and use to affect cooler performance.

Lab-scale experiments used a single refrigerated unit scaffold as the test object. We selected two typical ways to wrap that can possibly fulfill the curtain structure besides horizontal wrapping.

Cotton and wool shared the same shape, while linen had its own shape. The three methods of wrapping absorbent materials on scaffold are summarized in the following table:

Table 2-2 Material and wrapping methods

Materials type		Wrapping pattern
Cotton or wool thread	A	Vertical snaking twining
	B	Horizontal snaking twining
Single piece of linen	C	Whole piece wrapping on scaffold

2.5.1 Cooling Efficiency Calculation

The general percentage change from one period to another was calculated from the formula:

$$PR = \frac{(V_{present} - V_{past})}{V_{past}} \times 100\% \quad (1)$$

Where,

PR, Present value;

$V_{present}$, Present value;

V_{past} , Past value.

Based on the above general calculation formulation, to test the performance of fabric curtain, the cooling efficiency was calculated by:

$$\vartheta = [(t_1 - t_{inside}) / t_1] \times 100\% \quad (2)$$

Where,

ϑ , Cooling efficiency inside storage space of evaporative cooler model;

t_1 , Temperature of air flow blown into the container, °C ;

t_{inside} , Temperature inside the storage space, °C ;

And the average cooling efficiency was calculated by:

$$\vartheta_{average} = \left[\frac{(t_1 - \frac{t_2 + t_3}{2})}{t_1} \right] \times 100\% \quad (3)$$

Where,

$\vartheta_{average}$, Average cooling efficiency inside storage space of evaporative cooler model;

t_1 , Temperature of air flow blown into the container, °C ;

t_2 , Temperature inside the storage space at the position closest to the blower, °C ;

t_3 , Temperature inside the storage space at the position furthest from the blower, °C.

Assumptions:

- 1) Since the air blown into the container is from the inside of the lab, t_1 was room temperature;
- 2) We set up t_2 and t_3 at different positions inside of the scaffold; arithmetic mean of t_2 and t_3 represented the temperature inside the storage space.

The maximum cooling efficiency was calculated by:

$$\vartheta_{max} = Max\{\vartheta\} \quad (4)$$

Where,

ϑ_{max} , The maximum cooling efficiency.

The maximum average cooling efficiency can be calculated by:

$$\vartheta_{max(average)} = Max\{\vartheta_{average}\} \quad (5)$$

Where,

$\vartheta_{max(average)}$, The maximum average cooling efficiency.

2.5.2 Experiment Environment

To control certain elements, we conducted this experiment inside the laboratory. These elements included not allowing direct sunshine inside the lab, and closing the windows. The only power supply used was electricity to simulate the moving environment. Electricity powered the blower allowing airflow into the container.

2.5.3 Experiment Equipment Information

2.5.3.1 Scaffold:

This refrigerated storage frame unit, referred to as scaffold, is prototyped along

with the initial idea shown in figure 2-8, is made of plastic. We assume food will be stored inside the scaffold in practice. In this experiment, we manufactured scaffold using a rapid prototyping machine with dimensions 210mm high \times 55mm radius. The left drawing was finished using SolidWorks 2011, in which three circles and six columns make up the scaffold.

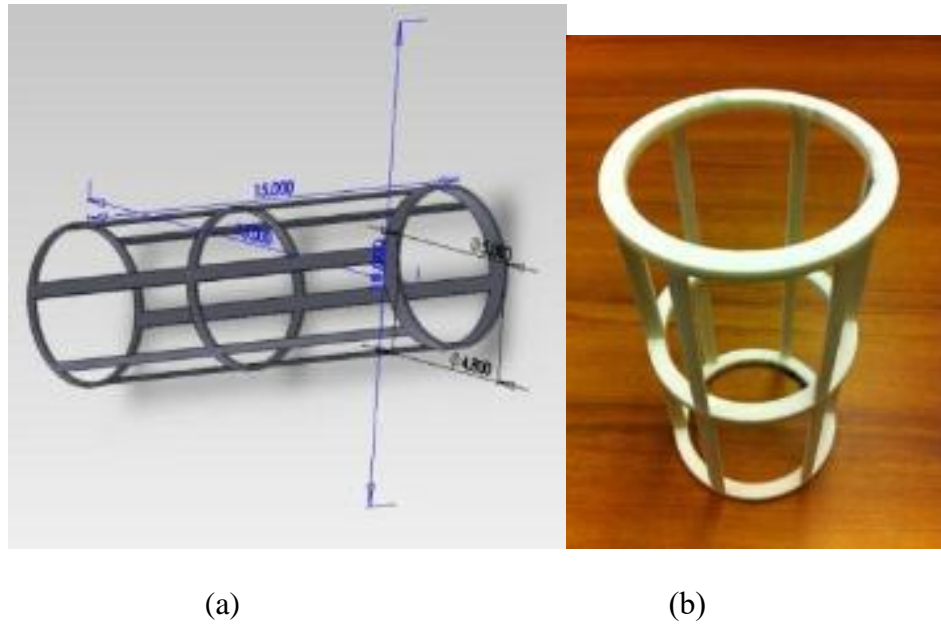


Figure 2-11 (a) Solidworks drawing and (b) product of single scaffold unit.

2.5.3.2 Crystal Container (Water Tank) With Cover:

The left image in figure 2-12 shows the water tank with cover drawing in SolidWorks 2011, and right image shows the actual product made, which is made of plastic; there are sinks on the cover and an opening fit for the blower on one side. The water container is sealed and is transparent so that we can observe the change of water level and material wrapping on the scaffold:

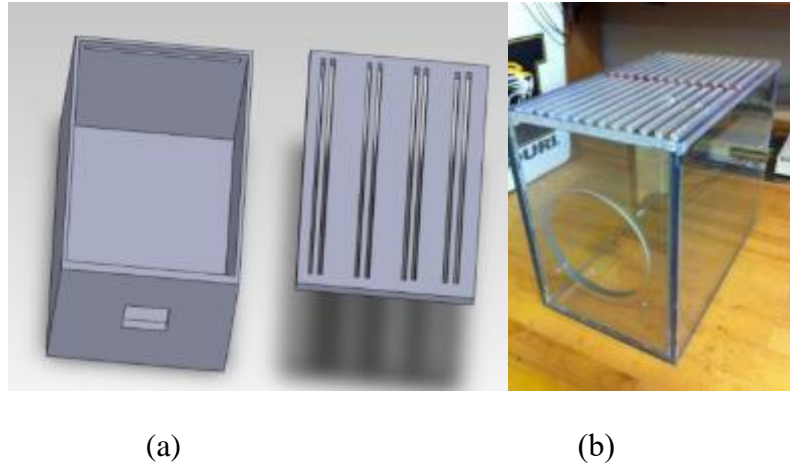


Figure 2-12 (a) Solidworks drawing and (b) product of container (water tank)

2.5.3.3 Absorbent Material:

Absorbent materials are considered to be ideal materials due to their abundance and low cost (William Adebisi Olosunde et al., 2009). The chosen absorbent materials were wool, cotton, and linen (a type of weave made of cotton).

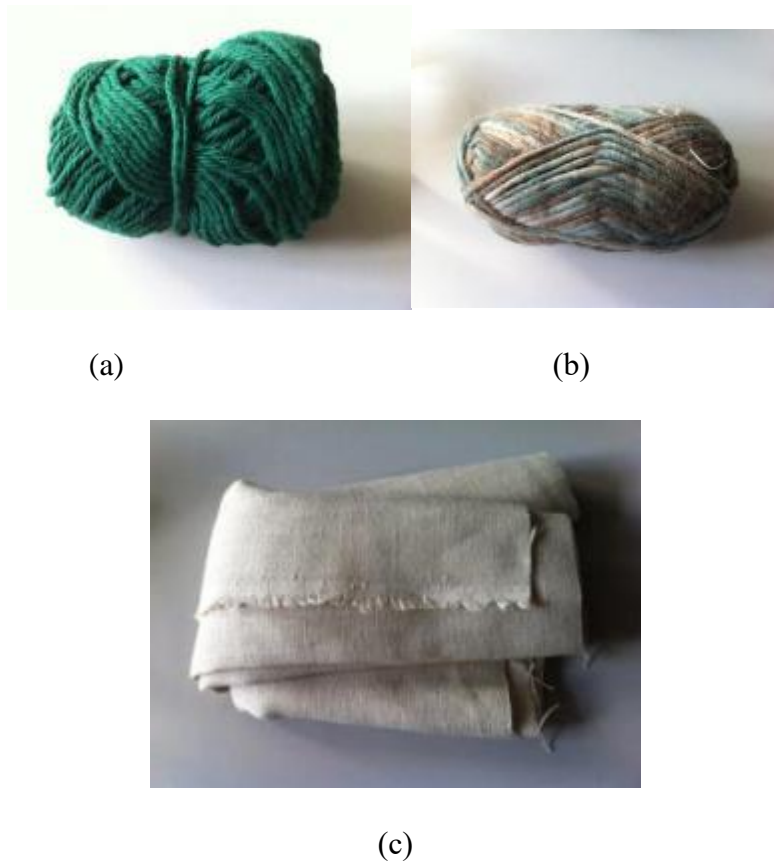


Figure 2-13 (a) Cotton threads, (b) woolen threads, and (c) linen piece (a type of weave made of cotton)

2.5.3.4 AC Cooling Fan



Figure 2-14 5V / 12V AC Cooling Fan

The 5V / 12V AC cooling fan has the dimension of 120mm x 25mm (4.72 X 0.98 Inch).

2.5.3.5 TK Thermocouple Input Type K Module



Figure 2-15 Thermocouples

Fluke 80 TK Thermocouple Input Type K Module was used to convert millivolts to TC voltage to measure temperature unit with temperature range: -50°C to 1000°C .

2.5.3.6 Humidity Sensors



Figure 2-16 Moisture sensor

HIH-5030/5031 Series covered filtered integrated circuit humidity sensor has detection range from 0 to 100%.

2.5.3.7 Data Acquisition Program

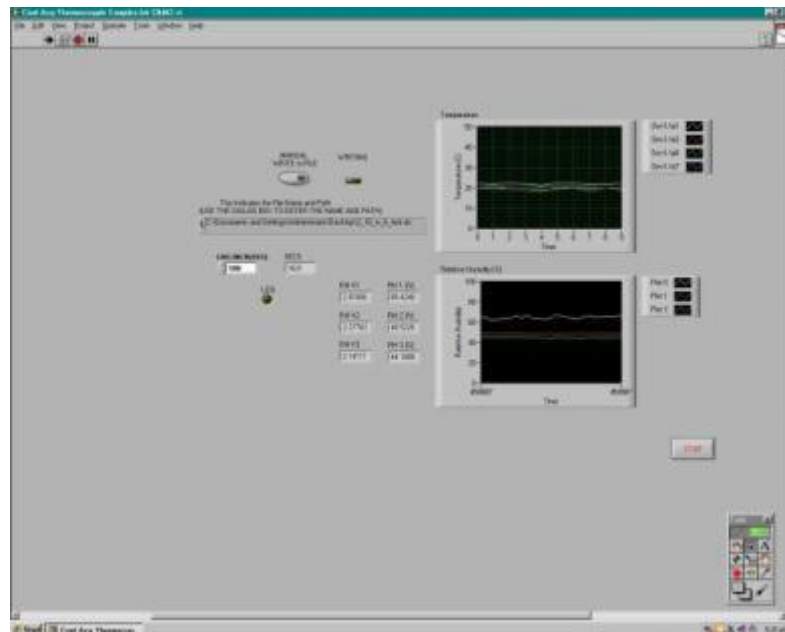


Figure 2-17 Data acquisition program

Lab View 8.6 program was used to create the program that can measure temperature and relative humidity, record time, temperature and relative humidity into a spreadsheet file in data logger fashion.

2.5.3.8 SCB-68 Shielded I/O Connector Block

A shielded I/O connector block for DAQ devices with built in Cold Junction Compensation (CJC) sensor and 68-pin Connectors was used to connect the DAQ device to thermocouples via conductor cable with accuracy of $\pm 1^{\circ}\text{C}$.

We connected four thermocouples and three moisture sensors with input section of connector and also connected output section with computer program:



Figure 2-18 I/O connector

2.5.4 Experiment Procedures

2.5.4.1 Water Preparation.



Figure 2-19 600 ml water in a plastic bottle

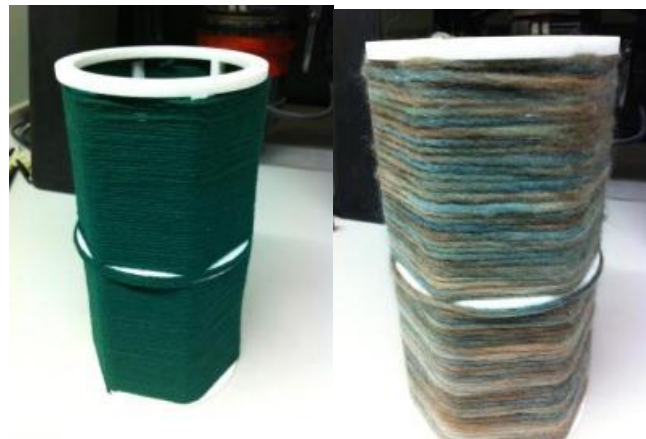
Have 600 ml water in a plastic bottle sat in room temperature before each case of experiments conducted.

2.5.4.2 Fabric Fibers Wrapping



(a) (b)

Figure 2-20 (a) Wrapping cotton thread and (b) wool thread onto scaffold vertically



(a) (b)



(c)

Figure 2-21 (a) Wrapping cotton thread, (b) wool thread onto scaffold horizontally, and (c) linen piece wrapping around scaffold

In this step, fiber materials were rapped onto the scaffold as designated way shown

in above figures.

2.5.4.3 Sensors Installation

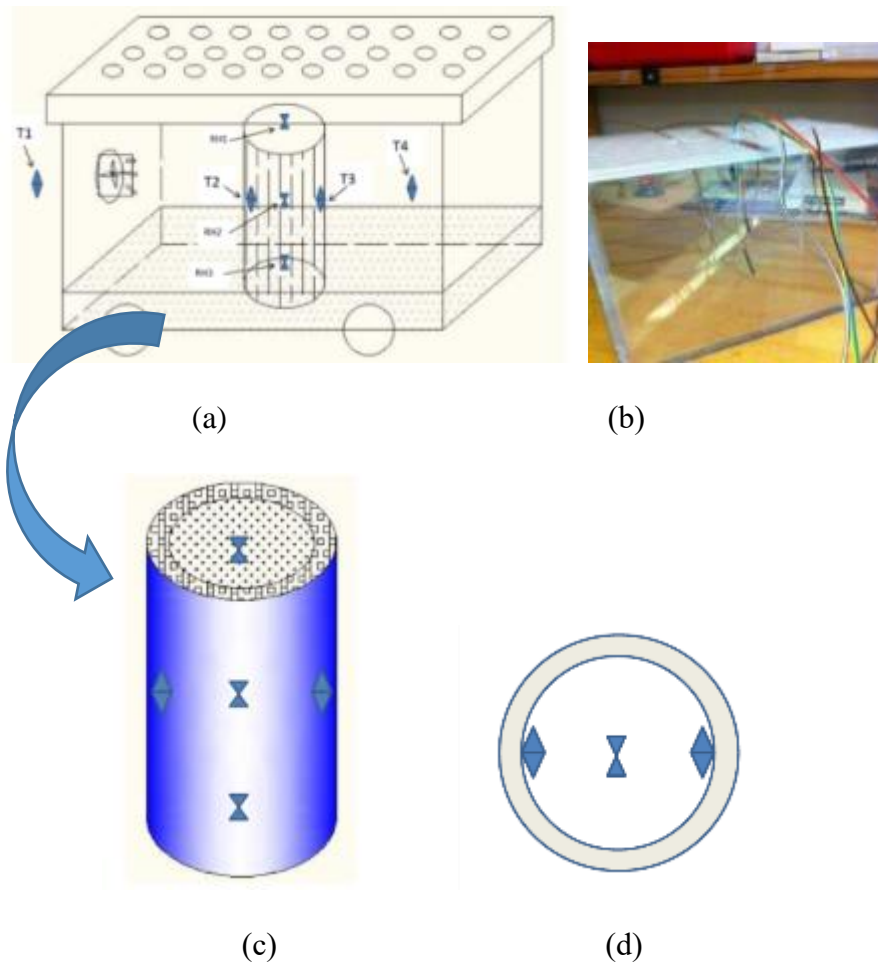


Figure 2-22 (a) Drawing of prescribed position; (b) sensors at diagnostic position; (c) front view of prescribed position model; (d) top view of prescribed position model

Lay thermocouples and moisture sensors at prescribed positions shown in above figure; connect the thermocouples and moisture sensors with the central connector, which is imported into the computer program

2.5.4.4 Scaffold Layout



Figure 2-23 Scaffold with cotton threads in container

After the sensors were set, lay scaffold into the transparent water container, make sure the sensors were at the right positions.

2.5.4.5 Water Injection



Figure 2-24 Pour water into container while the scaffold stands inside the water container

Pour the prepared 600ml water into container, make sure the fibers attached with the scaffold soak in the water, and then take the cover immediately to start the data collection soon.

2.5.4.6 Data Collection.

Run fan and data acquisition program then record temperature and moisture change. The testing duration for each group was 200 minutes, recording data every three minutes. We run three replications of experiment, each replication has eighteen cases;

the interval between two adjacent cases is 5 hours, we dry and change material during these 5 hours; the interval between two replications is 24 hours; all case contents are summarized in the following table:

Table 2-3 Case content

Case#	Material	Wrapping method	Blowing power (Volt)
1	Cotton threads	Vertical snaking twining	0
2	Cotton threads	Horizontal snaking twining	0
3	Woolen threads	Vertical snaking twining	0
4	Woolen threads	Horizontal snaking twining	0
5	Linen piece	Whole piece wrapping on frame	0
6	Cotton threads	Vertical snaking twining	5
7	Cotton threads	Horizontal snaking twining	5
8	Woolen threads	Vertical snaking twining	5
9	Woolen threads	Horizontal snaking twining	5
10	Linen piece	Whole piece wrapping on frame	5
11	Cotton threads	Vertical snaking twining	12
12	Cotton threads	Horizontal snaking twining	12
13	Woolen threads	Vertical snaking twining	12
14	Woolen threads	Horizontal snaking twining	12
15	Linen piece	Whole piece wrapping on frame	12
16	Only water	None	0
17	Only water	None	5
18	Only water	None	12

2.5.4.7 Water Consumption Measurement



Figure 2-25 Measuring water level change

Poured water from container to storage bottle and measure the changes of water level. Finally, cleaned and dried water container and fibers wrapped on the scaffold after the program is finished. Make sure water container and the fibers wrapped on the scaffold are completely dry before running the next case.

2.6 Prior Experiments Result

The experiment results showed the fiber-based evaporative cooler had significant cooling effect. Comparing with the ZECC's recoded lowest temperature that was 17.1°C while the environment temperature was 25°C (M.P. Islam & Morimoto, 2011), the lowest temperature during the whole experiment was 8.61°C while the environment temperature was 22.9°C. Also in same case, the average temperature during steady state is around 10 °C that is within the ideal storage temperature scale of 0°C to 15°C (Hardenburg, Robert E., Chien Yi Wang, & Alley E. Watada, 1989) for most of the fruits and vegetables. This temperature range is estimated to extend the shelf life of fruits and vegetables by 5-15 days. The cooling effect could maintain this low temperature as long as there is sufficient water supply. Different materials and wrapping methods have different effects on cooling performance, as well as the air flow speed and relative humidity. The two best combinations of material and wrapping method in terms of cooling efficiency were cotton threads in vertical wrapping way and whole linen piece wrapping.

The significant cooling performance of the new single-scaffold structure fiber-based evaporative cooler in the laboratory built a promising base for a deeper study on the heat and mass transfer during the cooling process, which can help understand the cooling phenomena for the design, and may provide insights to improve the cooler structure. In addition, we are motivated to explore the cooling performance of a multi-scaffold structure, as well as their use in a moving transport application.

CHAPTER 3

METHODOLOGY DEVELOPMENT

In prior research, a new fiber-based absorbent evaporative cooling (fbaEC) system model using absorbent fabric fiber wrapping in curtain structure on scaffolding for short-term transport and storage was built in laboratory scale, and a series of laboratory scale experiments were designed and conducted to statistically verify the basic concept of the new model. Through experiments, three kinds of absorbent fabric materials in common use were applied based on their water absorbent characteristic to decrease temperature and then to increase humidity, which contributes to keeping food and other products that require low temperature and high humidity to stay fresh longer.

The lowest temperature created through experiment was 8°C when the environment temperature was 22°C, the average temperature during stable stage is around 10°C that could last as long as there is sufficient water supply; while the lowest temperature through experiments on zero energy cool chamber conducted by other researchers was 17.1°C while the environment temperature was 25°C; the fbaEC had a significant better cooling result. In the future, once the cooler is used for transport, we propose it can achieve zero energy consumption of electricity, which is a potential advantage. Comparing with the existing evaporative cooling design, fbaEC does not need extra power source to conduct water from tank to convection plane which is a vertical layout, and this configuration achieves energy savings, and is reliable since the water can be moved up continuously through fibers' suction as long as there is water supply.

The following potential steps are proposed for this research.

Step 1: Build a heat and mass transfer mathematical model for a single-scaffold structure followed by the validation;

Step 2: Design and conduct the experiments on testing the fbaEC in a real transport environment followed by the statistics analysis;

Step 3: Build a heat transfer mathematical model for multi-scaffold structure.

3.1 Heat Transfer Mathematical Model On Single-Scaffold Structure

An in-depth analysis of the fiber-based absorbent evaporative cooling (fbaEC) is needed for further development of the model. In order to properly apply fbaEC for practical usage, we need to understand its thermodynamic, flow, and heat transfer properties (Lie, Su, Lai, & Lin, 2006). Convection is the main form of heat transfer to enable the phase change between water and vapors, so that heat can be moved from the warm air around the curtain to the vapors. Taking ZECC as an example, the water molecules in the filler between the brick walls evaporate under the influence of the outside unsaturated air through a cooling process that uses the latent energy of evaporation required for a changing the physical state from liquid to vapor. During this process, the heat required for the water evaporation process is removed from the water, the filler and the brick walls creating a temperature in the inner wall of the ZECC that is lower than the dry-bulb temperature (M. Islam, Morimoto, & Hatou, 2013). When evaporation heat transfer is considered, the experimental measurement and prediction of the heat transfer coefficients are two major aspects of research (Zhang, Zhang, Chen, & Yuan, 2008). A good model can help design and predict the performance of the cooler. Researchers have developed several heat and mass transfer models for different types of evaporative cooler design. Exhaustive studies have been carried on different configurations of spray air interaction, which is the main method of current evaporative cooler design. Most of the studies were initiated from the equation for convection, also known as Newton's Law of Cooling that can be expressed as

$$q = h_c A dT$$

where

q = heat transferred per unit time (Watts)

A = heat transfer area of the surface (m^2)

h_c = convective heat transfer coefficient of the process ($W/(m^2K)$ or $W/(m^2°C)$)

dT = temperature difference between the surface and the bulk fluid (K or °C)

Fiber-based absorbent evaporative cooling (fbaEC) derives a new structure with the vertical fiber curtain, which converts the convection plate from a horizontal direction to a vertical direction, thus the convection heat transfer equation cannot be directly used. Since there is no global model to cover all evaporative cooling design regardless of structure variety, and considering the uniqueness of the fbaEC structure, we need to transform the basic convection heat transfer equation to adjust for the vertical curtain structure convection situation. To achieve this, following steps need to be followed:

Step 1. Define the heat transfer process

A different heat transfer process requires a different heat transfer model; to accurately define the heat transfer process is the most basis step for the heat transfer study. In this step, we need to know: firstly, what is the initial nature of the heat transfer process; secondly, what is the path of airflow; thirdly, how does the airflow exchange heat with water; finally, how to achieve the cooling inside the scaffold (storage space).

Step 2. Make assumptions and build model frame based on cooling process

Once we define the heat transfer process, it is necessary to make assumptions for heat transfer study based on the first step: firstly, we assume the airflow is made of pure dry air; secondly, we assume the airflow velocity is constant. Then we need to determine the general model frame so that we can generate the equation to express the cooling process.

Step 3. Identify the detailed heat exchange scenario

The detailed heat exchange scenarios determine the derivation methods and value of factors in the general equation. For example, the situation of force convection on a flat plate and the situation of force convection on a cylinder have different heat transfer coefficients; and the situation of force convection on a vertical flat plate and the situation of force convection on a horizontal flat plate also have different heat transfer coefficient derivation methods. For a fiber-based curtain structure, we need to: firstly, determine the curtain structure character; secondly, use air meter measure and determine if there is significant airflow passing through the curtain and getting inside of the scaffold (storage space); thirdly, based on above two conditions, determine and find the proper methodology to derive the model elements.

Step 4. Derive each factor to complete the model

Once we identified the detailed heat exchange scenario, based on a general model equation, we can target the proper methods to derive each factor in the equation.

In the initial model assumption, only the heat transfer coefficient is estimated, and is the most important unknown factor that needs to be calculated through experiments that give the results of temperature and relative humidity. Empirical model and values have been determined by former research, e.g. “Transport Phenomena in Multiphase System” (Faghri & Zhang, 2006) summarized various methods to conduct the heat transfer coefficient. Combining other factors of airflow speed and convection plate area, etc., the empirical value of the heat transfer coefficient can be found, and then the heat transfer model will be completed.

In this study, the cotton and linen have been tested as the two best materials of all three materials that had been tested, and have most significant cooling effect. The heat

transfer coefficients of the two materials will be derived individually, and these coefficients will be validated for robustness.

3.2 Mass Transfer Mathematical Model On Single-Scaffold Cooling Structure

For this study, the heat transfer model becomes the basis for the mass transfer model. During the cooling process, the sensible heat from airflow transfers to the latent heat of water. According to the fbaEC design, vapors release the heat into the atmosphere, thereby cooling the inside of the scaffold, and water supplies endurance of the cooling effect. The energy balance can derive the mass transfer model, in which one of the most factors we want to know about is the amount of mass change.

The general model equation of mass transfer is the following:

$$q = mh_{lv}$$

In which, the q is the total heat of mass transfer, the m is the amount of water transferred, the h_{lv} is the latent heat transfer coefficient. The amount of water transferred can be calculated if we know the total heat of mass transfer and the latent heat transfer coefficient. The value of latent heat transfer coefficient can be found in empirical tables, and the heat transfer model will indicate the total heat of mass transfer.

Based on the product requirement, and through the mass transfer model, it will be useful to find the necessary water amount within certain conditions, e.g. the temperature change requirement, etc. Once we know the water amount that supports the required cooling, we can ensure the correct supply and avoid water waste.

In this part, the data collected from prior experiments will be applied to validate the mass transfer model. We will compare the measurement amount of water during the experiments and the theoretical amount of water determined through mass transfer calculation.

3.3 Experiments On Testing the fbaEC in Real Transport Environment

The initial design of the fiber-based absorbent evaporative cooler (fbaEC) is ultimately for transporting the products that need cooling like fruits and vegetables in the safe temperature range of 0-15°C. To validate the cooling performance in a realistic moving environment, a set of experiments for testing the cooling performance initially started to test single-scaffold structure, needs to be designed and conducted. Similar to the prior experiments on single-scaffold structure, the experiment equipment, case contents, experiment procedure and data collection process will be described.

3.3.1 Experiment Purpose and Cooling Efficiency Calculation

The new set of experiments will measure the cooling efficiency and performance of fbaEC in a realistic transport mode for single scaffold. In this new set of experiments, we still use the same methodology from the prior experiments to calculate the evaporative cooling efficiency. The detailed equations were shown in section 2.6.1.

3.3.2 Experimental Environment and Assumptions

The core difference between this new set of experiments and prior experiments is the experimental environment. For this new set of experiments, we move the equipment from inside the laboratory to the outdoors. All measurement and testing are based on cooling performance in a natural environment. We make following assumptions:

- 1) Compared with the assumptions of prior experiments, the airflow inlet temperature is environment temperature that is natural outdoor weather temperature.
- 2) We still set up t_2 and t_3 at different positions inside of the scaffold; arithmetic means of t_2 and t_3 still represents the temperature inside the storage space.

3.3.3 Experimental Equipment

- 1) Scaffold

We will use the same scaffolds for this set of experiments; the detailed dimensions and materials for making the scaffold were shown in section 2.6.3.

2) Transparent container

We still use the same transparent water tank that was used in the prior experiments to simulate the truck container, the details of water tank dimensions and design drawings were shown in section 2.6.3.

3) Fabric fibers

In prior experiments, we tested three kinds of fabric materials, cotton threads, woolen threads, and linen piece. The results showed cotton thread and linen piece had best cooling performance. In this set of experiments, we will test the cotton threads to validate the fbaEC in a realistic transport environment.

4) Sensors

We will use same thermal sensors and relative humidity sensors with prior experiments, to measure the change of temperature and relative humidity during experiments.

5) Data collection system

The data acquisition program (DAP) was shown in section 2.6.3; and Shielded I/O Connector Block for DAP devices with built in Cold Junction Compensation (CJC) sensor and 68-pin connectors were used to connect the DAP device to thermocouples via conductor cable with accuracy: $\pm 1^{\circ}\text{C}$. We also connected four thermocouples and three moisture sensors with input section of connector and also connected output section with a laptop program.

6) Vehicle

We will set the water container with the scaffold, sensors on a car roof; the laptop with DAP and I/O connector will be set up inside of the vehicle to run the data collection system while simulating the truck cargo moving environment.

3.3.4 Experiment Procedure

- 1) Allow exact amount of water to sit at environment temperature.
- 2) Wrapped cotton threads onto the single scaffold in prescribed patterns.
- 3) Set up the scaffold into container; tie the scaffold with the edge of container to make sure the scaffold will not fall during testing.
- 4) Set up the sensors at prescribed positions; connect the sensors with the data collection box that is also needs to be connected with laptop shown in following picture:



Figure 3-1 Data Acquisition System Connected with Sensors and Laptop and Sensor T1 position.

Sensor T1 measures the environment temperature (shown in above figure), sensors T2 and T3 measure the temperature inside scaffold, sensor T4 measures the temperature inside of water container but outside scaffold.

- 5) Set up whole container onto the vehicle roof and tie the container with the roof rack as shown in the following figure to make sure it will not move while driving.



Figure 3-2 Cooler Set Up on Vehicle

6) Pour water into bottom of container; set up the cover of container and tape it with the container so that it will not move or slide during driving.

7) Start to drive and run the DAP then record temperature and moisture change. All cases were driven on the same road path. Testing duration for each case was 30 minutes, recording data every three minutes. We ran three replications of the experiment. Each replication had 4 cases; all case contents are summarized in the following table:

Table 3-1 Experiment case content

Case #	Material	Wrapping method	Average Vehicle Speed
1	Cotton threads	Vertical snaking twining	0 mph
2	Cotton threads	Vertical snaking twining	15 mph
3	Cotton threads	Vertical snaking twining	30 mph
4	Cotton threads	Vertical snaking twining	45 mph

8) After each case was completed, pour remaining water to storage bottle and measure the change of water level.

The key point for the new experiments is to setup the container with scaffold(s) on the vehicle, then measure the temperature and relative humidity during the moving process. The experiments for testing the cooling performance in a realistic transport environment will provide a better understanding of the attributes of the fbaEC design.

3.3.5 Experiment Results Analysis

Once the experimental data are collected, the statistical analysis will be conducted to compare the experiment results to prior research that was conducted in the laboratory.

Furthermore, the basic statistical analysis will demonstrate the cooling effect for the alternative hypothesis that H1: there is not significant temperature difference between the inside and outside of scaffolds while there is water added into the water container.

Then the linear correlation analysis will further explore the relation among variables through the alternative hypothesis that H1: there are significant linear relationships among the cooling efficiency (maximum average cooling efficiency, maximum cooling efficiency, maximum average temperature difference and maximum temperature difference) and the speed, environment temperature, environment relative humidity.

In addition, sensitivity analysis will be conducted to help understand the influence of factors of speed and environment relative humidity on the cooling performance.

3.4 Heat and Mass Transfer Mathematical Model On Multi-Scaffold Structure

The fiber-based absorbent evaporative cooler (fbaEC) was initially tested with only one scaffold. Since it has been theoretically verified with both laboratory scale and real transport environment, we can extend our study to a multi-scaffold structure. In this study, to achieve the heat and mass transfer model for a multi-scaffold structure, similarly, we will use the following steps:

Step 1. Determine the multi-scaffold layout.

The heat and mass transfer configuration can be very different from a single-scaffold structure, as the layout of a multi-scaffold structure is much more complicated than a single-scaffolds structure. A multi-scaffold heat transfer model cannot be derived from a single scaffold structure by simple scaling. For example, the total cooling ability

of a three-scaffold cooler is not just three times of the cooling ability of a single-scaffold cooler. Even for the same number of scaffolds, different layout scenarios also derive different models, and the cooling performance could also be different. The reason is when the airflow passes through three scaffolds in line, for example, the velocity decreases nonlinearly along the path. Based on the initial design shown in figure 2-9, the scaffolds were initially layout in an aligned direction.

Step 2. Build the general heat and mass transfer model equation.

Based on an aligned multi-scaffold layout, we need to generate the general model equation to express the heat and mass transfer process according to: firstly, what is the airflow path; secondly, how does airflow exchange heat with water; finally, find out if there is any difference in heat and mass transfer pattern between each scaffold.

Step 3. Derive each factor to complete the model.

Once we targeted the general frame model of heat and mass transfer for aligned multi-scaffold layout structure, we can develop the methodology to derive the detailed factors according to the different scenarios, e.g. with respect to airflow velocity.

In this study, we will build a base to develop two models, for cotton threads and linen piece individually in future, with the difference in materials represented in the model.

3.5 Summary

A comprehensive in-depth analysis of the fiber-based absorbent evaporative cooler (fbaEC) can provide a useful tool to predict the minimum amount of water consumption during cooling, which offers a solid foundation for future development, particularly for the structure improvement that can lead to a better temperature decreasing. If we do not understand the logic behind the effects, there will not be sufficient background to derive future improvements.

The experiment testing the cooling performance of fbaEC in real transport environment is the extension of prior experiment in laboratory, which has more factors that can potentially have effect on the cooling efficiency. The experiments can practically validate the cooling performance when the cooler is used for short-term transportation, and further generate the support to promote this study to the future steps.

CHAPTER 4

HEAT AND MASS TRANSFER MATHEMATICAL MODEL FOR A SINGLE-SCAFFOLD STRUCTURE OF FIBER-BASED ABSORBENT EVAPORATIVE COOLER

Based on the dissertation objective and outline, this chapter presents the result of the heat and mass transfer mathematical model for a single-scaffold structure of a fiber-based absorbent evaporative cooler. The mass transfer model will follow the heat transfer model, and the validation will be at the end of this chapter.

Nomenclature			
v	Airflow speed, v=a or b m/s	Pr	Prandtl number, the ratio of momentum diffusivity to thermal diffusivity
H	Height of scaffold, m	Re	Reynold's number, the ratio of momentum forces to viscous forces and consequently quantifies the relative importance of these two types of forces for given flow conditions.
D	Diameter of scaffold, m	k	Conductivity
x	Travel distance of airflow, m	Nu_x	Nusselt Number, the ratio of convective to conductive heat transfer across the boundary.
α	Thermal diffusivity	h	Heat transfer coefficient
T_i	Temperature at each position, °C, $i = 1,2,3,4$	h_{lv}	Specific latent heat for water
t	Time, s	q	Amount of heat transferred (Heat Flux)
γ	Kinematic viscosity	m	Mass of water, g
θ	Correction coefficient	\dot{m}	Mass transfer of water per unit, g/s

4.1 Heat Transfer

Forced convection is the main driving force of heat transfer to enable the phase change between water and vapors, so that heat can be moved from the warm air around the curtain to the vapors.

Through a heat exchange process, the airflow exchanges heat with the water attached to the fibers and the water inside the scaffold. The airflow loses heat by dropping temperature, which is sensible heat; meanwhile, water gains heat by the phase changing from liquid to vapor, which is latent heat. Since the latent heat that air loses and the sensible heat that water gains are significantly negligible, we assume that the

sensible heat from airflow equals the latent heat of evaporation. This balance can be described as follows:

$$q = mh_{lv} = hc A dT$$

Where,

q = heat transferred per unit time (Watts)

m = the amount of water transferred

h_{lv} = the latent heat transfer coefficient

A = heat transfer area of the surface (m^2)

h_c = convective heat transfer coefficient of the process ($W/(m^2K)$ or $W/(m^2°C)$)

dT = temperature difference between the surface and the bulk fluid (K or °C)

Kachhwaha & Prabhakar (2009) researched heat and mass transfer study for a direct evaporative cooler. The structure of the cooler is water-spray based, the airflow exchanges heat directly with the cooling pad. Their study is based on the wet bulb temperature change, the number of mass transfer unit (NTU) is given by:

$$NTU = \frac{h \times A}{m_a \times C_{pa}}$$

where h is the heat transfer coefficient; A is the surface area of cooling pad; m_a is the mass flow rate of dry air; C_{pa} is heat capacity rates; the correlation presented for heat transfer is given as:

$$Nu = \gamma \times (Re^{0.8}) \times (Pr^{0.33})$$

In 2003, Camargo and Ebinuma et al. (2003) developed another mathematical model for direct evaporative cooling air condition system based on water dripping structure. In the study of the psychometric process, dry air is considered as a single gas characterized by an average molecular mass equal to 28.9645 (Camargo, Ebinuma, & Cardoso, 2003). The elementary sensible heat is:

$$\delta Q_s = h_c dA(T_s - T)$$

Where h_c is the convective heat transfer coefficient, A is the area of heat transfer surface, T_s is the water surface temperature and T is bulk temperature. The h_c coefficient is determined from the Nusselt number (Nu) expressed as a function of the Reynolds number (Re) and Prandtl number (Pr) shown as following:

$$Nu = 0.10 \times \left(\frac{l_e}{l}\right)^{0.12} Re^{0.8} Pr^{1/3}$$

Where l_e is the characteristic length and l is the pad thickness.

The proposed fbaEC derives a new column scaffold structure with vertical fiber curtain, through which the airflow can blow through the column. The new structure converts the convection interface from single solid horizontal or vertical plate to semi-penetrated column with water inside, thus cannot directly use convection heat transfer equation. Since there is no global model to cover all evaporative cooling design regardless structure variety, and considering the uniqueness of the fbaEC structure, we need to transform the basic convection heat transfer equation to adjust the vertical convection situation. In the initial model assumption, the heat transfer coefficient is estimated to be the main unknown factor that needs to be calculated through experiments, which give the results of temperature and relative humidity. Combining other factors of airflow speed and convection plate area, etc. the empirical value of heat transfer coefficient can be found, and then the heat transfer model will be completed. Finally, the amount of water that needs to be used for evaporation can be optimized.

In this study, the methodology will initially focus on the heat and mass transfer in an experiment that uses only one scaffold as simulated storage space. The airflow path derives the heat and mass transfer model based on if the airflow can pass through the scaffold: 1) if the airflow significantly passes the curtain, exchanges heat inside the scaffold, then the whole cooling process needs to be considered as flow blowing

through a porous medium shell; 2) if the airflow does not significantly pass the curtain, which means the airflow velocity can be negligible, then the cooling process is the flow blowing through a cylinder. An air meter is used to measure the speed of air flow pass through the scaffold and the speed of air flow enters into the water container, which corresponding to the blowing power in the prior laboratory experiment. The maximum air flow speed inside the scaffold is less than 0.01 m/s which can be negligible.

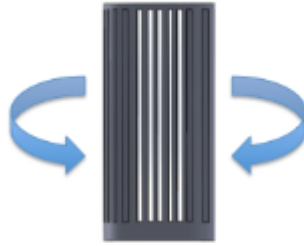


Figure 4-1 Airflow blow around the scaffold's surface

The main part where the heat exchange happens is when airflow blows the surface of scaffolds, the air exchanges heat with the water attached on the fiber curtain. For this part, we assume the scaffold is a unit shape of a circular cylinder, and according to the convective heat transfer coefficients for heat and mass transfer mode and geometry of flowing across a circular cylinder (Faghri & Zhang, 2006), the transfer coefficient can be expressed by the following:

$$h = \frac{Nu_x k}{x} \quad (1)$$

In which, the Nusselt number for the situation of flow across a circular cylinder can be expressed as following, as the air flow blowing across the scaffold:

$$\overline{Nu} = 0.3 + \frac{0.62 Re^{1/2} Pr^{1/3}}{[1 + (0.4/Pr)^{2/3}]^{1/4}} \times [1 + (Re/282000)^{5/8}]^{4/5} \quad (2)$$

The Reynolds number is defined by the airflow speed, scaffold's diameter and air dynamic viscosity as following:

$$Re = \frac{aD}{\gamma} \quad (3)$$

The Prandtl number is defined by the air dynamic viscosity and air thermal diffusivity as following:

$$Pr = \frac{\gamma}{\alpha} \quad (4)$$

From equation (1), (2), (3) and (4), following equation can be obtained:

$$\bar{h} = \frac{\overline{Nuk}}{D} = 0.3D^{-1} + \left\{ \frac{0.62\left(\frac{aD}{\gamma}\right)^{1/2}\left(\frac{\gamma}{\alpha}\right)^{1/3}}{\left[1+\left(\frac{0.4\alpha}{\gamma}\right)^{2/3}\right]^{1/4}} \times \left[1 + \left(\frac{aD}{282000\gamma}\right)^{5/8}\right]^{4/5} \right\} kD^{-1} \quad (5)$$

For the fiber-based absorbent evaporative cooler, we define θ as correction coefficient due to the reason that during experiments, it is not necessary the whole scaffold would be soaked by water; the correction coefficient could also represent the partial area of convection surface. Then the heat transfer coefficient for the single-scaffold structure cooler can be expressed as following:

$$h = \theta \bar{h} \quad (6)$$

4.2 Mass Transfer

Once the heat transfer coefficients are found, mass transfer can be processed by following principle:

$$q = hA\Delta T = \dot{m}h_{lv} \quad (7)$$

As the evaporation process includes two stages:

a. Transition stage

This stage starts at the beginning of evaporation; the temperature starts to drop non-linearly from the room temperature until the temperature becomes relatively stable. In this stage, the evaporation process is divided into many finite micro intervals, for each interval, the initial temperature T_{in} is room temperature and the end temperature T_{out} is the temperature by the end of the interval. Then each micro interval is considered as steady stage i.

Based on equation (7), the surface area of scaffold is:

$$A = \pi DH \quad (8)$$

The temperature change can be defined as following:

$$\Delta T_{transfer} = |T_{out} - T_{in}| \quad (9)$$

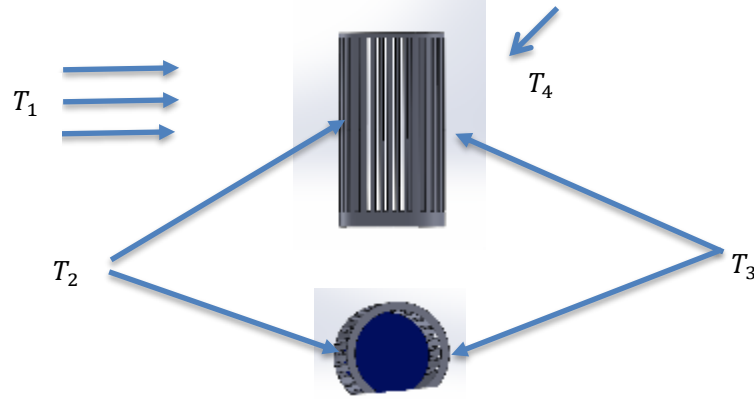


Figure 4-2 The sectional view and top view of the positions of T_2 and T_3

Specifically, for the evaporation that happens on the surface of scaffold, the temperature change is defined as the difference between the room temperature T_1 and outlet temperature T_3 (Shown in above figure 4-2) as following:

$$\Delta T_{transfer} = |T_3 - T_1| \quad (10)$$

From equation (7), (8), (9) and (10), the mass transfer of water can be obtained by the following:

$$m_{i,transfer} = \frac{q}{h_{lv}} = \frac{hA\Delta T}{h_{lv}} = \frac{hA(T_3 - T_1)}{h_{lv}} \quad (11)$$

The mass of water in transition stage can be expressed by the following:

$$m_{transfer} = \sum_{i=1}^n m_{i,transfer} dt \quad (12)$$

b. Steady Stage

This stage starts once the temperature stay in relative stable range, and it will last for a long time, as long as the water supply is sufficient and the environment condition stays the same. As the temperature amplitude is assumed negligible, the temperature change can be defined as the difference in steady temperatures as following:

$$\Delta T_{steady} = |T_{3,steady} - T_1| \quad (16)$$

Similar with equation 14, the mass transfer of water in steady stage can be expressed by following:

$$m_{steady} = \frac{q}{h_{lv}} = \frac{hA\Delta T}{h_{lv}} = \frac{hA\Delta T(|T_{3,steady} - T_1|)}{h_{lv}} \quad (17)$$

And the amount of mass of water in steady stage can be expressed by the following:

$$m_{steady} = m_{steady}t \quad (18)$$

Combine the amount of mass of water from two stages of evaporation, the total amount of water consumes through whole process of evaporation can be calculated by the following:

$$m_{Total} = m_{transfer} + m_{steady} \quad (19)$$

The prior research supplied the data of temperature during experiment for validation; by using the collected data, we can predict the total amount of water that we should consume during each experiment case, and then the measurement value of water amount change will be compared with predicted value. The correction coefficient θ will be defined based on the comparison.

4.3 Results and Discussion

The prior laboratory experiment tested two levels of blowing power, 5 volts and 12 volts, which corresponding to two air flow velocities for forced convection scenarios, which is measured by an air meter: $a = 3 \text{ m/s}$ and $a = 6 \text{ m/s}$. The height of the scaffold is 210 mm ; the diameter of the scaffold is 110 mm . According to the experiment assumptions, the empirical value of dry air property at the temperature 300K is summarized as follows:

$$\gamma = 1.568 \times 10^{-5} \text{ m}^2/\text{s}$$

$$k = 2.624 \times 10^{-5} \text{ kW/mK}$$

$$\alpha = 22.07 \times 10^{-6} m^2/s$$

Therefore, the Nusselt number is obtained as:

$$\overline{Nu} = 81.5$$

The theoretical average heat transfer coefficient for all the cases that had 3 m/s velocity airflow blowing is:

$$\bar{h} = 19.5 w/m^2K;$$

And the theoretical average heat transfer coefficient for all the cases that had 6 m/s velocity airflow blowing is:

$$\bar{h} = 29.4 w/m^2K$$

Since in prior experiments the cases with cotton and linen were the materials that showed a significantly better cooling performance than woolen (Guo, 2012), all twelve cases use cotton and linen in three replications, are used to validate the heat and transfer mathematical model to determine the value of correction factor of the heat transfer coefficient. The selected cases from prior experiment contents (Guo, 2012) are summarized in the following table:

Table 4-1 Contents of Selected Cases for Validation

Case Number (#)	Material	Wrapping Method	Blowing power (Airflow Velocity)
6	Cotton	Vertical	5 V (3m/s)
10	Linen	Whole piece wrapping	5 V (3m/s)
11	Cotton	Vertical	12 V (6m/s)
15	Linen	Whole piece wrapping	12 V (6m/s)

To test the temperature changes inside the scaffold, the prior experiment recorded the inlet and outlet temperature point every three minutes; we assume this recorded temperature represented the average temperature within a period of three minutes, and we treat each period as a finite element. Each case of experiment endured 201 minutes that consists of sixty-seven elements. The total amount of water consumption that

happened in the scaffold during the whole cooling process equals the summation of the amount of water consumption of each finite element. Therefore, by applying the theoretical heat transfer coefficient to the heat and mass transfer mathematical model, the amount of water consumption on the scaffold for all the cases that used cotton and linen as absorbent materials is summarized in the following table:

Table 4-2 Calculation Results of Water Consumption on Scaffold

Case number/ Result	Calculation results (g)		
	Replication 1	Replication 2	Replication 3
Case #6	76.35	60.57	55.85
Case #10	85.54	87.97	63.65
Case #11	121.13	113.19	99.81
Case #15	129.47	76.38	93.6

According to the above table, based on the temperature recorded from prior experiment (Guo, 2012), the calculation result of water consumption shows similar trend with the prior experiment results analysis shown in Table 4-3. Case #11, with the whole piece of linen wrapped on the scaffold, consumed relatively much more water than other cases, which also produced the highest cooling efficiency among all experiment cases.

The prior experiment physically measured the water consumption of the whole cooler for each case. The measurement result is shown in following table:

Table 4-3 Measurement Results of Total Water Consumption of Whole Cooler

Case number/ Result	Actual water consumption (g)		
	Replication 1	Replication 2	Replication 3
Case #6	90	80	70
Case #10	100	110	80
Case #11	140	130	120
Case #15	140	90	110

The above water consumption includes two parts, one is the water consumption that happened on the scaffold, and the other part is the water consumption that happened on

the area surrounded by the scaffold. To separate the water consumption of scaffold from the total amount of water consumption, based on the mathematical model of the forced convection when the airflow blows the horizontal water surface, the average heat transfer coefficient is obtained as follows:

$$\bar{h} = \frac{\overline{Nu}k}{D}$$

In which,

$$\overline{Nu} = 0.332R_e^{1/2}P_r^{1/3}$$

Therefore, the average transfer coefficient when the airflow velocity is 3m/s at the temperature 300K is $\bar{h} = 15.96$; the average transfer coefficient when the airflow velocity is 6m/s at the temperature 300K is $\bar{h} = 29.59$.

Similar to calculating the water consumption of the scaffold, the water consumption that happened around the scaffold is forced convection for horizontal water surface, is summarized in the following table:

Table 4-4 Water Consumption from Surrounded Water Area

Case number/ Result	Surrounded area water consumption (g)		
	Replication 1	Replication 2	Replication 3
Case #6	9.63	9.04	8.7
Case #10	11.27	12.34	9.06
Case #11	16.11	15.56	14.15
Case #15	14.02	13.59	16.25

The actual amount of water consumption that only happened on the scaffold can be obtained from the difference between the total amount of water consumption and the amount of water consumption that happened on the surrounded water area, which is shown in the following table:

Table 4-5 Actual Water Consumption of Scaffold

Case number/ Result	Actual water consumption (g)		
	Replication 1	Replication 2	Replication 3

Case #6	80.37	70.96	61.3
Case #10	88.73	97.66	70.94
Case #11	123.89	114.44	105.85
Case #15	125.98	76.41	93.75

Therefore, the following figure shows the comparison between actual water consumption and calculation results for the selected four cases.

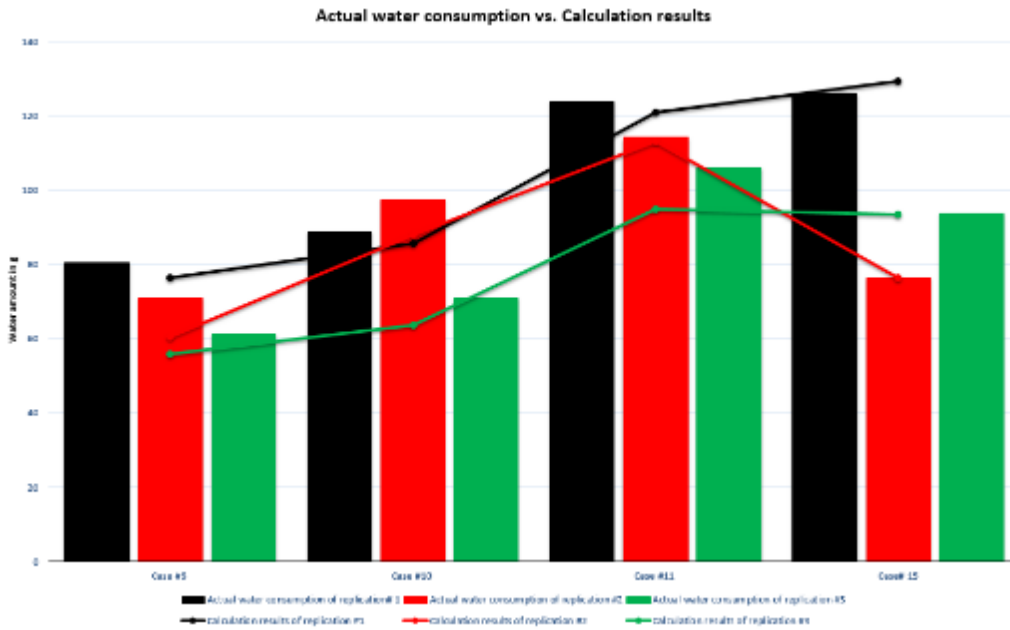


Figure 4-3 Comparison between actual water consumption and calculation results

In above figure, the black columns represent the actual water consumption of replication #1, the red columns represent the actual water consumption of replication #2, and the green columns represent the actual water consumption of replication #3; The black line represents the calculation result of replication #1, the red line represent the calculation result of replication #2, and the green line represent the calculation result of replication #3. The above chart shows the consistency between the actual water consumption of scaffold and the calculation results based on the heat and mass transfer mathematical model. To numerically compare the actual water consumption and the theoretical calculation results, the error is defined as following:

$$\frac{\text{Actual water consumption} - \text{Theoretical calculation result}}{\text{Theoretical calculation result}} \times 100\%$$

And the result is shown in following table and figure:

Table 4-6 Error Summary between Actual Water Consumption of scaffold and Calculation Results

Case number/ Result	Error			Average Error
	(Actual-Theory)/Actual			
Case #6	5%	15%	9%	10%
Case #10	4%	10%	10%	8%
Case #11	2%	1%	10%	5%
Case# 15	-3%	0%	0%	-1%

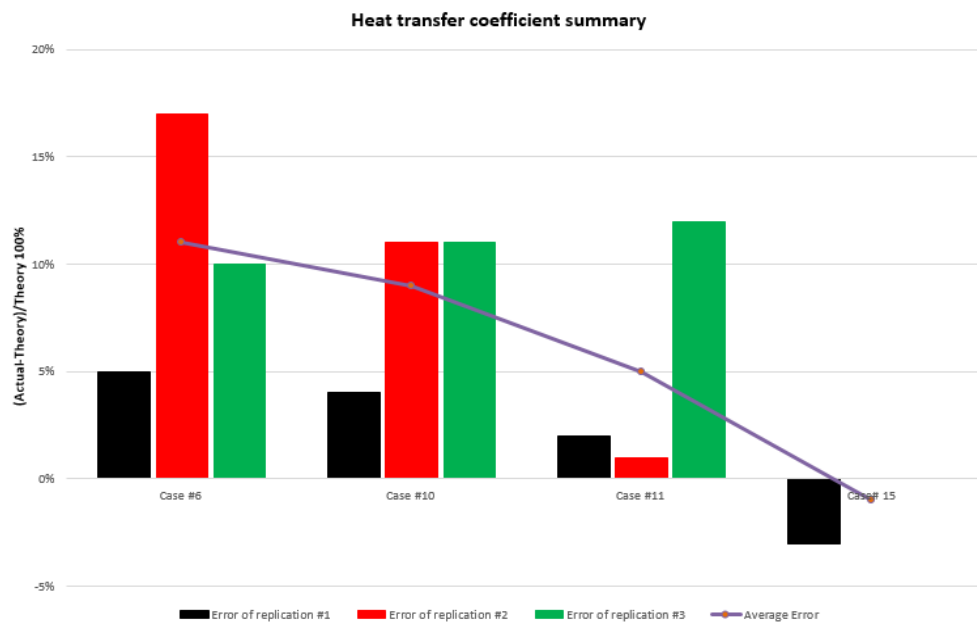


Figure 4-4 Error summary between actual water consumption and calculation results

The above table 4-6 also suggests the difference between the value of theoretical average heat transfer coefficient and the actual empirical value of average heat transfer coefficient, which is defined as θ , the correction coefficient. For the cases that used cotton vertical wrapping with 3 m/s blowing velocity, the actual average heat transfer coefficient is 111% of theoretical value, $h = 1.11\bar{h}$; for the cases that used cotton vertical wrapping with 6 m/s blowing velocity, the actual average heat transfer coefficient is 105% of theoretical value, $h = 1.05\bar{h}$; for the cases that used linen whole piece wrapping with 3 m/s blowing velocity, the actual average heat transfer coefficient is 109% of theoretical value, $h = 1.09\bar{h}$; and for the cases that used linen whole piece

wrapping with 6 m/s blowing velocity, the actual average heat transfer coefficient is 99% of theoretical value, $h = 0.99\bar{h}$. All the above results are summarized in following table, and the error decreases as the blowing speed increases:

Table 4-7 Heat Transfer Coefficient Summary

Case number/ Result	Heat transfer coefficient	
	Theoretical value	Empirical value
Case #6	15.96	17.72
Case #10	15.96	17.4
Case #11	29.59	31.07
Case# 15	29.59	29.29

There are several factors that may have caused the error: 1) the measurement accuracy; 2) airflow velocity stability; 3) the surface characteristics may have changed, for example, the density of the curtain and the curtain surface humidity.

4.4 Summary

Once the heat transfer coefficient is determined, the minimum amount of water consumption during cooling can be predicted using the heat and mass transfer mathematical model, as long as the environment temperature, target temperature and scaffold characteristics (dimension) are given.

Following example provides a demonstration of the model:

In the case that fbaEC has a single-scaffold structure with cotton threads as the fiber material and the diameter of 10 cm and the height of 25 cm; the air flow speed is 10m/s with normal room temperature, the designated temperature decreasing is 10 °C. Determine the unit time water consumption during the steady stage.

According to the single-scaffold structure heat and mass mathematical model, the heat transfer coefficient can be expressed by following:

$$\bar{h} = \frac{\overline{Nu}k}{D} = 0.3D^{-1} + \left\{ \frac{0.62 \left(\frac{aD}{\gamma}\right)^{1/2} \left(\frac{\gamma}{\alpha}\right)^{1/3}}{\left[1 + \left(\frac{0.4\alpha}{\gamma}\right)^{2/3}\right]^{1/4}} \times \left[1 + \left(\frac{aD}{282000\gamma}\right)^{5/8}\right]^{4/5} \right\}$$

Where,

$$v = a = 10 \text{ m/s}$$

$$D = 0.1 \text{ m/s}$$

$$\gamma = 1.568 \times 10^{-5} \text{ m}^2/\text{s}$$

$$k = 2.624 \times 10^{-5} \text{ kW/mK}$$

$$\alpha = 22.07 \times 10^{-6} \text{ m}^2/\text{s}$$

$$h_{lv} = 2257 \text{ J/g}$$

$$Re = \frac{aD}{\gamma} = 63775.5102$$

$$Pr = \frac{\gamma}{\alpha} = 0.707$$

$$\overline{Nu} = 0.3 + \frac{0.62 Re^{1/2} Pr^{1/3}}{\left[1 + \left(0.4/Pr\right)^{2/3}\right]^{1/4}} \times \left[1 + \left(Re/282000\right)^{5/8}\right]^{4/5} = 160.1$$

The heat transfer coefficient is:

$$\bar{h} = 42$$

The unit time water consumption is

$$\dot{m} = \frac{q}{h_{lv}} = \frac{\bar{h}A\Delta T}{h_{lv}} = \frac{42 \times 0.25 \times 0.1 \times 10}{2257} = 0.0037 \text{ g/s}$$

The heat and mass transfer mathematical model also provides a tool to help improve the cooler design that achieves the designated cooling performance, for example, through modifying the scaffold structure and air flow speed, etc. Take above example as illustration: in the case that the unit water consumption is 0.0037g/s, the air flow speed is 10m/s with normal room temperature, if the designated temperature is 11 °C, determine the height of scaffold with the diameter of 10 cm.

As we know the scaffold surface area can be calculated as:

$$A = \frac{m h_{lv}}{h \Delta T} = 0.018 m^2$$

The height of the scaffold can be calculated by:

$$H = \frac{A}{D} = 18 \text{ cm}$$

Therefore, the height of scaffold should be 18 cm to achieve the designated temperature decrease.

CHAPTER 5

EXPERIMENTS ON TESTING THE fbaEC COOLING PERFORMANCE IN REAL TRANSPORT ENVIRONMENT

Twelve groups of experiments that combined three replications of four cases were conducted. An extra three groups also compared cases that tested cooling performance of fbaEC under the circumstances where the cooler had no water. We drove a vehicle at four speeds of 0 mph, 15 mph, 30 mph and 45 mph, on the same curvy paved country route that avoided the traffic and other distraction factors, to test the cooling performance of fiber-based absorbent evaporative cooler (fbaEC) with same type of cotton fabric material, and all groups of experiment used same vertical fabric wrapping method.

5.1 Experiment Result

There are three graphics in each case of experiments representing the temperature changes at four different positions during three replications, in which “T1” represents the environment temperature that shows the temperature change in weather environment; both “T2” and “T3” represent the temperature inside the scaffold, in which “T2” was set near the front of vehicle, and “T3” was set near the back of vehicle; “T4” represents the temperature inside the water container but outside the scaffold (shown following figure).

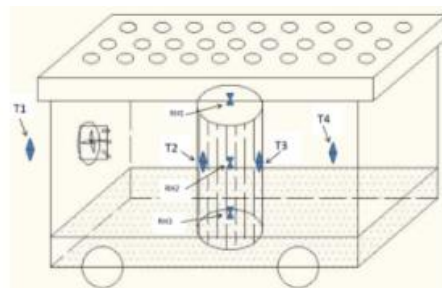


Figure 5-1 Thermal couples' positions

5.1.1 Speed 0 MPH

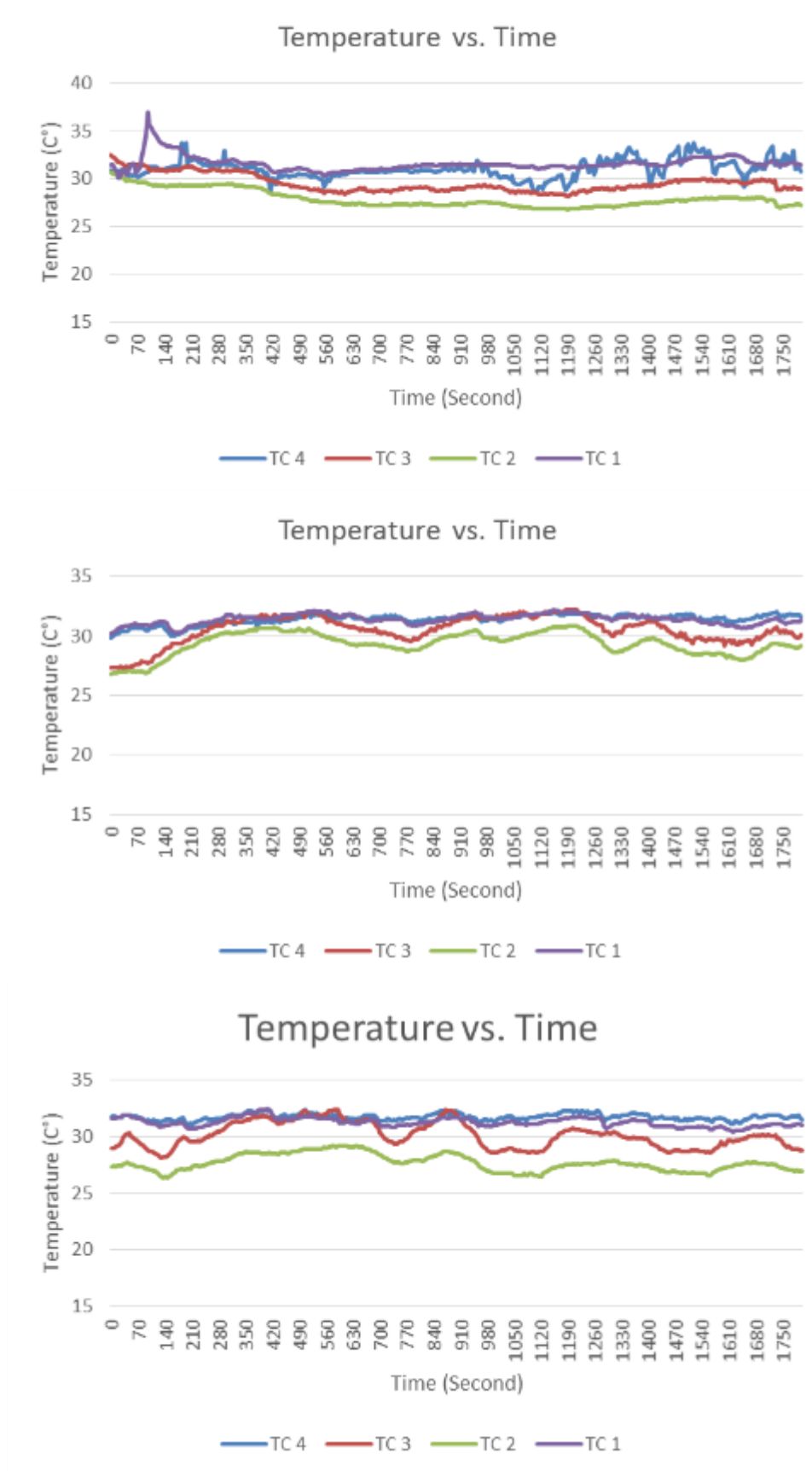


Figure 5-2 Temperature vs. time of three replications in case that driving test at speed

of 0 mph

In above figures, the purple line represents the environment temperature; the green line represents the temperature at the position inside the scaffolding near the front of vehicle; the red line represents the temperature inside the scaffolding at the position near the back of vehicle; the blue line represents the temperature outside the scaffolding inside the water container, which is also near the back of vehicle.

In this case, three replications show that environment temperature was stable; the average environment temperature of three replications was 31.58 °C, 31.39 °C and 30.92 °C respectively; the temperature outside the scaffolding inside the water container did not change much, but all temperatures inside the scaffolding decreased as time passed; the lowest temperature inside the scaffolding in each replication were 26.7 °C , 26.8 °C and 25.8 °C respectively; the maximum differences between the temperature inside of the scaffolding and environment temperature in each replication were 7.5 °C , 4 °C and 4.7 °C respectively; the maximum average cooling efficiency in each replication were 17.97%, 11.97% and 13.44%, respectively; and the maximum cooling efficiency were 20.27%, 12.94% and 15.41% respectively. The environment relative humidity was 36%, 43% and 39% respectively.

5.1.2 Speed 15 MPH

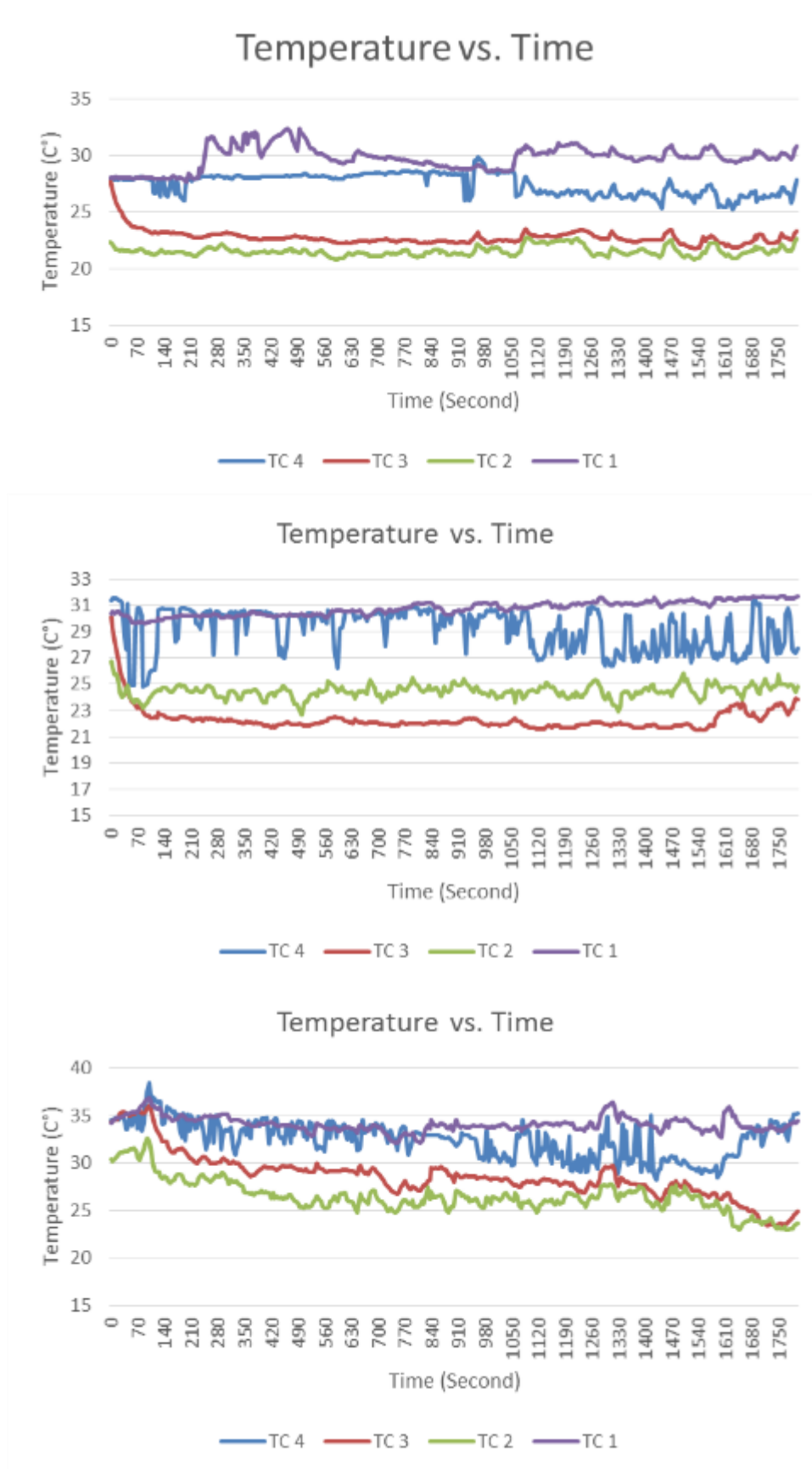
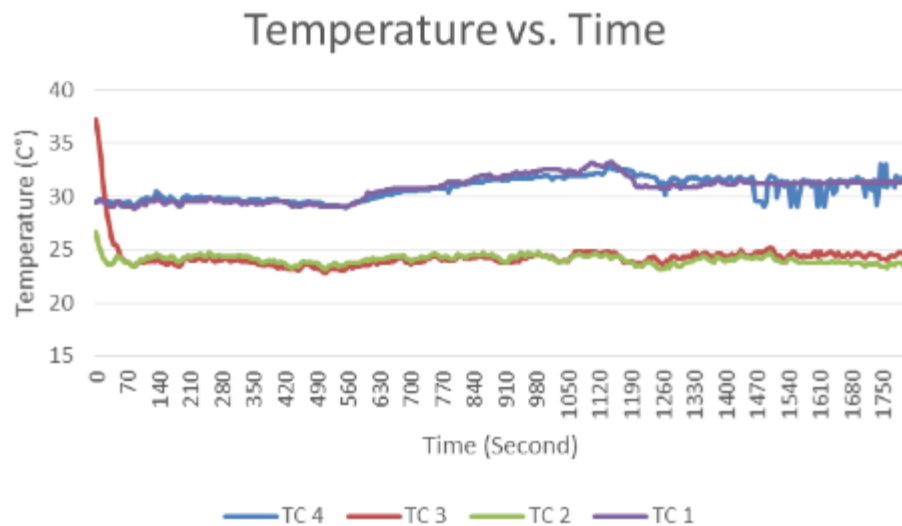


Figure 5-3 Temperature vs. time of three replications in case that driving test at speed

of 15 mph

In this case, three replications show that environment temperature was relatively stable; the average environment temperature was 30.33 °C, 30.93 °C and 30.98 °C respectively; the temperature outside the scaffolding inside the water container did not change much as well as environment temperature; however, all temperatures inside the scaffolding decreased obviously as time passed; the lowest temperature inside the scaffolding in each replication was 20.8 °C, 21.4 °C and 22.9 °C respectively; the maximum differences between the temperature inside of the scaffolding and environment temperature in each replication were 13.8 °C, 10.6 °C and 12 °C respectively; the maximum average cooling efficiency in each replication were 37.07%, 31.41% and 32.41% respectively; and the maximum cooling efficiency were 39.08%, 33.13% and 33.43% respectively. The environment relative humidity was 47%, 40% and 39% respectively.

5.1.3 Speed 30 MPH



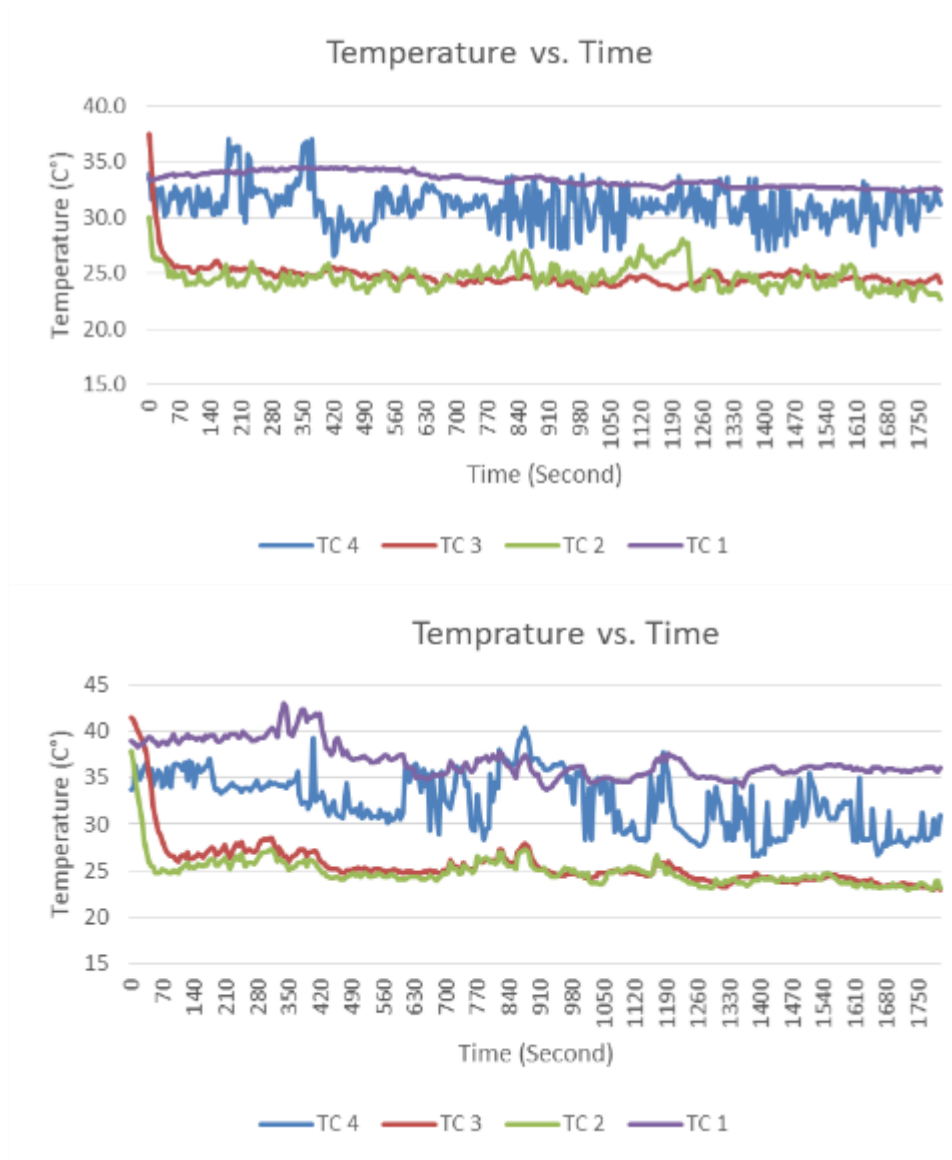
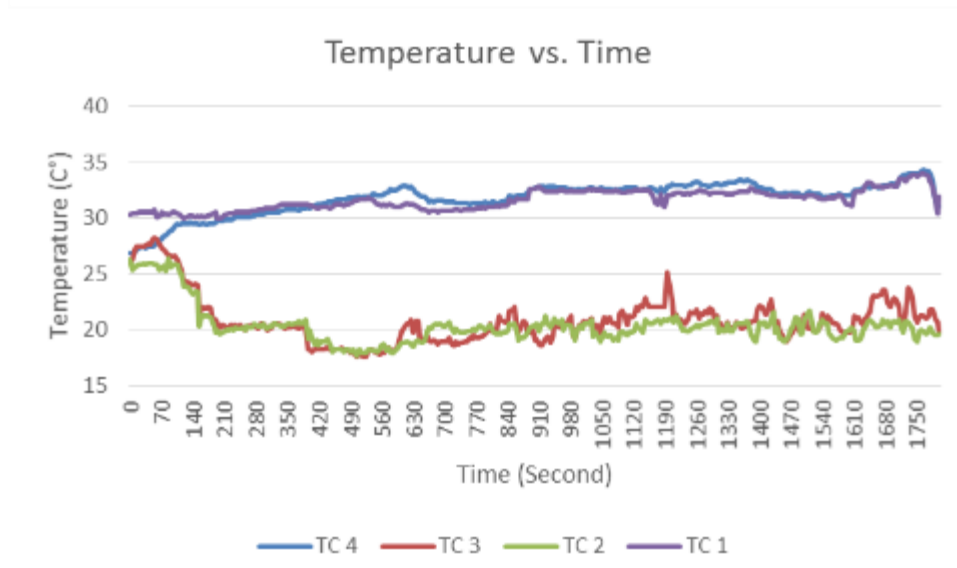
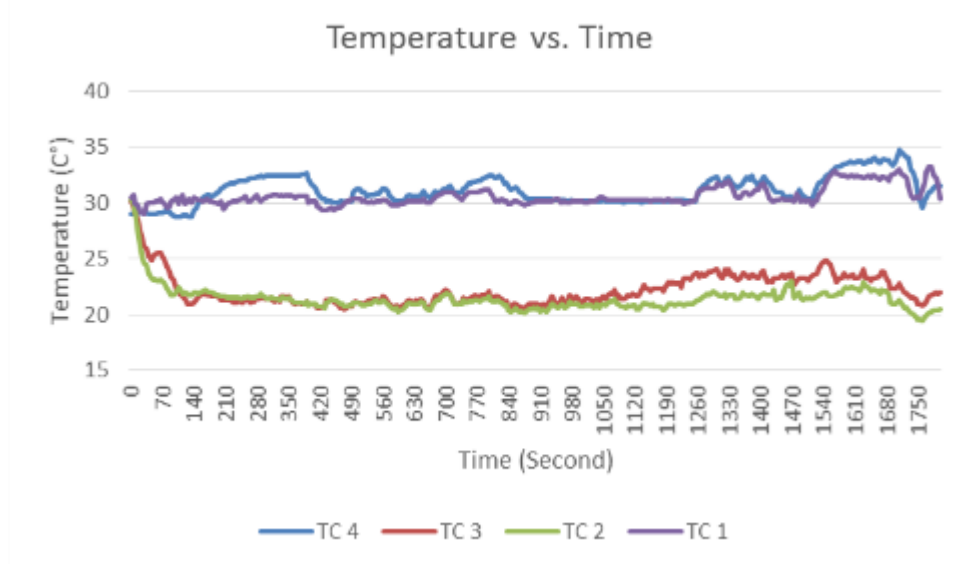


Figure 5-4 Temperature vs. time of three replications in case that driving test at speed of 30 mph

In this case, three replications show that environment temperature was still keeping relatively stable; the average environment temperature was 30.89°C, 33.21°C and 36.59°C respectively; the temperature outside the scaffolding inside the water container kept stable but lower than the environment temperature; as expected, all temperatures inside the scaffolding decreased obviously as time passed; the lowest temperature inside the scaffolding in each replication was 22.8°C, 22.6°C and 22.9°C respectively; the maximum differences between the temperature inside of the scaffolding and environment temperature in each replication were 9.2°C, 11°C and 17.2°C respectively;

the maximum average cooling efficiency in each replication were 27.03%, 30.17% and 39.07% respectively; and the maximum cooling efficiency were 27.63%, 32.07% and 40% respectively. The environment relative humidity was 48%, 39% and 30% respectively.

5.1.4 Speed 45 MPH



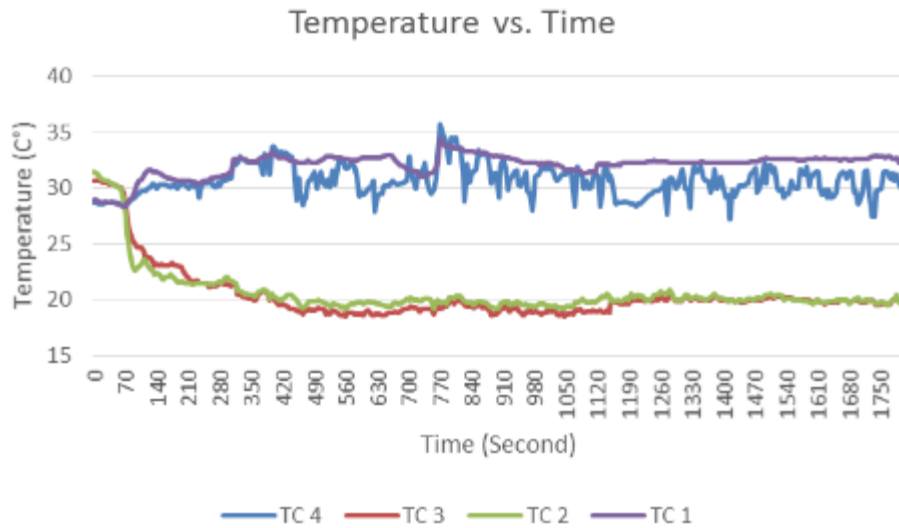


Figure 5-5 Temperature vs. time of three replications in case that driving test at speed of 45 mph

In this case, three replications show that environment temperature kept relatively stable; the average environment temperature was 30.6 °C , 31.9 °C and 32.05 °C respectively; the temperature outside the scaffolding inside the water container kept stable but lower than the environment temperature as well as previous cases; also as expected, all temperatures inside the scaffolding decreased obviously as time passed; the lowest temperature inside the scaffolding in each replication was 19.5°C, 17.6°C and 18.5°C respectively; the maximum differences between the temperature inside of the scaffolding and environment temperature in each replication were 13.2°C, 14.8°C and 15.3°C respectively; the maximum average cooling efficiency in each replication were 37.39%, 44.15% and 43.6% respectively; and the maximum cooling efficiency were 39.64%, 44.48% and 44.48% respectively. The environment relative humidity was 43%, 37% and 39% respectively.

5.1.5 Extra Compare Cases

To compare and demonstrate that the cooling effect of fbaEC comes from the effect of evaporation, the extra compare cases were conducted while there is no water in either container or scaffolds at all.

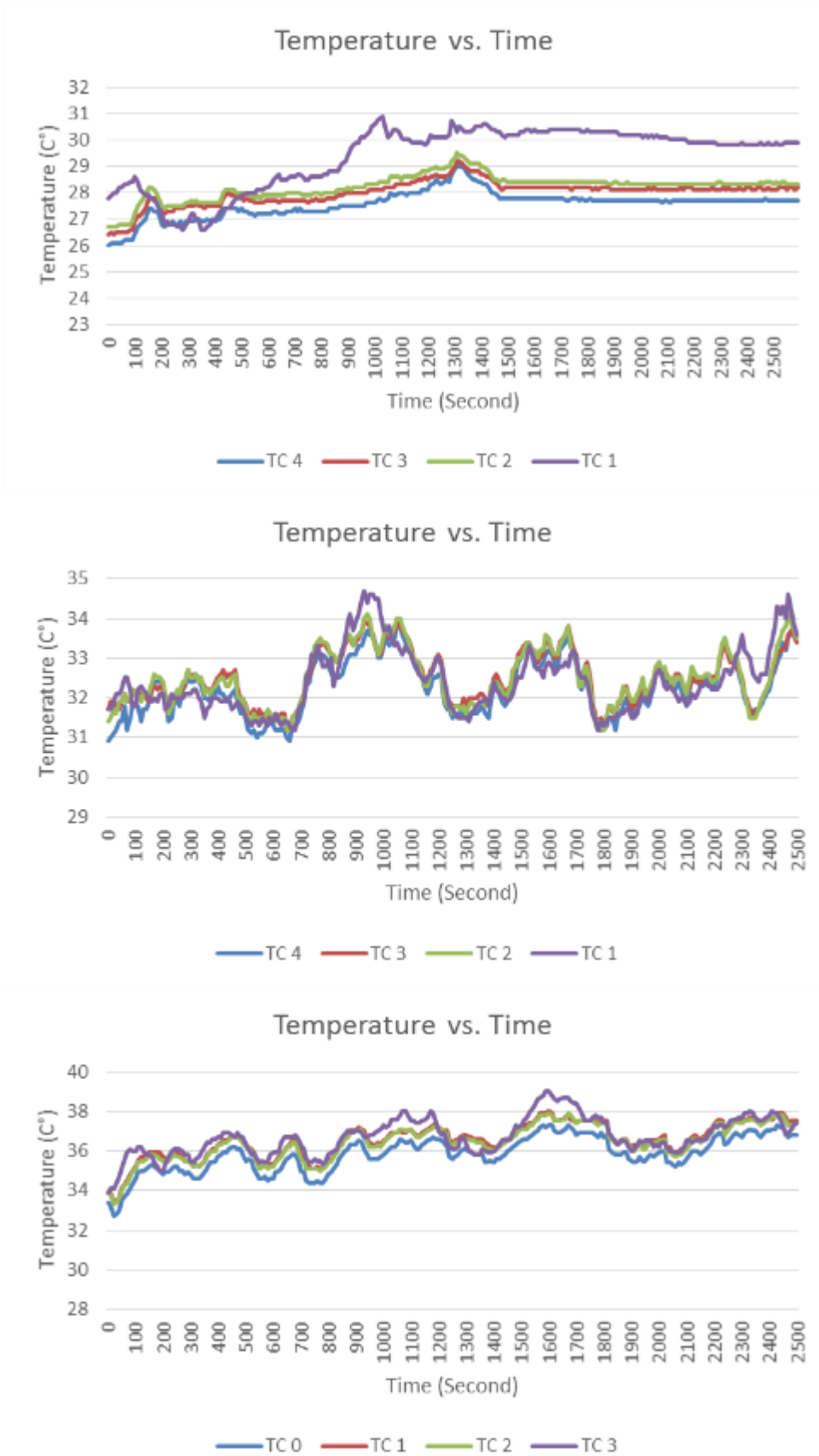


Figure 5-6 Temperature vs. time example of three replications in case that driving test at speed of 15 mph, 30 mph and 45 mph, while running without water inside

In this case, all temperatures at different positions showed no obvious difference during experiment, all temperatures changed as most similar trend and kept relatively stable.

5.2 Water Consumption

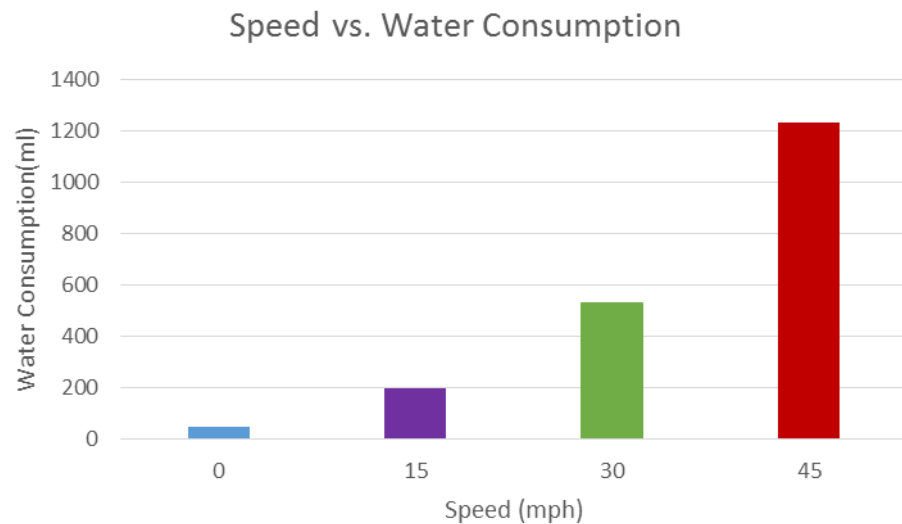


Figure 5-7 The average amount of consumed water among three replication at each driving speed while testing

Experiment results showed water consumption was linearly consistent with driving speed and cooling efficiency. The most water consumption happened in the case of driving speed of 45mph, which created the maximum cooling efficiency of 44.48%; the least water consumption happened in the case of driving speed of 0mph, which created the minimum cooling efficiency of 12.94%.

5.3 Statistical Analysis

5.3.1 Temperature Comparison

The basic statistical analysis on all cases that tested fbaEC cooling performance which driving at speed of 0 mph, 15 mph, 30 mph and 45 mph showed the temperatures inside scaffold with water inside, were consistently significantly lower than environment temperature; and the temperatures inside scaffold of extra case without

water that tested fbaEC cooling performance, were not significantly lower than environment temperature.

5.3.2 Basic Assumptions and Analysis

The dataset contains eight variables, where driving speed, average environmental temperature (T1), and environment relative humidity are predictor variables, and water consumption, maximum average cooling efficiency, maximum cooling efficiency, maximum average temperature difference and maximum temperature difference are response variables. Among those three predictor variables, the environment temperature and environment relative humidity were known by measurement, and the dataset could be divided into different groups based on the control predictor variable speed. For each group, we firstly analyze the correlation between predictor variables (Temperature, Humidity) and response variables.

5.3.2.1 General Correlation Analysis

The following figures show the correlation coefficients for response variables (Water Consumption, maximum average cooling efficiency, maximum cooling efficiency, maximum average temperature difference and maximum temperature difference) and predictor variables (Temperature, Humidity) for each group.

	Average Environmental Temperature
Water Consumption	NA
Maximum Average Cooling Efficiency	0.5394194
Maximum Cooling Efficiency	0.4524075
Maximum Average Temperature Difference	0.5719729
Maximum Temperature Difference	0.5784805
	Environment Relative Humidity
Water Consumption	NA
Maximum Average Cooling Efficiency	-0.9328153
Maximum Cooling Efficiency	-0.9642060
Maximum Average Temperature Difference	-0.9179916
Maximum Temperature Difference	-0.9148074

Figure 5-8 Correlation analysis among variables for group #1 ($v = 0\text{mph}$)

According to the result, the correlation between water consumption and other variables are not applicable, as the value of the differences among observed water

consumptions of cases are not significantly detected due to the measurement resolution.

This also applies for next group #2 with driving speed of 15mph.

	Average Environmental Temperature
Water Consumption	NA
Maximum Average Cooling Efficiency	-0.4892215
Maximum Cooling Efficiency	-0.5913380
Max temperature difference	0.2274177
Max temperature difference.1	-0.2240096
	Environment Relative Humidity
Water Consumption	NA
Maximum Average Cooling Efficiency	0.63714421
Maximum Cooling Efficiency	0.72587623
Max temperature difference	-0.04981406
Max temperature difference.1	0.39449393

Figure 5-9 Correlation analysis among variables for group #2 (v = 15mph)

	Average Environmental Temperature
Water Consumption	0.9144532
Maximum Average Cooling Efficiency	0.9868208
Maximum Cooling Efficiency	0.9985144
Maximum Average Temperature Difference	0.9900889
Maximum Temperature Difference	0.9799641
	Environment Relative Humidity
Water Consumption	-0.8660254
Maximum Average Cooling Efficiency	-0.9639072
Maximum Cooling Efficiency	-0.9869917
Maximum Average Temperature Difference	-0.9694384
Maximum Temperature Difference	-0.9531016

Figure 5-10 Correlation analysis among variables for group #3 (v = 30mph)

	Average Environmental Temperature
Water Consumption	0.9955668
Maximum Average Cooling Efficiency	0.9860025
Maximum Cooling Efficiency	0.9955668
Maximum Average Temperature Difference	0.9914301
Maximum Temperature Difference	0.9908034
	Environment Relative Humidity
Water Consumption	-0.9449112
Maximum Average Cooling Efficiency	-0.9663498
Maximum Cooling Efficiency	-0.9449112
Maximum Average Temperature Difference	-0.9563193
Maximum Temperature Difference	-0.8454468

Figure 5-11 Correlation analysis among variables for group #4 (v = 45mph)

According to the above result, we can conclude as following:

(1) The correlation between driving speed and water consumption is positively significant. Water consumption is not significantly related with other predictor variables while the cooler is in static status and with lower speed.

(2) Among the groups #1, #3 and #4, the average of values of correlation coefficients for environment relative humidity and cooling efficiency are lower than -0.90, suggesting the environment humidity and cooling efficiency (maximum average cooling efficiency, maximum cooling efficiency, maximum average temperature difference and maximum temperature difference) are highly negatively correlated, which indicates that the higher the environment relative humidity, the lower the cooling efficiency; this observation doesn't apply to group #2 with lower driving speed of 15 mph.

(3) When Speed is fast, the environment temperature is highly correlated with water consumption and cooling efficiency. Thus, the correlation coefficients between environment temperature and water consumption, cooling efficiency respectively increase as speed goes up.

5.3.2.2 Effect of Environment Relative Humidity on Cooling Efficiency

The following figures are scatter plots for environment relative humidity and four cooling efficiency variables respectively. Normally the X axis represents the predictor variable and Y axis represents the dependent variable, but in each plot, we switched two axis to recognize the correlation among factors easily: the Y axis represents the environment relative humidity; the X axis represents the maximum cooling efficiency (a), the maximum average cooling efficiency (b), the maximum temperature difference (c), and the maximum average temperature difference (d); red line and spots refer to group 1 with speed of 0 mph, , yellow line and spots refer to group 2 with speed of 15 mph, blue line and spots refer to group 3 with speed of 30 mph, and green line and spots

refer to group 4 with speed of 45 mph. The straight lines represent the least squares lines of each group; they are the least squares estimate for cooling efficiency based on the environment humidity. These figures show similar slope trend for all groups except group #2, and the intercepts increase as speed increases.

Moreover, all p-values are around 0.10 except group #2. Thus we can conclude that given 90% confidence interval, there is a significant linear relationship between cooling efficiency (maximum average cooling efficiency, maximum cooling efficiency, maximum average temperature difference and maximum temperature difference) and environment relative humidity when the cooler is under static status and driving with higher speed.

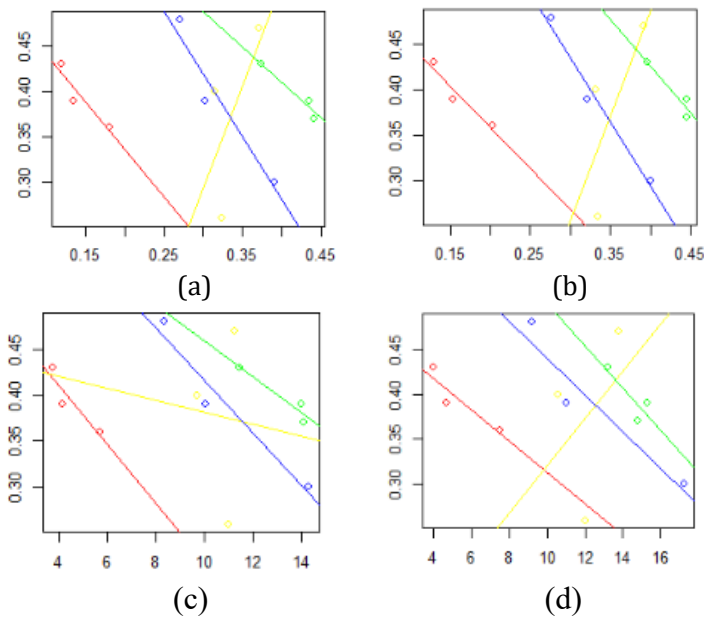


Figure 5-12 Scatter plots among environment relative humidity and four cooling efficiency variables

5.3.2.3 Effect of Environment Temperature on Cooling Efficiency

Similar to previous section, the following figures are scatter plots for environment temperature and other four cooling efficiency variables ((a) maximum average cooling efficiency, (b) maximum cooling efficiency, (c) maximum average temperature difference and (d) maximum temperature difference) respectively. The color of red,

yellow, blue and green refer to group #1 with speed of 0 mph, group #2 with speed of 15 mph, group #3 with speed of 30 mph, and group #4 with speed of 45 mph respectively.

The linear regression model was given by ordinary least squares method. The result shows that the slope parameters are more stable while speed is high and the intercepts decreases as speed increases. Also the p-value decreases as speed increases, in which the four P-values of four cooling efficiency variables in group 3 (speed of 30 mph) are 0.0888, and the four P-values in group #4 (speed of 45 mph) are 0.0841, which indicates the linear relationship between environment temperature and cooling efficiency is more significantly positive related as speed increases.

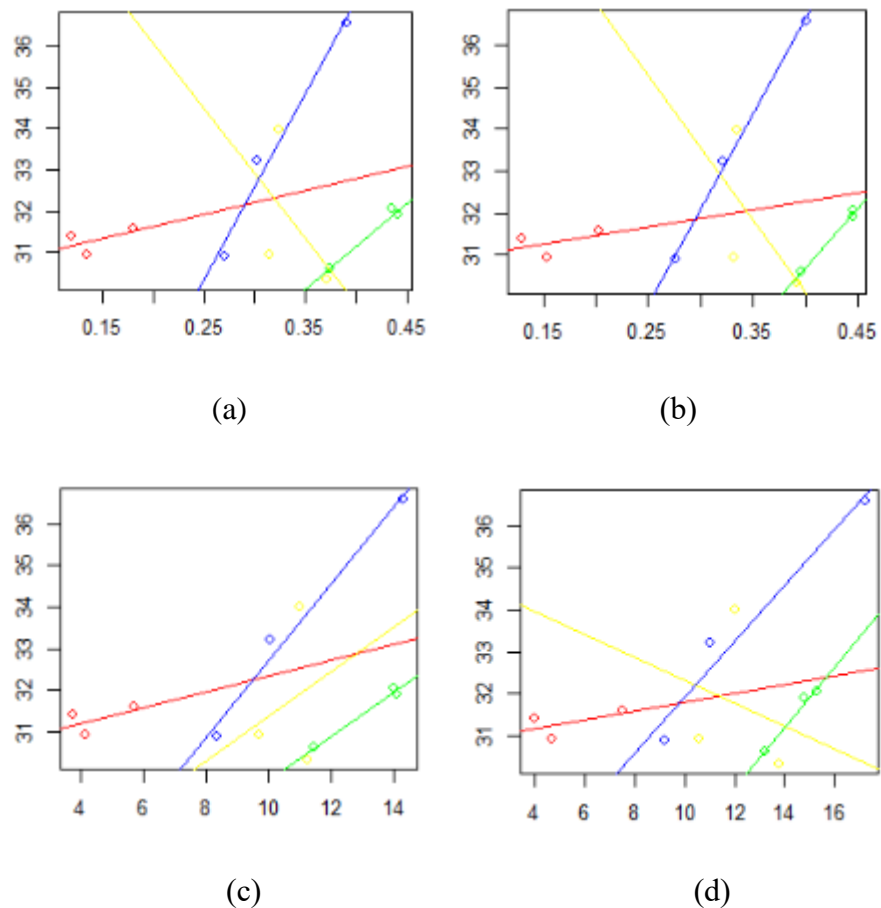


Figure 5-13 Scatter plots among environment relative humidity and four cooling efficiency variables

5.3.3 Linear Regression Analysis

5.3.3.1 Analysis Method Based On Prior Probability

The above result shows a linear correlation among speed and cooling efficiency, and this assumption is also proven in table 5-3. And according to above result of previous section, the alternative hypothesis is set up as following (also defined in section 3.3.5):

H1: There are significant linear relationships between cooling efficiency (maximum average cooling efficiency, maximum cooling efficiency, maximum average temperature difference and maximum temperature difference) and the environment temperature, environment relative humidity, respectively. Given different value of Speed (0 mph, 15 mph, 30 mph and 45 mph), the distributions are expressed as the following:

$$V = 0 : H = kX + (b_0 + 0)$$

$$V = 15 : H = kX + (b_0 + \Delta)$$

$$V = 30 : H = kX + (b_0 + 2\Delta)$$

$$V = 45 : H = kX + (b_0 + 3\Delta)$$

In which,

H = Environment relative humidity;

X = Cooling efficiency (maximum average cooling efficiency, maximum cooling efficiency, maximum average temperature difference and maximum temperature difference);

b_0 = The origin intercept value while the speed is 0 mph;

Δ = The intercept change when the speed changes every 15 mph;

$1/k$ = The effect of humidity on cooling efficiency.

The slope parameter k represents the change of environment relative humidity when the related predictor variable (cooling efficiency) changes one unit. So the inverse of slope parameter represents the change of cooling efficiency when the environment relative humidity changes one unit. The intercepts show the effect of the speed. Thus, the difference between the greatest intercept and the least intercept which is $\Delta v=3\Delta$, equals to the three times of change of environment relative humidity when speed changes every 15 mph. Therefore, the change of cooling efficiency when speed changes on unit could be obtained as following:

$$dt_{cooling\ efficiency} = -\frac{\Delta}{15k}$$

The value of k could be calculated and the value of $1/k$ is the following:

-0.9308259 -0.8932412 -37.5691202 -48.9143409

As shown above, when the environment relative humidity increases each 1%, the maximum average cooling efficiency will be decreased by 0.93%, the maximum cooling efficiency will be decreased by 0.89%, the maximum average temperature difference will be decreased by 0.37°C and the maximum temperature difference will be decreased by 0.48°C.

5.3.3.2 Analysis Based on Post Probability

Basic statistics analysis suggested the correlation among response variables (Water Consumption, Maximum Average Cooling Efficiency, Maximum Cooling Efficiency, Maximum Average temperature difference and Maximum temperature difference) and predictor variables (Temperature, Humidity) for group #2 with driving speed of 15 mph varies from other three groups, the stability of fbaEC with lower speed caused the unstable cooling performance, which can be reflected by the figures in section 5.1.2. To accurately analyze the further linear relation among variables, since the fbaEC is

used for short-term transportation and storage, and the cooling performance is more stable with either static status or higher speed, we select groups with higher speeds which are group #3 and group #4 and select group with static status that is group #1 to continuously create the regression model. The sum of squared differences of each group could be expressed as following:

$$SS_1 = (kX_1 + b_0 - y_1)^2$$

$$SS_3 = (kX_3 + b_0 + 2\Delta - y_3)^2$$

$$SS_4 = (kX_4 + b_0 + 3\Delta - y_4)^2$$

In which, y is the observed value.

When $SS_1 = 0$, the unbiased estimation for b_0 could be obtained as the following:

$$B_0 = \text{mean}\{-(kX_1 - y_1)\} = 0.5486792$$

Two methods could be considered used to calculate Δ that is the intercept change when the speed changes every 15 mph:

Method I: Unbiased Estimation

Since $\text{mean}\{-(kX_3 - y_3)\}$ and $\text{mean}\{-(kX_4 - y_4)\}$ are the unbiased estimation for $(b_0 + 2\Delta)$ and $(b_0 + 3\Delta)$ respectively, we can calculate the estimation for Δ directly.

Method II: OLS (Ordinary Least Square) Method

Let $SS = SS_1 + SS_3 + SS_4$, and under the circumstances that $b_0, k, X = \{x_1, x_3, x_4\}$, $Y = \{y_1, y_3, y_4\}$ are known factors, SS could be a function of Δ that has the minimal value when

$$\Delta = (2 * \sum (kx_3 - y_3) + 3 * \sum (kx_4 - y_4) - 5b_0) / 13$$

The following figures show the regression result, in which the dark lines represent the unbiased estimation and bright lines represent the OLS results.

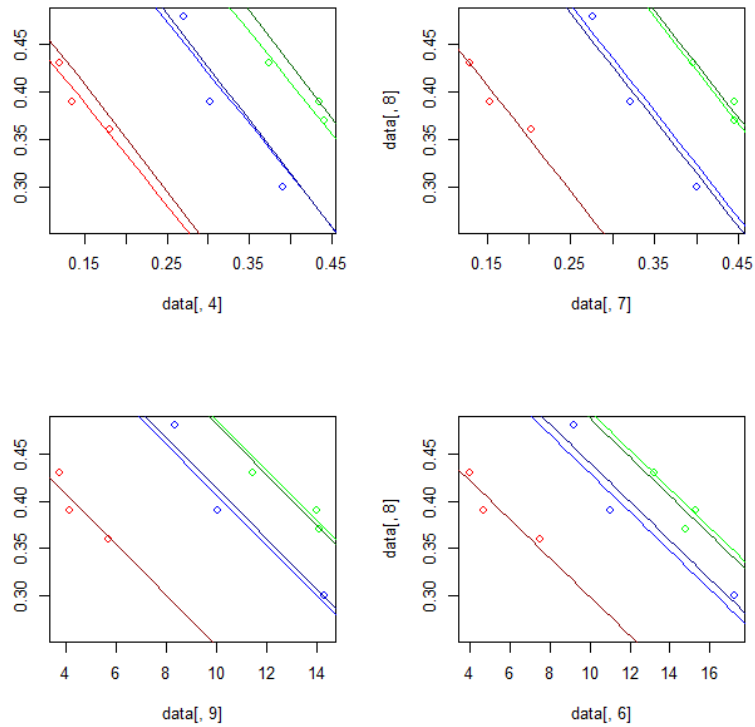


Figure 5-14 Regression results from two methods comparison

According to observation about above figures, the two methods indicate similar result and the calculation shows that when speed changes 1 unit that is 1 mph, the maximum average cooling efficiency, the maximum cooling efficiency, the maximum average temperature difference and the maximum temperature difference change as following by two methods respectively:

Unbiased estimation:

0.006125246 0.005990610 0.194716476 0.204364025

OLS:

0.006016937 0.005863132 0.198739060 0.212289134

As shown above, when the driving speed increases each 1 mph, the maximum average cooling efficiency will be increased by 0.6%, the maximum cooling efficiency will be increased by 0.59%, the maximum average temperature difference will be

increased by 0.19°C and the maximum temperature difference will be decreased by 0.2°C.

Therefore, the statistics results conclude the linear relation among speed and cooling efficiency given the environment relative humidity. Compare with the value of 1/k that is the effect of environment relative humidity on cooling efficiency, variable speed is less sensitive on the cooling efficiency than environment relative humidity, which indicates when changing one unit of speed and environment relative humidity respectively while keep another variable constant, the environment relative humidity change leads to more obvious change on cooling efficiency.

Table 5-1 Summary of effects of environment relative humidity and speed on the cooling efficiency

Variables	Environment Relative Humidity (Changes 1%)	Speed (Changes 1 mph)
Maximum Average Cooling Efficiency	0.93%	0.6%
Maximum Cooling Efficiency	0.86%	0.59%
Maximum Average Temperature Difference	0.37 °C	0.19 °C
The Maximum Temperature Difference	0.48 °C	0.2 °C

5.3.3.3 Regression Model

Based on all above result, the fitted regression model among environment humidity, speed and cooling efficiency could be calculated and expressed as the following:

$$H = -1.074315C_1 + 0.5486792 + 0.006464084S$$

$$H = -1.119518C_2 + 0.5747699 + 0.006563884S$$

$$H = -0.0266176C_3 + 0.5138930 + 0.005289958S$$

$$H = -0.02044395C_4 + 0.5037304 + 0.004340018S$$

In which,

H, Environment Relative Humidity

C_1 , Maximum Average Cooling Efficiency

C_2 , Maximum Cooling Efficiency

C_3 , Maximum Average Temperature difference

C_4 , Maximum Temperature difference

S, Speed

We can continue to transform above models to following:

$$C_1 = -0.9308259H + 0.5107249 + 0.006016937S$$

$$C_2 = -0.8932412H + 0.5134082 + 0.005863132S$$

$$C_3 = -37.56912H + 19.30651 + 0.1987391S$$

$$C_4 = -48.91434H + 24.63964 + 0.2122891S$$

5.3.3.4 Model Validation

A model validation was conducted with comparing estimated values and observed values for data of all variables by using Welch Two Sample t-test, the p-values are much larger than 0.05. It suggests not to reject the null hypothesis that the estimated values and observed values have no difference, so we can conclude the above regression models are valid. The following figure show the result.

Welch Two Sample t-test

```
data: chisq.prel[-c(4:6)] and chisq.data1[-c(4:6)]
t = 0.012823, df = 15.998, p-value = 0.9899
alternative hypothesis: true difference in means is not equal to 0
95 percent confidence interval:
 -0.1259802  0.1275135
sample estimates:
mean of x mean of y
0.2949778 0.2942111
```

```

Welch Two Sample t-test

data: chisq.pre2[-c(4:6)] and chisq.data2[-c(4:6)]
t = 0.0162, df = 15.999, p-value = 0.9873
alternative hypothesis: true difference in means is not equal to 0
95 percent confidence interval:
 -0.1226469  0.1245358
sample estimates:
mean of x mean of y
0.3086000 0.3076556

Welch Two Sample t-test

data: chisq.pre3[-c(4:6)] and chisq.data3[-c(4:6)]
t = -0.014858, df = 15.994, p-value = 0.9883
alternative hypothesis: true difference in means is not equal to 0
95 percent confidence interval:
 -4.334427  4.274094
sample estimates:
mean of x mean of y
 9.497756  9.527922

Welch Two Sample t-test

data: chisq.pre4[-c(4:6)] and chisq.data4[-c(4:6)]
t = -0.044276, df = 15.993, p-value = 0.9652
alternative hypothesis: true difference in means is not equal to 0
95 percent confidence interval:
 -4.888103  4.688103
sample estimates:
mean of x mean of y
10.66667 10.76667

```

Figure 5-15 Regression model statistics validation result

An example can demonstrate the above regression model:

When the environment relative humidity is 40% and the driving speed is 35 mph, the cooling efficiency for a 30-minute transportation can be calculated through above model as following:

Maximum Average Cooling Efficiency:

$$C_1 = -0.9308259 * 0.4 + 0.5107249 + 0.006016937 * 20 = 0.258733$$

Maximum Cooling Efficiency

$$C_2 = -0.8932412 * 0.4 + 0.5134082 + 0.005863132 * 20 = 0.273374$$

Maximum Average Temperature difference

$$C_3 = -37.56912 * 0.4 + 19.30651 + 0.1987391 * 20 = 8.253644^\circ\text{C}$$

Maximum Temperature difference

$$C_4 = -48.91434 * 0.4 + 24.63964 + 0.2122891 * 20 = 9.3196896^\circ\text{C}$$

5.3.4 Analysis on Effect of Speed on Water Consumption

According to the correlation analysis among water consumption and other predictor variables, the correlation between water consumption and environment temperature, and the correlation between water consumption and environment relative humidity are not significantly correlated while the speed is low; therefore, considering the regression model that includes speed, environment temperature and relative humidity, the further F-test shows that the effects of environment temperature and relative humidity on the water consumption can be neglected, following table shows the result, in which, the P value of speed is less than 0.05 while other variables' P value is greater than 0.05, suggesting we can concludes the above result.

Table 5-2 F-test result on the predictor variables to the amount of water consumption

Analysis of Variance					
Source	D F	Sum of Squares	Mean Square	F Value	Pr > F
Model	3	2490933	830311	182.69	<.0001
Error	8	36359	4544.81940		
Corrected Total	11	2527292			
Parameter Estimates					
Variable	D F	Parameter Estimate	Standard Error	t Value	Pr > t
Intercept	1	764.86467	768.23282	1.00	0.3486
Speed	1	0.98025	0.04239	23.12	<.0001
Environment Temperature	1	-14.63605	18.67933	-0.78	0.4559
Environment Relative Humidity	1	-684.36999	528.60780	-1.29	0.2316

Based on above result, the driving speed is most significant variable to predict the water consumption, then we presume the correlation between speed and water consumption follow the nonlinear relation as following:

$$W = a * S^k + b$$

In which,

W= the amount of water consumption;

S= Speed in mph;

To derive the above model, firstly we substitute following:

$$W' = W - b \text{ and}$$

$$S' = S/15$$

Then,

$$W' = a' * S'^k$$

The value of a' and b could be obtained by letting $S' = 0$ and $S' = 1$ as following:

$$a' = 150$$

$$b = 50$$

Then based on the ordinary least square method, we can calculate the value of k , which is following:

$$k = 1.865$$

Therefore, the fit model for speed and water consumption could be obtained as following:

$$W = 150 \times (S/15)^{1.865} + 50$$

Another F-test statistically validates the above regression model shows the model fit is significant (shown in following table):

Table 5-3 F-test result on the regression model among speed and water consumption

Analysis of Variance					
Source	D F	Sum of Squares	Mean Square	F Value	Pr > F
Model	1	2482587	2482587	555.33	<.0001
Error	10	44704	4470.43199		
Corrected Total	11	2527292			

The above equation can be used to predict the minimum water consumption of fbaEC during transport process; an example can be used for demonstration:

When the driving speed is 20 mph, the amount of water consumption in 30 minutes can be calculated through above equation as:

$$W = 150 \times (20/15)^{1.865} + 50 = 306.5 \text{ ml}$$

5.4 Discussion and Summary

According to the comprehensive statistics analysis, fbaEC's cooling performance was statistically supported during practical driving tests. Generally, the driving speed is one of main factors that affected the cooling efficiency. The faster we drove, the better cooling efficiency we achieved. The maximum cooling efficiency during whole experiment was 44.48% with the driving speed of 45mph, which also achieved the lowest temperature of 17.6°C while the environment temperature was 31.9°C, and the temperature inside scaffold stays around the lowest temperature as long as other predicted variables keep relatively stable.

The heat from direct sun shine (solar radiation) had effect (Jakimavicius, Kriauciuniene, Gailiusis, & Sarauskiene, 2013) during tests, which added extra heat to the whole fbaEC system. The recommended storage temperature for most fruits and vegetables ranges from 0°C to 15°C (Hardenburg et al., 1989), the temperature inside the scaffold could be decreased more to meet the recommended temperature range if

the radiation heat effects was limited by modifying the water container design which could be changed to non-transparent material or improve the scaffold dimension, etc. The initial design of fbaEC for eventual use will combine with the truck compartment, which could avoid the solar radiant heat effect in the future.

The cooling capacity of fbaEC is also limited by environment relative humidity and environment temperature. Given these two factors, the theoretical lowest temperature limit through evaporative cooling is called dew-point. By inquiring the dew point through psychrometric chart, the comparison between the fbaEC's lowest temperature through the driving experiment and the dew point is summarized in following table:

Table 5-4 Comparison between driving experiment result and dew-point

Replication	Speed	Lowest Temperature (°C)	Dew Point (°C)	Difference	Average Environmental Temperature	Environment Relative Humidity
1	0	26.7	14.7	82%	31.58	0.36
2	0	26.8	17.3	55%	31.39	0.43
3	0	25.8	15.4	68%	30.92	0.39
1	15	20.8	17.8	17%	30.33	0.47
2	15	21.4	15.8	35%	30.93	0.40
3	15	22.9	16.8	36%	33.98	0.36
1	30	22.8	18.6	23%	30.89	0.48
2	30	22.6	17.4	30%	33.21	0.39
3	30	22.9	16.2	41%	36.59	0.30
1	45	19.5	16.6	17%	30.60	0.43
2	45	17.6	15.4	14%	31.90	0.37
3	45	18.5	16.3	13%	32.05	0.39

The above table indicates the driving speed is an influencing factor on the evaporation efficiency in the certain environment. The higher the driving speed, the smaller the difference between the lowest temperature and the dew-point.

Similarly, the comparison of the lowest temperature through prior experiments in laboratory and the dew point is summarized in following table:

Table 5-5 Comparison between prior lab experiment result and dew-point

Material	Replication	Blow Power	Lowest Temperature	Dew Point (°C)	Difference	Average Environmental Temperature	Environment Relative Humidity
----------	-------------	------------	--------------------	----------------	------------	-----------------------------------	-------------------------------

			(°C)				
Cotton	1	5	10.5	8.6	22%	22.5	40.9%
Cotton	2	5	13.9	11.7	19%	23.2	48.1%
Cotton	3	5	14.4	11.7	23%	23.3	48%
Cotton	1	12	10.2	8.5	20%	22.5	40.6%
Cotton	2	12	12.1	9	34%	23	40.7%
Cotton	3	12	12.3	10.7	15%	24	42.9%
Linen	1	5	8.61	7.4	16%	22.9	37.4%
Linen	2	5	9.79	8.5	15%	23.3	38.8%
Linen	3	5	14.3	10.5	36%	22.6	45.2%
Linen	1	12	10.5	8.5	24%	23.9	37.4%
Linen	2	12	14.1	9.9	42%	23	43.2%
Linen	3	12	13.2	9.6	38%	22.5	43.9%

The lowest temperature achieved through the driving test is 9°C that is higher than the lowest temperature through the prior laboratory experiments. The above two tables also show the different levels of dew points since the average environment temperature for each series of experiment were different; and the environment temperature of prior laboratory experiment were much lower than that of driving test. Therefore, another method that can further decrease the temperature inside the cooler is changing the environment factors through structure redesign, for example, to lower the immediate surrounding temperature by creating a new cooler environment, etc.

The cooling efficiency is also significantly related with environment relative humidity. For each case, generally the lower the environment relative humidity, the higher cooling efficiency it achieved.

The following table summarizes the experiments on testing the fbaEC cooling performance in real transport environment:

Table 5-6 Driving Test Experiment Result Summary

Replication	Speed	Water Consumption (ml)	Lowest Temperature (°C)	Average Environmental Temperature	Maximum Temperature Difference (°C)	Maximum Cooling Efficiency	Environment Relative Humidity
1	0	50	26.7	31.58	7.5	20.27%	0.36
2	0	50	26.8	31.39	4.0	12.94%	0.43
3	0	50	25.8	30.92	4.7	15.41%	0.39
1	15	200	20.8	30.33	13.8	39.08%	0.47
2	15	200	21.4	30.93	10.6	33.13%	0.40

3	15	200	22.9	33.98	12.0	33.43%	0.26
1	30	500	22.8	30.89	9.2	27.63%	0.48
2	30	500	22.6	33.21	11.0	32.07%	0.39
3	30	600	22.9	36.59	17.2	40.00%	0.30
1	45	1100	19.5	30.60	13.2	39.64%	0.43
2	45	1300	17.6	31.90	14.8	44.48%	0.37
3	45	1300	18.5	32.05	15.3	44.48%	0.39

CHAPTER 6

HEAT AND MASS TRANSFER MATHEMATICAL MODEL FOR A MULTI-SCAFFOLD STRUCTURE OF FIBER-BASED ABSORBENT EVAPORATIVE COOLER

To expand and enrich the original fbaEC design based on a single scaffold structure, this chapter presents the development of a heat and mass transfer mathematical model for a multi-scaffold structure of fiber-based absorbent evaporative cooler. The mass transfer model will follow the heat transfer model.

Nomenclature			
		N_L	Number of scaffold rows
V	Air flow velocity	N_T	Number of scaffolds in each row
V_{max}	Maximum airflow velocity	T_o	Outlet temperature
D	Scaffold diameter	T_i	Inlet temperature
S_T	Transverse pitch measured between scaffolds	T_s	The temperature inside of scaffold
S_L	Longitudinal pitch measured between scaffolds	ΔT	Temperature difference
h	Average heat transfer coefficient	ΔT_{lm}	Log-mean temperature difference
N	Total number of scaffolds	t	Cooling duration
L	The length of whole multi-scaffold structure	k	Conductivity
D	Diameter of scaffold, m	γ	Kinematic viscosity
α	Thermal diffusivity	$Re_{D,max}$	Reynolds number based on maximum airflow velocity occurring within the scaffolds
ρ	Air flow density	C_1, C_2	Correction factor

In this study, we initially develop a methodology to predict the amount of water consumption during cooling with an aligned arrangement of multi-scaffold structure; since the air flow fluid will not experience a significant change with the single row or single line structure than the single scaffold (Faghri & Zhang, 2006), and follow the original design of fbaEC shown in figure 2-9, the minimum number of scaffolds is 2×2 . However, for better practical experiment performance, 3×3 is believed to be the better starting number for future experiment validation.



Figure 6-1 2×2 Multi-scaffold illustration

Based on the observation of prior experiment results on the single scaffold, the whole cooling process includes two stages. The first one is a transition stage that starts from the beginning of cooling, in which the temperature inside the scaffold decreases from the environment temperature. The next stage is a steady stage that follows the transition stage, in which the temperature inside the scaffold keeps relatively stable. Since the transition duration is significantly short among the whole cooling process, and it is negligible if the cooling duration is long enough, we focus on the water consumption when it is in the steady stage.

Typically, it is reasonable to find out the average heat transfer coefficient for the whole multi-scaffold structure cooler. The average heat transfer coefficient is defined as the following:

$$\bar{h} = \overline{Nu_D} \frac{k}{D} \quad (1)$$

According to Faghri & Zhang (2006), if the number of scaffold rows is greater and equal to 20, as well as other conditions shown in following:

$$N_L \geq 20$$

$$0.7 \lesssim Pr \lesssim 500$$

$$10 \lesssim Re_{D,max} \lesssim 2 \times 10^6$$

The average Nusselt number can be expressed by following:

$$\overline{Nu_{D(N_L \geq 20)}} = C_1 Re_{D,max}^m Pr^{0.36} \left(\frac{Pr}{Pr_s}\right)^{1/4} \quad (2)$$

In which, the constant C_1 and m can be found in the empirical table based on the scaffold configuration and the Reynolds number. The Prandtl number is defined by

the air dynamic viscosity and air thermal diffusivity as following, and Pr_s is the Prandtl number at the condition when the scaffolds' temperature is steady.

$$Pr = \frac{\gamma}{\alpha} \quad (3)$$

The Reynolds number is based on the maximum air flow velocity within the whole scaffolds structure, and can be defined as the following:

$$Re_{D,max}^m = \rho V_{max} D / \gamma \quad (4)$$

The maximum air flow velocity is defined as the following:

$$V_{max} = \frac{S_T}{S_T - D} V \quad (5)$$

If the number of scaffolds rows is less than 20, a new constant C_2 is introduced as a correction factor, which can also be found in the empirical table, according to Faghri & Zhang (2006), based on the scaffolds' configuration and the number of the scaffolds' rows. The average Nusselt number can be expressed in following:

$$\overline{Nu_{D(N_L < 20)}} = C_2 \overline{Nu_{D(N_L \geq 20)}} \quad (6)$$

To accurately reflect the temperature changes in the whole scaffold structure, since the temperature distribution various at different positions, we define the temperature difference as a log-mean temperature difference, shown in the following:

$$\Delta T_{lm} = \frac{(T_S - T_i) - (T_S - T_o)}{\ln\left(\frac{T_S - T_i}{T_S - T_o}\right)} \quad (7)$$

$$\frac{T_S - T_i}{T_S - T_o} = \exp\left(-\frac{\pi D N \bar{h}}{\rho V N_T S_T c_p}\right) \quad (8)$$

As long as the total number of scaffolds is known, q' , the average heat transfer rate per unit length of the whole scaffold structure can be obtained by the following:

$$q' = N(\pi D \bar{h} \Delta T_{lm}) \quad (9)$$

Therefore, the total heat transferred during cooling is the following:

$$Q = q' L t \quad (10)$$

The heat balance assumption suggests the sensible heat that air flow losses equals to the latent heat that water gains, thus the amount of water consumed during cooling process can be obtained by the following:

$$m_{total} = \frac{Q}{h_{lv}} \quad (11)$$

In which, h_{lv} is the latent heat transfer coefficient (previously shown in Chapter 4).

The above heat and mass transfer mathematical model is built to present the heat and mass transfer process during cooling for the multi-scaffold structure, and to predict the minimum amount of water consumption. This is the initial step of study on the multi-scaffold structure's cooling performance. The model validation is suggested to conduct a series of experiments, which is similarly with the single-scaffold structure experiment. The experiments can start in laboratory environment, but with a 3×3 layout that has a better practical experiment performance. Then the experiments in a real transport environment will be needed for further validation.

CHAPTER 7

CONCLUSION AND FUTURE STUDY

7.1 Research Summary

Evaporative cooling has been demonstrated as one of the most effective alternatives for sustainable refrigeration technology, particularly in areas with high temperature and low humidity. The natural process of moving heat from surrounding air to water vapor produces a considerable cooling effect. The earliest application called “Zero Energy Cool Chamber” (ZECC), based on evaporative cooling to benefit food storage was made in the 1980s, that effectively preserved agricultural products for a certain amount of time, and extended food shelf life. Afterwards, there were many research and ZECC product applications developed in different sizes and locations. Partially using natural and non-human-made power to cool is a huge energy saver and one of the advantages of evaporative cooling, especially for evaporative air conditioner products that use a pump to move water up then spray down to the pad structure which is the heat exchange medium.

To provide an alternative to traditional refrigerated trucks that rely on fossil energy, and extend the capability of evaporative cooling technology for transport, a fiber-based absorbent evaporative cooler (fbaEC) model was developed in laboratory scale. A series of experiments were designed to conceptually test the model performance that produces cooling, while simulating a transport environment in a laboratory through absorbent character of fabric fiber and without external electricity. The results from the prior experiment showed the cooling performance in laboratory environment was statistically significant with certain fabric materials and certain curtain structure.

To continuously explore the fbaEC’s insight on the cooling process, and its cooling performance, the following aspects were studied in this dissertation.

7.1.1 Heat and Mass Transfer Mathematical Model Development for Single-scaffold

Structure

To comprehensively understand the mechanism of the cooling process by fiber-based absorbent evaporative cooler (fbaEC) model, and expand the cooling application for practical use in transport, in this dissertation, a complete heat and mass transfer mathematical model was built to study the evaporative cooling process using a single scaffold, and to predict the minimum water consumption during cooling.

Convection is the main form of heat transfer to enable the phase change between water and vapors, so that heat can be moved from warm air around the curtain to vapor state. Using the theory of energy balance of heat and mass transfer process, the curtain structure character, and air flow blowing scenario, we derived the method to calculate the total heat amount that is the predictable factor for water consumption amount.

The heat and mass transfer mathematical model explains the heat flow and mass transformation process that explains the cooling process of fbaEC for a single-scaffold structure. To quantitatively predict the minimum water consumption during cooling that can help the future input control to avoid the unnecessary waste, the key to the whole model is the heat transfer coefficient that was also unknown. By substituting the given factors, a theoretical heat transfer coefficient was found to complete the theoretical model. Then a series of model validation was conducted to revise the heat transfer coefficient for fbaEC.

7.1.2 Cooling Effect Validation in Transport Environment

The fiber-based absorbent evaporative cooling (fbaEC) was designed for both food storage and transportation. The laboratory experiments have proven that fbaEC has a significant cooling effect while in simulated static and transporting environment, which

builds a solid base to expand the research to next level that is validating the fbaEC performance in real practical storage and transport environment.

In this dissertation, a series of experiments were designed and conducted that move evaporative cooler model as well as other equipment to the outdoors. Similar procedures with the prior experiments were used to monitor and measure the temperature changes inside the scaffold which supported the curtain structure to produce cooling effect. Four levels of speeds of 0 mph, 15 mph, 30 mph and 45 mph were tested with identical cotton fiber, while driving the vehicle on the road.

The experimental results consistently indicated the fbaEC's cooling effect. The results showed the maximum cooling efficiency during whole experiment was 44.48% with the driving speed of 45mph, which also achieved the lowest temperature of 17.6°C while the environment temperature was 31.9°C.

The following table shows the comparison of results from ZECC, a prior laboratory experiment, and the driving experiments for single-scaffold structure. The fbaEC's cooling efficiency is higher than ZECC, and the difference between dew point and lowest temperature of fbaEC is smaller than ZECC; particularly, the cooler in the real transport environment has the best cooling effect of all in terms to the dew point comparison.

Table 7-1 Comparison Among Different Experiment Results

	Lowest temperature (°C)	Environment Temperature (°C)	Cooling Efficiency	Dew Point (°C)	Difference Between Dew Point and Lowest Temperature
ZECC (*Tested with food inside the chamber)	17.1	25	32%	10.5	63%
Prior Laboratory Experiment	8.61	22.9	62%	7.4	16%
Driving Experiment	17.6	31.9	45%	15.4	14%

The statistical analysis supported the experiment results. The cooling effect during the whole experiment was statistically significant, the temperatures inside the scaffold with water, were consistently significantly lower than the environment temperature.

There is a high correlation among cooling efficiency and driving speed, environment temperature and environment relative humidity. Driving speed and environment temperature have a positive effect on the cooling efficiency, meanwhile environment relative humidity has a negative effect on the cooling efficiency. Moreover, the statistical results showed the linear relationship between environment factors and cooling efficiency is more significantly related when the cooler is under static status or with high speed. The sensitivity analysis also concludes that environment factors are more likely to affect the cooling efficiency than the driving speed.

A linear regression model was generated by using the data set from experiments, and a model validation was conducted. It suggests not to reject the null hypothesis that the estimated values and observed values have no difference, thus it is concluded the regression models are valid.

7.1.3 Heat and Mass Transfer Mathematical Model Extension for Multi-Scaffold Structure

Followed the similar model development procedure for the single-scaffold structure, a heat and mass transfer mathematical model on multiple scaffolds structure was built to explore the future evaporative cooling configuration.

The scaffolds layout arrangement matched with the original fbaEC design. The method to find the heat transfer coefficient for the whole cooler is derived, then the minimum unit time water consumption for the whole cooler with a multi-scaffolds structure can be calculated through the model.

7.2 Future Study

Based on all above of study results, following aspects are suggested for the future study on fiber-based absorbent evaporative cooling system, to further validate the cooling effect and improve the cooling performance.

7.2.1 Validation Experiment of Multi-Scaffold Structure's Cooling Efficiency

The study and experiments on the fiber-based absorbent evaporative cooler with a single-scaffold structure and the heat and mass transfer mathematic model on the multi-scaffold structure, have built a solid base for the next step study and experiments on the multi-scaffold structure. Exploring the cooling performance of multi-scaffold structure is suggested to improve the fiber-based absorbent evaporative cooling design.

Firstly, the experiments in lab scale to verify the multi-scaffold structure will be estimated similarly with the prior experiments on single-scaffold structure, which is suggested to start with a 3×3 align layout arrangement. More thermal sensors are proposed to use during experiments to measure the temperature changes at different position in a multi-scaffold structure. The experiment procedure and the statistical analysis methods are proposed similarly with the prior laboratory experiments for the single-scaffold structure, as well as the heat and mass transfer model validation.

Furthermore, once the laboratory experiments verified the cooling performance of multi-scaffold structure, the next step will be the driving experiment for the cooler with multi-scaffold structure in a real transport environment. Similar with the driving experiment on the single-scaffold structure, all data of temperature changes during cooling process need to be collected and statistically analyzed to validate the multi-structure's cooling effect, and to summarize the correlation among predictor variables (driving speed, environment factors, etc.) and cooling efficiency.

7.2.2 fbaEC Structure Improvement

All the analysis results from experiments become the basis to improve the cooler design, and to create better cooling performance in future.

During the experiments of testing fbaEC with a single-scaffold structure in the real transport environment, the radiation heat from direct sun shine through the transparent water container added extra heat to the whole fbaEC system. Future improvement of fbaEC material for water container that can use non-transparent material, is suggested to avoid the solar radiant heat effect, which is discussed in section 5.4. It is believed to potentially decrease the temperature inside of scaffolding furthermore.

In addition, by changing the surrounding environment of scaffold through structure modification to lower the surrounding temperature and relative humidity of scaffold, can directly decrease the dew-point for scaffold environment, which breaks the original limitation of cooling capacity of scaffold. Therefore, the temperature inside the scaffold can be further decreased, eventually meeting the 0-15 °C temperature range recommended for transporting fruits and vegetables.

A closed water loop circulation system is also suggested for future research, since the water changes to vapor during heat transfer process, then vapors escape from the cooler, the close water loop circulation system can possibly avoid the need to replenish the water. That would be especially valuable for the areas where have limited access to water resources.

7.3 Contribution

In this dissertation, all the research and study on the fiber-based absorbent evaporative cooling (fbaEC) has achieved following three main aspects:

- 1) Developed a heat and mass transfer mathematical model to predict the minimum water consumption for the single-scaffold structure cooling system.

The model can be used to explore the insight of cooling process, and further calculate the water consumption under designated factors of temperature change range and transport time duration. Meanwhile, the single-scaffold cooler structure can also be improved based on the model, to achieve different cooling effect.

2) Consistently demonstrated its cooling performance and significant temperature decreasing without external electricity while running the whole system in the real transport environment.

The fbaEC shows a better cooling effects than ZECC, in respect to laboratory environment and transport environment, respectively. In this study, although the lowest temperature inside cooler through the driving experiment did not meet the recommended temperature range of transporting fruits and vegetables, which is 0-15°C, the fbaEC's advantages of sustainability and energy saving has been statistically proven.

3) Built a heat and mass transfer mathematical base for future study on the multi-scaffold structure.

The complete heat and mass transfer mathematical model for the single scaffold provided a solid base for the extension mathematical model for the multi-scaffold structure cooling system. This model is the initial step to explore the future validation of multi-scaffold structure's cooling effect. The initial fbaEC design using a multi-scaffold structure can be implemented and improved based on the model.

All in all, as the original design was to provide an alternative method to preserve food products and extend their shelf life for people living in rural dry areas where have limited access to electricity and high technology, it is possible to extend fbaEC for use with pharmaceutical products as well, for example, vaccines and other medicines that need to be kept in lower temperature during storage and transportation.

REFERENCE

- Abbouda, S., & Almuhanha, E. (2012). Improvement of Evaporative Cooling System Efficiency in Greenhouses. *International Journal of Latest Trends in Agriculture and Food Sciences*, 2(2).
- Air Resources Board. (2014). *Transport Refrigerators Technology Assessment*. California Environmental Protection Agency.
- Amer, O., Boukhanouf, R., & Ibrahim, H. (2015). A Review of Evaporative Cooling Technologies. *International Journal of Environmental Science and Development*, 6(2).
- Anyanwu, E. E. (2003). Design and measured performance of a porous evaporative cooler for preservation of fruits and vegetables. *Energy Conversion and Management*, (45 (2004)), 2187–2195.
- Basediya, A. Lal, Samuel, D. V. K., & Beera, V. (2011). Evaporative cooling system for storage of fruits and vegetables - a review. <https://doi.org/10.1007/s13197-011-0311-6>
- Boucekara, H., Kedous-Lebouc, A., Dupuis, C., & Allab, F. (2008). Prediction and optimisation of geometrical properties of the refrigerant bed in an AMRR cycle. *International Journal of Refrigeration*, 31, 1224–1230.
- Buker, M., & Riffat, S. (2015). Recent developments in solar assisted liquid desiccant evaporative cooling technology-A review. *Energy and Buildings*, 96, 95–108.
- Camargo, J. R., Ebinuma, C. D., & Cardoso, S. (2003). A MATHEMATICAL MODEL FOR DIRECT EVAPORATIVE COOLING AIR CONDITIONING SYSTEM. *Engenharia Térmica*, 30–34.
- Chouksey RG. (1985). Design of passive ventilated and evaporatively cooled storage structures for potato and other semi perishables.

- Das SK, & Chandra P. (2001). Economic analysis of evaporatively cooled storage of horticultural produce. *Agric Eng Today*, 25 (3-4) , 1–9.
- Evaporate Cooling | Heating & Cooling | Alabama Power. (n.d.). Retrieved November 8, 2015, from <http://www.alabamapower.com/business/services/architects-engineers/library/space-heating-cooling/evaporate-cooling.asp>
- Faghri, A., & Zhang, Z. (2006). *Transport Phenomena in Multiphase System*. Elsevier Inc.
- FDA. Advanced Notice of Proposed Rulemaking (ANPRM) (2010).
- Ganesan, M., Balasubramanian, K., & Bhavani, R. (2004). Effect of water on the shelf-life of brinjal in zero-energy cool chamber. *J Indian Inst Sci*, (84), 1–7.
- Gómez, E. V., Martínez, F. C. R., & González, A. T. (2010). The phenomenon of evaporative cooling from a humid surface as an alternative method for air-conditioning. *INTERNATIONAL JOURNAL OF ENERGY AND ENVIRONMENT*, 1(1), 69–96.
- Guo, X. (2012). *Fiber-Based Absorbent Configuration in Evaporative Cooling* (MS Thesis). University of Missouri, Columbia, Missouri.
- Hardenburg, Robert E., Chien Yi Wang, & Alley E. Watada. (1989). The Commercial Storage of Fruits, Vegetables, Florist and Nursery Stocks, United States Department of Agriculture Handbook #66.
- Helsen, A., & Willmot, J. (1991). Wet air cooling of fruits, vegetables and flowers. Current practice in Europe. Technical innovation in freezing and refrigeration of fruits and vegetables. *International Institute of Refrigeration*, 169–77.
- Islam, M., Morimoto, T., & Hatou, K. (2013). Dynamic optimization of inside temperature of Zero Energy Cool Chamber for storing fruits and vegetables using neural networks and genetic algorithms. *Computers and Electronics in*

Agriculture, 95, 98–107.

- Islam, M. P., & Morimoto, T. (2011). Identification and control of temperature in a zero energy cool chamber for fruits and vegetables (pp. 1078–1083). Presented at the System Integration (SII), 2011 IEEE/SICE International Symposium on, Kyoto: IEEE.
- Islam, M. P., & Morimoto, T. (2014). A new zero energy cool chamber with a solar-driven adsorption refrigerator. *Renewable Energy*, 72, 367–376.
- Jain, D. (2006). Development and testing of two-stage evaporative cooler. *Building and Environment*, (42 (2007)), 2549–2554.
- Jakimavicius, D., Kriauciuniene, J., Gailiusis, B., & Sarauskiene, D. (2013). Assessment of uncertainty in estimating the evaporation from the Curonian Lagoon. *Baltica*, 26.
- J.M. Wu, X. Huang, & H. Zhang. (2008). Numerical investigation on the heat and mass transfer in a direct evaporative cooler. *Applied Thermal Engineering*, (29 (2009)), 195–201.
- Kachhwaha, S. S., & Prabhakar, S. (2009). Heat and mass transfer study in a direct evaporative cooler. *Journal Of Scientific & Industrial Research*, (Vol.69), 705–710.
- Kalpana Rayaguru, Md K. Khan, & Sahoo N. R. (2009). Water use optimization in zero energy cool chambers for short term storage of fruits and vegetables in coastal area. *J Food Sci Technol*, (July–August 2010), 437–441.
- Khader, V. (1999). Textbook on food storage and preservation (5th edn.). Kalyani Pub, India.
- Lie, Y., Su, F., Lai, R., & Lin, T. (2006). Experimental study of evaporation heat transfer characteristics of refrigerants R-134a and R-407C in horizontal small tubes.

- International Journal of Heat and Mass Transfer*, 49, 207–218.
- Longmone AP. (2003). Evaporative cooling of good products by vacuum. *Food Trade Rev (Pennwalt Ltd)*, (47), 13–16.
- Love, R. (2009). Chillin’ at the Symposium with Plato: Refrigeration in the Ancient World. *ASHRAE Transactions*, 115(1), 106.
- Mehere, S., Mudafale, K., & Prayagi, S. (2014). Review of Direct Evaporative Cooling System with Its Applications. *International Journal of Engineeing Research and General Science*, 2(6).
- Mogaji, T., & Fapetu, O. (2011). Development of an evaporative cooling eyetem for the preservation of fresh vegetables. *African Journal of Food Science*, 5(4), 255–266.
- Mohit Saluja. (2011). Absorbent Textiles.
- Montazeri, H., Blocken, B., & Hensen, J. (2015). CFD analysis of impact of physical parameters on evaporative cooling by a mist spray system. *Applied Thermal Engineering*, 75, 608–622.
- Ndukwu, M. C., & Manuwa, S. I. (2014). Review of research and application of evaporative cooling in preservation of fresh agricultural produce. *Int J Agric & Biol Eng*, Vol. 7(No.5), 85.
- Noble, N. (2003). Evaporative Cooling. *Practical Action*. United Kingdom. Retrieved from <http://answers.practicalaction.org/our-resources/item/evaporative-cooling>
- Patil, C., Hirde, K., & Badnera, R. (2013). The Concept of Indirect Evaporative Cooling. *International Journal of Engineering Science and Innovative Technology*, 2(5).
- Popular Plastics and Packaging. (2014). *Food industry focuses on better packaging and smarter process technology for less spoilage*.
- Prabha A, Sharma HR, Goel AK, & Ranjana V. (2006). Changes in ascorbic acid

- content of lemon fruits stored in zero energy cool chamber and under ambient atmosphere. *J Dairy Foods HS*, 25(1), 73–75.
- Ranjan, R., Murthy, J., & Garimella, S. (2011). A microscale model for thin-film evaporation in capillary wick structures. *CTRC Research Publications*.
- Roy, K., & Khurdiya, D. (1982). Keep vegetables fresh in summer. *Indian Hort*, 1(27), 5–6.
- Roy, S. (1984). Post harvest storage of fruits and vegetables in a specially designed built in space (pp. 190–193). Presented at the Proc. Intl. Workshop on Energy conservation in buildings., Roorkee,UP,India.
- Roy, S. K., & Khurdiya, D. S. (1986). Studies on Evaporative Cooled Zero-energy Input Cool Chamber for the Storage of Horticulture Produce. *Indian Food Packer*, 40, 26–31.
- Roy, S. K., & Pal, R. K. (1991). A LOW COST ZERO ENERGY COOL CHAMBER FOR SHORT TERM STORAGE OF MANGO. *International Society for Horticultural Science*, 291(59).
- Sandooja, J., Sharma, R., Pandit, M., & Batra, B. (1987). Storage studies to tomato in zero-energy cool chamber in relation to storage of maturity and packaging material used. *Haryana Agric Univ J Res.*, 17(3), 216–217.
- S.K Sharma, M.C. Nautiyal, & K. Issar. (n.d.). POSTHARVEST ROTTING, QUALITY AND SHELF LIFE OF APPLE AS AFFECTED BY CHEMICALS, GA TREATMENT AND PACKAGING.
- SN, J., & S, C. (2006). Selection of bricks and cooling pad for construction of evaporatively cooled storage structure. *Inst Engineers*, 87, 25–28.
- T.A. Taylor, D.R. Heldman, R.R. Chao, & H.L. Kramer. (1998). SIMULATION OF THE EVAPORATIVE COOLING PROCESS FOR TORTILLAS.

- Thompson AK. (1996). Post harvest technology of fruit and vegetable. *Oxford: Blackwell Science Ltd*, 136.
- Umbarkar SP, Bonde RS, & Kolase MN. (1991). Evaporatively cooled structures for orange (*Citrus reticulata*). *Indian J Agric Eng*, 1(1), 26–32.
- Used Evaporative Coolers | Coolers. (2014). Retrieved from <http://dalllac.com/used-evaporative-coolers/>
- Wagner, R. (n.d.). What Is a Reefer Truck? Retrieved November 2, 2016, from http://www.ehow.com/facts_5050431_reefer-truck.html
- Wasker, D., Nikam, S., & Garande, V. (1999). Effect of different packaging materials on storage behaviour of sapota under room temperature and cool chamber. *Indian J Agric Res.*, 33, 240–244.
- Western Environmental Services Corporation. (n.d.). Evaporative Cooling Basics. Retrieved November 14, 2015, from <http://www.wescorhvac.com/Evaporative%20cooling%20white%20paper.htm>
- Westlake, D. (n.d.). Sideswept Bangs: Improved Methods Of Transporting Food. Retrieved November 2, 2016, from <http://sidesweptbangs.blogspot.com/2013/05/improved-methods-of-transporting-food.html>
- William Adebisi Olosunde, J.C. Igbeka, & Taiwo Olufemi Olurin. (2009). Performance Evaluation of Absorbent Materials in Evaporative Cooling System for the Storage of Fruits and Vegetables. *International Journal of Food Engineering*, Volume 5,(Issue 3). <https://doi.org/10.2202/1556-3758.1376>
- Wojtala, G. (n.d.). *Interstate Food Transportation Assessment project*.
- World Bank. (2014). Food Loss and Waste a Barrier to Poverty Reduction. Retrieved October 24, 2015, from <http://www.worldbank.org/en/news/press->

release/2014/02/27/food-loss-waste-barrier-poverty-reduction

- Xuan, Y. M., Xiao, F., Niu, X. F., Huang, X., & Wang, S. W. (2012). Research and application of evaporative cooling in China: A review (I) –research. *Renewable and Sustainable Energy Reviews*, *16*, 3535–3546.
- Yuan, F., & Chen, Q. (2012). A global optimization method for evaporative cooling systems based on the entransy theory. *Energy*, *42*, 181–191.
- Zhang, X., Zhang, X., Chen, Y., & Yuan, X. (2008). Heat transfer characteristics for evaporation of R417A flowing inside horizontal smooth and internally grooved tubes. *Energy Conversion and Management*, *49*.

APPENDIX

In this section, an example raw data set table is listed as following, to show the temperature changes from one replication of case with driving speed of 45 mph during driving experiment.

Time (s)	TC 4 (°C)	TC 3 (°C)	TC 2 (°C)	TC 1 (°C)
0	26.9	26.2	26.3	30.3
5	26.9	26.3	25.4	30.4
10	27	27.2	25.6	30.4
15	27.2	27.4	25.7	30.4
20	27.3	27.5	25.8	30.5
25	27.4	27.5	25.9	30.5
30	27.4	27.4	26	30.5
35	27.3	27.6	25.9	30.5
40	27.4	27.7	26	30.5
45	27.5	27.7	26	30.5
50	27.5	28.2	26	30.6
55	27.6	28.3	25.9	30.8
60	27.8	28.1	25.8	30.1
65	28	27.7	25.4	30.2
70	28.2	27.3	25.6	30.5
75	28.4	27.2	25.7	30.3
80	28.5	27	25.3	30.4
85	28.7	26.7	26.4	30.3
90	28.9	26.6	25.6	30.4
95	29	26.5	25.8	30.5
100	29.3	26.6	25.8	30.5
105	29.5	26.3	25.8	30.4
110	29.4	25.7	25.1	30.3
115	29.5	25.4	25	30.2
120	29.5	24.3	23.9	30
125	29.5	24.3	23.9	30.1
130	29.5	24.2	23.8	30.2
135	29.6	24.1	23.6	30.2
140	29.5	24	23.2	30.2
145	29.5	24.1	23.4	30.1
150	29.5	24	23.4	30.2
155	29.4	21.1	20.3	30.1
160	29.5	22.1	21.3	30.2
165	29.5	21.9	21.3	30.1
170	29.4	21.9	21.3	30.2
175	29.5	22	21.2	30.2

180	29.5	21.9	21.1	30.3
185	29.5	20.8	20.6	30.4
190	29.6	20.9	19.8	30.5
195	29.7	20.5	20	30
200	29.7	20.2	19.6	30
205	29.8	20.4	19.8	30.1
210	29.9	20.3	19.9	30.3
215	29.9	20.2	20	30.3
220	29.9	20.2	20	30.4
225	29.9	20.4	20.1	30.4
230	30	20.3	20	30.4
235	30.1	20.4	20.2	30.5
240	30.1	20.1	20.1	30.6
245	30.1	20.4	20.1	30.5
250	30.1	20.2	20.2	30.5
255	30.1	20	20	30.5
260	30.1	20.3	20.3	30.6
265	30.1	20.2	20.2	30.6
270	30.2	20.4	20.2	30.7
275	30.2	20.4	20.6	30.7
280	30.3	20.3	20.4	30.7
285	30.3	20.1	20.3	30.8
290	30.3	20.5	20.3	30.8
295	30.3	20.6	20.6	30.8
300	30.4	20.4	20.3	30.9
305	30.5	20	20.1	30.9
310	30.6	20.1	20.3	30.9
315	30.6	20.2	20.3	30.9
320	30.6	20.5	20.5	30.9
325	30.6	20.5	20.5	31
330	30.6	20.6	20.4	31.1
335	30.7	20.4	20.3	31.2
340	30.7	20.3	20.3	31.2
345	30.8	20.1	20.3	31.2
350	30.8	20.3	20.5	31.3
355	30.8	20.2	20.5	31.2
360	30.8	20.3	20.4	31.2
365	30.8	20.3	20.6	31.3
370	30.8	20.2	20.6	31.3
375	30.7	20.1	20.8	31.3
380	30.9	20.2	20.6	31.3
385	30.9	20.4	20.6	31.3
390	30.9	20.1	20.9	31.3
395	31	18.3	19.2	31.2
400	30.9	18.2	20	31.1

405	31	18	19.3	31.1
410	31.1	18.2	18.7	31
415	31.2	18.2	19.1	30.9
420	31.3	18.2	18.6	30.9
425	31.3	18.2	19	31
430	31.4	18.3	19	31
435	31.4	18.4	19	31
440	31.5	18.4	19.2	31
445	31.5	18.2	18.7	30.9
450	31.5	18.1	18	31
455	31.6	18.2	18.3	31.2
460	31.7	18.3	18.2	31.2
465	31.7	18.3	18.3	31.2
470	31.7	18.4	18.3	31.2
475	31.7	18.3	18	31.1
480	31.7	18.1	18.2	31.2
485	31.8	18.3	18.2	31.3
490	31.8	17.9	18	31.4
495	31.8	18	18.2	31.5
500	31.8	17.9	18	31.6
505	31.9	17.6	17.7	31.6
510	31.9	18	18.2	31.7
515	31.8	17.7	17.9	31.7
520	31.9	17.6	17.9	31.7
525	31.9	17.6	17.9	31.7
530	31.9	18.1	18.2	31.8
535	31.9	18.2	18.2	31.7
540	32.2	18.3	18.1	31.7
545	32.2	18	18.1	31.5
550	32.1	17.9	18	31.3
555	32.1	17.8	18.2	31.2
560	32.1	17.9	18.6	31.1
565	32.2	17.9	18.7	31.2
570	32.3	18.3	18.1	31.1
575	32.4	18.4	18.4	31.2
580	32.6	18.2	18	31.2
585	32.5	18	17.9	31.1
590	32.5	18.2	18.1	31
595	32.6	18.5	18.4	31
600	32.7	19.1	18.6	31
605	32.9	19.9	18.8	31.1
610	33	20.2	18.8	31.3
615	32.9	20.5	18.9	31.4
620	32.7	20.5	18.8	31.3
625	32.8	20.9	18.7	31.3

630	32.6	19.8	18.5	31.2
635	32.3	20.8	18.9	31.1
640	32.2	20.8	19.1	31
645	32.1	19.2	19	30.9
650	31.9	19.1	18.8	30.8
655	31.9	19.3	19.1	30.8
660	31.7	19.4	19.9	30.7
665	31.5	19.1	20.2	30.6
670	31.6	18.9	20.1	30.7
675	31.5	19.1	20.4	30.7
680	31.6	18.9	20.5	30.7
685	31.6	18.7	20.4	30.6
690	31.6	18.9	20.6	30.7
695	31.6	18.9	20.3	30.7
700	31.5	19	20.3	30.7
705	31.5	19	20.4	30.7
710	31.5	19.3	20.7	30.7
715	31.5	18.7	20.1	30.7
720	31.5	18.6	19.8	30.8
725	31.4	19	20.1	30.8
730	31.4	18.7	19.9	30.8
735	31.4	18.8	19.7	30.7
740	31.4	18.8	19.7	30.8
745	31.4	18.9	19.8	30.8
750	31.4	18.9	19.9	30.8
755	31.3	19.3	19.9	30.8
760	31.4	19.2	20	30.8
765	31.4	19.5	20.1	30.8
770	31.4	19.3	20	30.9
775	31.4	19.3	20.3	30.9
780	31.4	19.4	20.3	30.9
785	31.4	19.4	20.2	31
790	31.5	19.6	20	30.9
795	31.4	19.9	20.2	31
800	31.4	20.5	20.4	31
805	31.5	19.9	20.1	31
810	31.5	20	19.8	31
815	31.4	20	19.6	31.1
820	31.4	21.2	19.8	31
825	31.5	20.9	19.6	31.1
830	31.5	20.8	19.7	31.1
835	31.6	20.7	19.7	31.1
840	31.7	20.9	20	31.3
845	32	21.7	20.5	31.7
850	31.9	21.7	20.4	31.5

855	31.9	22.1	20.6	31.5
860	32	19.8	19.8	31.8
865	32	19.8	19.1	31.7
870	32.1	20.3	19.3	31.7
875	32.1	20.8	19.3	31.7
880	32.2	20.6	19.5	31.7
885	32.3	19.7	19.8	31.7
890	32.6	19.7	20.2	32.6
895	32.6	20.1	20.3	32.6
900	32.7	19.1	20.3	32.6
905	32.7	19.2	20.6	32.7
910	32.8	18.7	19.9	32.9
915	32.8	18.6	20.5	32.6
920	32.8	19	20.5	32.5
925	32.7	19.2	21.2	32.4
930	32.8	19.4	20.6	32.4
935	32.8	18.8	20.2	32.4
940	32.8	19.5	20.7	32.4
945	32.8	20.4	21	32.4
950	32.7	20.4	20.7	32.4
955	32.7	20.2	20.5	32.5
960	32.7	20.5	20.9	32.5
965	32.7	20.4	20	32.5
970	32.7	20.6	20.4	32.4
975	32.6	20.8	20.4	32.4
980	32.6	21.3	20.3	32.5
985	32.6	19.7	19.9	32.4
990	32.5	19.2	19.1	32.4
995	32.6	20.1	20.1	32.4
1000	32.6	20.4	20.3	32.4
1005	32.5	20.4	20.1	32.4
1010	32.6	20.8	20.6	32.4
1015	32.6	20.6	20.5	32.5
1020	32.7	20.8	20.5	32.6
1025	32.7	21	20.9	32.5
1030	32.7	19.9	19.4	32.6
1035	32.6	20.4	19.8	32.5
1040	32.6	20.3	19.4	32.5
1045	32.7	19.8	19	32.5
1050	32.7	20.4	19.3	32.5
1055	32.6	21.1	19.8	32.4
1060	32.6	20.7	19.4	32.4
1065	32.6	21.1	19.5	32.4
1070	32.6	20.8	19.5	32.4
1075	32.5	20.5	19.1	32.4

1080	32.6	20.6	19.3	32.5
1085	32.5	20.2	19.1	32.4
1090	32.6	21.5	19.7	32.4
1095	32.6	21.7	19.9	32.3
1100	32.7	21.1	19.6	32.3
1105	32.7	20.4	19.5	32.4
1110	32.7	21.3	19.8	32.4
1115	32.7	21.1	19.7	32.4
1120	32.7	21.2	19.9	32.5
1125	32.7	22	20.6	32.5
1130	32.6	21.7	20.2	32.5
1135	32.5	22.2	20.1	32.5
1140	32.6	22.1	19.7	32.5
1145	32.6	22.8	20.9	32.5
1150	32.6	22.5	20.8	32.5
1155	32.7	22.1	20.6	32.5
1160	32.7	22	20.6	32.2
1165	32.6	22	20.7	31.7
1170	32.5	22	20.8	31.4
1175	32.4	22	20.9	31.2
1180	32.7	22	20.6	32.2
1185	32.4	22.1	20.9	31.1
1190	32.4	22	20.9	31
1195	32.8	25.2	20.8	32
1200	32.9	23.9	21	32.1
1205	33.1	22.6	21	32.2
1210	33	21.1	20.7	32.2
1215	33	21.4	21.2	32.3
1220	33	20.8	20.8	32.3
1225	33	20.9	20.2	32.3
1230	33	20.7	20	32.2
1235	32.9	20.6	20	32.2
1240	33	20.9	19.9	32.3
1245	33	21.6	20	32.2
1250	33.1	21.5	20.1	32.3
1255	33.2	21.5	20.2	32.3
1260	33.3	21.8	20.4	32.4
1265	33.2	21	20.2	32.5
1270	33.1	21.5	20.4	32.5
1275	33	21.4	20.4	32.4
1280	33	21.7	20.5	32.4
1285	32.9	21.5	20.5	32.3
1290	32.9	21.9	20.8	32.2
1295	33	21.8	20.8	32.3
1300	33.1	21	20.5	32.3

1305	33.1	21.2	21	32.3
1310	33.1	20.1	19.7	32.3
1315	33	20.5	20.1	32.3
1320	33.1	19.9	19.9	32.3
1325	33.1	20	20	32.2
1330	33.2	20.7	20.6	32.2
1335	33.2	20.1	19.9	32.2
1340	33.2	20.2	19.9	32.2
1345	33.2	20.3	20.4	32.3
1350	33.3	20.7	20.6	32.3
1355	33.4	20.6	20.5	32.4
1360	33.4	20.1	20.5	32.4
1365	33.3	20.2	20.5	32.4
1370	33.4	20.7	20.8	32.4
1375	33.4	20.7	20.7	32.4
1380	33.3	20.7	19.8	32.7
1385	33.2	20.8	19.2	32.6
1390	33.1	20.8	19	32.4
1395	32.9	21.7	19.4	32.4
1400	32.7	22.2	20.7	32.4
1405	32.7	22	20.6	32.3
1410	32.6	21.6	20.7	32.3
1415	32.6	21.4	20.3	32.2
1420	32.6	21.9	20.3	32.2
1425	32.6	22.7	20.9	32.1
1430	32.4	21.2	21.6	32.1
1435	32.2	19.9	19.7	32
1440	32.2	20.8	20.2	32
1445	32.2	19.7	19.2	31.9
1450	32.2	19.5	19.2	31.9
1455	32.3	19.1	18.9	31.9
1460	32.3	19	19.1	31.9
1465	32.2	19.3	19.5	32
1470	32.3	19.8	20.2	32
1475	32.3	19.7	20.2	31.9
1480	32.3	20.5	21.1	31.9
1485	32.3	20.1	21	31.9
1490	32.1	19.8	19.6	31.9
1495	32	20.2	19.6	31.9
1500	32	21.4	20.9	31.8
1505	32.3	20.2	21.4	32.1
1510	32.4	20.1	21.7	32.1
1515	32.3	20.2	21.3	32.1
1520	32.2	19.9	19.9	32
1525	32.2	19.9	19.8	31.9

1530	32.2	20	20	31.8
1535	32.2	20.3	20.5	31.8
1540	31.8	21.5	20.9	31.7
1545	31.9	20.6	20.5	31.7
1550	31.9	21.3	20.6	31.8
1555	31.9	21.1	19.8	31.8
1560	32	20.8	19.4	31.8
1565	32.1	20.6	19.2	31.8
1570	32.1	20.5	19.1	31.9
1575	32.2	20.4	19.2	32
1580	32.2	20	19.3	32
1585	32.1	19.8	19.3	31.8
1590	32.1	19.8	19.8	31.4
1595	32	19.8	19.9	31.3
1600	32.1	19.8	20	31.2
1605	32.2	19.9	20.2	31.1
1610	32.5	21.2	19.9	32.3
1615	32.5	21	19.1	32.4
1620	32.5	21.1	19.1	32.4
1625	32.6	20.7	19.2	32.4
1630	32.7	20.4	20.1	32.5
1635	32.8	20.9	20.1	32.8
1640	32.8	21.2	20.7	33.2
1645	32.7	21.6	20.9	33.2
1650	32.9	22.9	20.7	33.1
1655	32.9	23.1	20.6	32.9
1660	32.9	23	20.2	32.8
1665	32.7	23.1	20.3	32.8
1670	32.9	23.2	20.4	32.8
1675	33	23.5	20.9	32.7
1680	33	23.6	20.6	32.8
1685	33	22.4	20.8	32.9
1690	33.1	22	20.2	33
1695	33.1	22.4	20.5	33
1700	33.1	22.8	20.8	32.9
1705	32.9	22.6	20.7	32.9
1710	33.6	21.9	20.9	33.6
1715	33.7	20.7	20.4	33.6
1720	33.9	20.2	19.8	33.5
1725	33.9	21.6	20.8	33.3
1730	34	23.8	20.7	33.7
1735	34	23.4	20.3	33.8
1740	34	22.8	20.2	33.9
1745	34	21.3	19.2	33.9
1750	34	20.7	19	33.8

1755	34	21.3	19.9	33.9
1760	34.2	21.3	20	34
1765	34.3	21.3	19.9	34
1770	34.2	21	19.6	33.9
1775	34.2	21.3	19.9	33.8
1780	34	21.8	20.2	33.3
1785	33.4	21.8	19.8	32.9
1790	31.6	21	19.5	31.7
1795	30.9	20.7	19.5	30.4
1800	31.1	19.8	19.6	31.9

VITA

Xiaoyu Guo earned his M.S. and Ph.D. in industrial engineering from the University of Missouri in 2012 and 2016, respectively. He earned his bachelor's degree in mechanical engineering from Tianjin Polytechnic University in 2009.